

Acoustic classification of Australian frogs for ecosystem surveys

A THESIS SUBMITTED TO
THE SCIENCE AND ENGINEERING FACULTY
OF QUEENSLAND UNIVERSITY OF TECHNOLOGY
IN FULFILMENT OF THE REQUIREMENTS FOR THE DEGREE OF
DOCTOR OF PHILOSOPHY

Jie Xie

School of Electrical Engineering and Computer Science
Science and Engineering Faculty
Queensland University of Technology

April 2016

Copyright in Relation to This Thesis

© Copyright 2016 by Jie Xie. All rights reserved.

Statement of Original Authorship

The work contained in this thesis has not been previously submitted to meet requirements for an award at this or any other higher education institution. To the best of my knowledge and belief, the thesis contains no material previously published or written by another person except where due reference is made.

Signature:

Date:

To my family

Abstract

Rapid decreases in frog populations, which are regarded as one of the most critical threats to global biodiversity, have been spotted from locations around the world. Causes of these declines can be summarised as follows: disease, habitat destruction and modification, exploitation, pollution, pesticide use, introduced species, and ultraviolet-B radiation (UV-B). On the one hand frogs play an important role in the whole ecosystem, but on the other frog populations are declining globally. To assess frog populations and optimise frog protection policies, monitoring frogs is becoming ever more necessary. Since frogs are much easier to be heard than seen, frog populations are often assessed by their vocalisations. In order to collect frog vocalisations, traditional manual methods require ecologists and volunteers to visit the field, which limits the scale for acoustic data collection. In contrast, recent advances in acoustic sensors provide a novel method to survey vocalising animals such as frogs. After deploying acoustic sensors in the field, they can automatically collect acoustic data at large spatial and temporal scales. The large volumes of raw acoustic data collected must be analysed to gain insights about frogs and the environment from the data. It has become very important to enable automated species identification in acoustic data. Also, since the data is collected from the field, the acoustic data tend to be very noisy and very often the desired signal (frog call) is weak. Very often, there are also multiple signals overlapping the frog calls. These characteristics pose a big challenge to performing automatic classification of frog species in acoustic data.

The research presented in this dissertation aims to investigate methods to build a robust and accurate classification prototype system for frog species in acoustic data. Two important aspects of a classification prototype system are investigated: feature extraction and classification, which consist of contributions towards three main objectives.

- (1) Develop an enhanced feature representation for frog call classification. Time-frequency information of frog calls can be effectively represented via the enhanced representation

of temporal, perceptual and cepstral features. The classification performance of various machine learning techniques is compared with different feature representations. Our proposed enhanced feature representation achieves the best classification accuracy which outperforms most previous studies.

- (2) Propose a novel feature representation based on adaptive wavelet packet decomposition.

To better capture the frequency domain information of frog calls with a good anti-noise ability, a novel feature representation, namely *adaptive frequency scaled wavelet packet decomposition sub-band cepstral coefficients*, is proposed. Compared with other cepstral coefficients, the proposed feature representation shows the best classification performance and a good anti-noise ability.

- (3) Design a robust classification system to study low signal-to-noise ratio (SNR) recordings with multiple simultaneously vocalising frog species. Two classification frameworks are employed to classify multiple simultaneously vocalising frog species.

- (a) Multiple-instance Multiple-label (MIML) learning

To use MIML learning for classifying multiple simultaneously vocalising frog species, individual syllables are first segmented. Then, various features are calculated from each segmented syllable. Next, a bag generator is applied to those extracted features to construct a suitable bag-of-syllable representation. Finally, three MIML learning algorithms are employed for the classification of frog vocalisations: MIML-SVM, MIML-KNN, and MIML-RBF.

- (b) Multiple-label (ML) learning

For the ML learning, acoustic features are first calculated without segmentation. Then, ML learning is used to classify simultaneously vocalising frog species using extracted features. Three main ML learning methods are compared: Binary relevance, Classifier Chains, Random k-labelsets, where the base classifier is a decision tree classifier. Furthermore, the frog abundance and species richness over three months are calculated based on the results of acoustic event detection and ML classification, respectively. Lastly, the correlation analysis between frog calling activity (frog abundance and species richness) and weather variables (mean temperature and rainfall) are studied to demonstrate the application of our proposed ML classification framework.

Our proposed approach achieves promising classification results compared with most previous studies. Novel feature representations and classification learning frameworks have different contributions to the performance of the classification system of frog vocalisations. To cope with high SNR recordings, we construct a novel feature representation including temporal, perceptual, and cepstral features. To improve the anti-noise ability of cepstral features, we develop a novel wavelet-based cepstral feature representation. To address low SNR recordings with multiple overlapping vocalising frog species, the classification frameworks of MIML learning and ML learning are proposed. To the best of this researcher's knowledge, it is the first time that MIML learning and ML learning are employed for automatic classification of multiple simultaneously vocalising frog species. With this developed classification system, the ecosystem at large spatial and temporal scales can be surveyed, which can help ecologists better understand the ecosystem.

Keywords

Bioacoustic monitoring
Soundscape ecology
Environmental audio analysis
Frog call classification
Spectrogram analysis
Acoustic feature extraction
Wavelet packet decomposition
Multiple-instance multiple-label learning
Multiple-label learning

Acknowledgments

First, I would like to express my sincere gratitude and thanks to Dr Jinglan Zhang (principal supervisor), for giving me an opportunity to study in Australia. During the entirety of this PhD study, I have learnt so much from her about having passion for work, combined with high motivation, which will benefit me throughout my life. I would also like to express my gratitude to Professor Paul Roe (associate supervisor), for his consistent instructions and supports through the last three years.

I would also like to thank Dr Michael Towsey for his provision of consistent guidance, discussions, and encouragement during my PhD study. Michael's attitude towards scientific research keeps motivating me go deeper into research.

I want to thank Professor Vinod Chandran for his support in writing my confirmation report and this thesis. Vinod's strong background knowledge in signal processing greatly helps me improve my understanding of this research.

I would also like to express my gratitude to my family, especially my grandparents, parents and my wife. They have always supported my overseas study. Without their support, I could not give my full attention to PhD study and the completion of this thesis. My sincere thanks also go to all my friends for their love, attention and support to my PhD study.

Finally, I extend my thanks to the China Scholarship Council (CSC), Queensland University of Technology and the Wet Tropics Management Authority for their financial support.

Table of Contents

Abstract	v
Keywords	ix
Acknowledgments	xi
List of Figures	xx
List of Tables	xxii
Abbreviations	
1 Introduction	1
1.1 Motivation and background	1
1.2 Basic concepts	2
1.2.1 Environmental audio data	2
1.2.2 Audio data analysis	3
1.2.3 Frog call structure	4
1.2.4 Acoustic event and background noise	5
1.2.5 Frog call classification	6
1.3 Research Challenges	6
1.4 Research questions	7
1.5 Aims and objectives	8
1.6 Significance and contributions	9

1.7	Thesis structure	11
2	Literature review	15
2.1	Overview	15
2.2	Signal pre-processing	17
2.2.1	Signal processing	17
2.2.2	Noise reduction	18
2.2.3	Syllable segmentation	18
2.3	Acoustic features for frog call classification	19
2.3.1	Time domain and frequency domain features for frog call classification	19
2.3.2	Time-frequency features for frog call classification	20
2.3.3	Cepstral features for frog call classification	21
2.3.4	Other features for frog call classification	21
2.4	Classifiers	22
2.5	MIML or ML learning for bioacoustic classification	23
2.6	Experiment results with state-of-the-art methods	24
2.6.1	Evaluation criteria	24
2.6.2	Previous experimental results	25
2.7	Research gap in current literature	25
2.7.1	Database	25
2.7.2	Signal pre-processing	27
2.7.3	Acoustic features	28
2.7.4	Classifiers	28
2.8	Summary	29
3	Frog call classification based on enhanced features and machine learning algorithms	31
3.1	Overview	31

3.2	Architecture of the classification system for frog calls	32
3.2.1	Data description	32
3.2.2	Syllable segmentation based on an adaptive end point detection	32
3.2.3	Pre-processing	35
3.2.4	Feature extraction	37
3.2.5	Classifier description	41
3.3	Experiment results	45
3.3.1	Effects of different machine learning techniques	45
3.3.2	Effects of different feature sets	46
3.3.3	Effects of different window size for MFCCs and perceptual features . .	46
3.3.4	Effects of noise	47
3.4	Discussion	49
3.5	Summary and limitations	49

4 Adaptive frequency scaled wavelet packet decomposition for frog call classification 51

4.1	Overview	51
4.2	Method	52
4.2.1	Sound recording and pre-processing	52
4.2.2	Spectrogram analysis for validation set	53
4.2.3	Syllable segmentation	54
4.2.4	Spectral peak track extraction	56
4.2.5	Syllable SPT features	58
4.2.6	Wavelet packet decomposition	59
4.2.7	WPD based on an adaptive frequency scale	60
4.2.8	Feature extraction based on adaptive frequency scaled WPD	60
4.2.9	Classification	64
4.3	Experiment result and discussion	65
4.3.1	Parameter tuning	65

4.3.2	Feature evaluation	66
4.3.3	Comparison between different feature sets	66
4.3.4	Comparison under different SNRs	70
4.3.5	Feature evaluation using the real world recordings	71
4.4	Summary and limitations	72
5	Multiple-instance multiple-label learning for the classification of frog calls with acoustic event detection	75
5.1	Overview	75
5.2	Materials and methods	76
5.2.1	Materials	76
5.2.2	Signal processing	77
5.2.3	Acoustic event detection for syllable segmentation	77
5.2.4	Feature extraction	81
5.2.5	Multiple-instance multiple-label classifiers	81
5.3	Experiment results	81
5.3.1	Parameter tuning	81
5.3.2	Classification	82
5.4	Discussion	84
5.5	Summary and limitations	85
6	Detecting frog calling activity based on acoustic event detection and multi-label learning	87
6.1	Overview	87
6.2	Materials and methods	88
6.2.1	Acquisition of frog call recordings	88
6.2.2	Frog abundance monitoring	89
6.2.3	Wavelet-based feature extraction for species richness analysis	91

6.2.4	Multi-label classification for species richness analysis	94
6.3	Experiment results	94
6.3.1	Experiment setup	94
6.3.2	Frog abundance detection	95
6.3.3	Frog species richness analysis	95
6.3.4	Comparison with MIML	96
6.3.5	Statistical analysis	97
6.4	Summary and limitations	98
7	Conclusion and future work	99
7.1	Summary of contributions	99
7.2	Limitations and future work	101
A	Waveform, spectrogram and SNR of frog species from David Stewart's CD	103
B	Waveform, spectrogram and SNR of six frog species from JCU recordings	105
C	Power spectral density (PSD) estimate of signal and noise (JCU recordings)	107
D	Confidence interval of signal and noise	109
References		119

List of Figures

1.1	Photos of frogs	2
1.2	An example of a spectrogram of environmental recording	4
1.3	Spectrogram of <i>Litoria caerulea</i>	5
1.4	Flowchart of a frog call classification system	6
1.5	An example of collected recording	8
1.6	Structure of the four main chapters of this thesis	12
2.1	Waveform, spectrum and spectrogram of one frog syllable	18
2.2	Acoustic event detection	22
3.1	Flowchart of frog call classification system using enhanced features	32
3.2	Härmä's segmentation algorithm	34
3.3	Syllable segmentation results	35
3.4	Distribution of syllable number for all frog species	36
3.5	Results of different classifiers	46
3.6	Classification results with different feature sets	47
3.7	Classification results of MFCCs with different window size	47
3.8	Classification results of TemPer with different window size	48
3.9	Sensitivity for different features for different levels of noise contamination	48
4.1	Block diagram of the frog call classification system for wavelet-based feature extraction	52
4.2	Distribution of number of syllables for all frog species	55

4.3	Segmentation results based on bandpass filtering	56
4.4	Spectral peak track extraction results	58
4.5	Adaptive wavelet packet tree for classifying twenty frog species	62
4.6	Description of three feature extraction methods including MFCCs, MWSCCs, and different statistical types of AWSCCs.	62
4.7	The feature vectors for 31 syllables of the single species, <i>Assa darlingtoni</i> . . .	68
4.8	Wavelet packet tree based on adaptive frequency scale for classifying ten and fifteen frog species.	70
4.9	Mel-scaled wavelet packet tree for frog call classification.	70
4.10	Sensitivity of five features for different levels of noise contamination.	71
5.1	Flowchart of a frog call classification system using MIML learning	76
5.2	Acoustic event detection results before (Left) and after (Right) event filtering based on dominant frequency	80
5.3	Acoustic event detection results after region growing	80
6.1	Flowchart of a frog call classification system using multi-label learning	88
6.2	Acoustic event detection for frog abundance monitoring using different methods	92
6.3	Frog abundance detection of different sites	95
6.4	Frog species richness distribution of three selected sites	96
6.5	Averaged frog species richness of different sites.	97

List of Tables

2.1	Summary of related work	19
2.2	A brief summary of classifiers used in previous studies.	23
2.3	Overview of frog call classification performance	26
3.1	Summary of scientific name, common name, and corresponding code	33
3.2	Comparision with previous used feature representations	49
4.1	Parameters of 18 frog species averaged of three randomly selected syllable samples in the commercial recording	53
4.2	Parameters of eight frog species obtained by averaging three randomly selected syllable samples from recordings of James Cook University	54
4.3	Parameters used for spectral peak extraction	57
4.4	Parameter setting for calculating spectral peak track.	66
4.5	Weighted classification accuracy (mean and standard deviation) comparison for five feature sets with two classifiers.	67
4.6	Classification accuracy of five features for the classification of twenty-four frog species using the SVM classifier	69
4.7	Paired statistical analysis of the results in Table 4.6	69
4.8	Classification accuracy (%) for classifying different number of frog species with four feature sets.	70
4.9	Classification accuracy using the JCU recordings.	72
5.1	Accuracy measure for MIML classifiers with different feature representations .	84
5.2	Example predictions with MIML-RBF.	84

6.1	Acoustic parameters of eight frog species averaged for ten randomly selected syllables	89
6.2	Classification results based on four feature sets and four multi-label learning algorithms.	96
A.1	Waveform, spectrogram, and SNR of CD	103
B.1	Waveform, spectrogram, and SNR of JCU recordings	105
C.1	PSD of JCU recordings	107
D.1	Confidence interval for CD recordings	109
D.2	Confidence interval for JCU recordings	109

List of Abbreviations

DFT	Discrete Fourier Transform
DCT	Discrete Cosine Transform
STFT	Short-Time Fourier Transform
LPCs	Linear Predictive Coding
MFCCs	Mel-Frequency Cepstral Coefficients
LDA	Linear Discriminant Analysis
K-NN	K-Nearest Neighbour
SVM	Support Vector Machine
ANN	Artificial Neural Network
RF	Random Forest
AED	Acoustic Event Detection
WPD	Wavelet Packet Decomposition
MIML	Multiple-Instance Multiple-Label
ML	Multiple-Label

Chapter 1

Introduction

1.1 Motivation and background

During the past decades, rapid decreases in frog populations, which are regarded as one of the most critical threats to the global biodiversity, have been spotted from locations around the world. Many environment problems are regarded as the reasons for these declines: disease, habitat destruction and modification, exploitation, pollution, pesticide use, introduced species, and ultraviolet-B radiation (UV-B). On one hand frog populations are declining rapidly worldwide, and on the other, frogs are greatly important to the global ecosystem.

- (1) Frogs are an integral part of the food web
- (2) Frogs are often used as environment indicators
- (3) Frogs are important in medical research that benefits humans

For those aforementioned reasons, increasing frog populations and optimising protection policies necessitates monitoring of frogs. Frogs are often much easier to be heard than to be seen (Figure 1.1). Also frog vocalisations are often employed for most communication; this offers a possible way to study and evaluate frog populations by detecting species-specific calls [Dorcas et al., 2009]. Therefore, frogs are often monitored via their vocalisations. Traditional manual monitoring methods require ecologists and volunteers to spend extensive time in the field for acoustic data collection. Although traditional methods can provide an accurate measure of daytime species and richness, it has a scale limitation in both spatial and temporal domains for this measurement. To address this limitation, recent advances in acoustic sensors provide a

way to automatically survey vocal animals (such as frogs). Deploying acoustic sensors in the field, frog vocalisations can then be automatically collected. Compared with the manual point-counting method, sensors can greatly extend the survey into larger spatial and temporal scales, and generate large volumes of acoustic data that needs to be analysed. Consequently, enabling automatic species identification in acoustic data has become important. However, since the recordings are automatically collected from the field, the audio data tends to be very noisy. Very often the desired signal (frog call) is weak, and there are multiple overlapping signals over the frog call. Furthermore, different frog species tend to call together to make a chorus. All those characteristics pose a big challenge in monitoring frog vocalisations automatically.



Figure 1.1: Photos of frogs to indicate that frogs are difficult to be seen in the field

1.2 Basic concepts

In this section, some basic concepts are given to better describe the research problem and questions, aims and objectives, significance and contributions that are presented in the thesis.

1.2.1 Environmental audio data

The audio data used in this study is mainly derived from two sources: David Stewart's CD [Stewart, 1999] and recordings collected by James Cook University (JCU)¹. David Stewart's CD is employed for the preliminary testing, and used for the experiments in Chapters 3 and 4. Recordings collected by JCU are used for Chapters 5 and 6. The reasons for using those two datasets are listed as follows.

¹All the recordings can be obtained from our group website: <https://www.ecosounds.org/>

- Almost all prior work studied frog recordings with an assumption that only one frog species exists in each individual recording; first, those previous methods are reviewed and a frog call classification system is developed to outperform the state-of-the-art, whereas the CD recordings are used for testing. In this thesis, CD recordings are used in Chapter 3 and 4.
- Compared with the CD recordings, most JCU recordings have multiple simultaneously vocalising frog species, which is in accord with the real environment. Chapters 5 and 6 focus on the investigation of JCU recordings, which is the real situation for most environmental recordings.

Compared with audio data collected in the laboratories and quiet places (such as on David Stewarts CD), environmental recordings are normally collected under unconstrained noisy conditions (such as JCU recordings). Consequently, the noise and variability issues need to be considered when coping with environmental audio data. In terms of the background noise, there are a wide variety of non-biological noises and a variety of animal sounds in the environmental recordings. These non-biological noises often come from different sources: rain, wind, human activities (e.g. traffic noise). Besides non-biological noises, many competitive animal sounds (e.g. birds when we are interested in frogs) are also recorded in the environmental recordings. The signal-to-noise ratio (SNR) of CD recordings and JCU recordings are listed in Table A.1 and Table B.1.

Since the power of signal and background noise in this study varies from recording to recording and call to call within the recording, Table D.1 and Table D.2 (Appendix D) show the confidence intervals of high and low SNR recordings for the power of signal and noise.

In the case of variability, it is produced in many aspects: call structure between species, population of one specific species, time and season changes. All those noises and variabilities make it challenging to develop a robust frog call classification system.

1.2.2 Audio data analysis

Audio data is usually considered as a mono-dimensional signal. To ease the tasks of understanding, comparison, modification, and resynthesis of signals [Rocchesso, 2003], audio data analysis is often developed to find the major features representing the time-varying audio

data. Many application areas of audio data analysis have been identified: speech processing, mechanical signal processing, bioacoustics analysis, etc. The two most important audio data analysis techniques are Short-time Fourier Transform (STFT) and Linear Predictive Coding (LPC). STFT is a Fourier-related transform, which determines the sinusoidal frequency and phase content of local sections of a signal as it changes over time [Allen, 1997]. LPC is mostly used to represent the spectral envelope of audio data based on the information of a linear predictive model [Deng and O'Shaughnessy, 2003]. After STFT, the audio data is transformed into its two dimensional representation (spectrogram), which is widely used for most bioacoustics analysis for its flexible implementation and good applicability. An example of a spectrogram of frog calls derived from a field recording is shown in Figure 1.2.

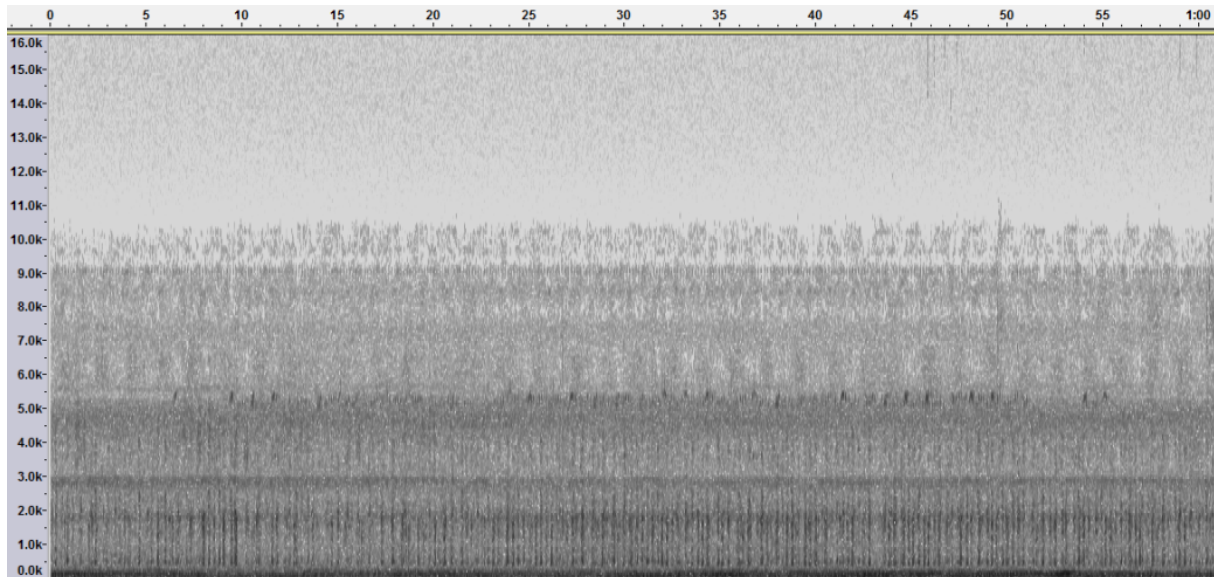


Figure 1.2: An example of spectrogram of environmental recording. The x-axis is time (seconds); the y-axis is frequency (kHz). The spectrogram is generated from a one-minute recording collected in Townsville, Queensland, on around 11.50 pm February 03 2013; the frog species in this recording is *Litoria caerulea*

1.2.3 Frog call structure

In contrast to the hierarchical structure of bird calls, frog calls have a relatively simple call structure [Somervuo et al., 2006]. The frog vocalisation structure mainly has two ingredients: call and syllable. A frog call is normally made up of several frog syllables (Figure 1.3).

One syllable is basically a sound that a frog produces with a single blow of air from the lungs [Huang et al., 2009]. For frog call classification, an elementary unit is one syllable. To get an

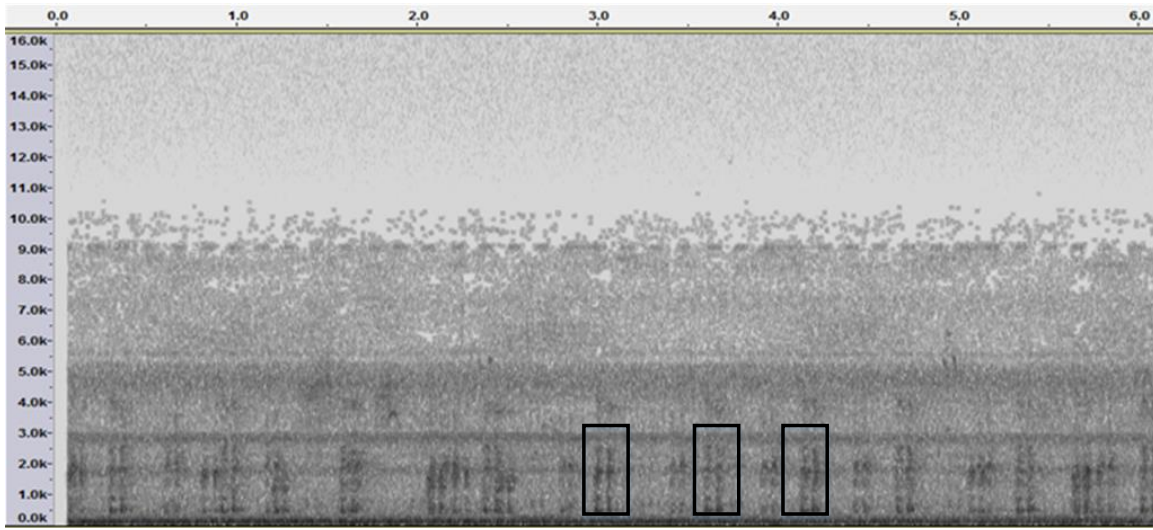


Figure 1.3: Spectrogram of *Litoria caerulea*, three syllable of *Litoria caerulea* are annotated with one black rectangle, respectively.

intuitive sense of the frog call structure, examples of different frog species in both waveform and spectrogram are shown in Table A.1 and Table B.1. For the waveform, x-axis and y-axis represent time and amplitude scales, respectively. The x-axis and y-axis of the spectrogram represent the time and frequency scales, respectively. The grey scale represents the acoustic intensity.

To the best of this researcher's knowledge, no serious research has explored the frequency range of different frog species. So far, Some researchers pointed out that ultrasound can be produced by few frog species [Arch et al., 2008, Narins et al., 2007]. In this research, we focus on those frog species, frequency of which are lower than 8000 Hz.

1.2.4 Acoustic event and background noise

An acoustic event is a localised region of high intensity in a spectrogram. As can be seen from Figure 1.5, there are lots of acoustic events in an one-minute recording. This study focuses on the frog vocalisations, and frog calls are regarded as signals. Consequently, all the other events are called background noise. In this study, both high and low SNR recordings are investigated to build a robust frog call classification system. Most previous studies present the frog call classification system using high SNR recordings. The high SNR recordings often assume that there is only one frog species in each individual recording with few background noises

($SNR \geq 15dB$). In contrast, most low SNR recordings consist of more than one frog species in an individual recording with lots of background noises ($SNR < 15dB$). For the low SNR recordings, Table C.1 shows the power spectral density of signal and noise. It can be seen that the noise in low SNR recordings is often generated by several sources and broadband, which covers different frequency bands and leads to the frequency overlapping between the signal and noise.

1.2.5 Frog call classification

A frog call classification system often consists of four parts (Figure 1.4): (1) signal pre-processing, which includes signal processing and noise reduction; (2) syllable segmentation, which is used to generate a basic classification unit for frog calls; (3) feature extraction; and (4) classification.

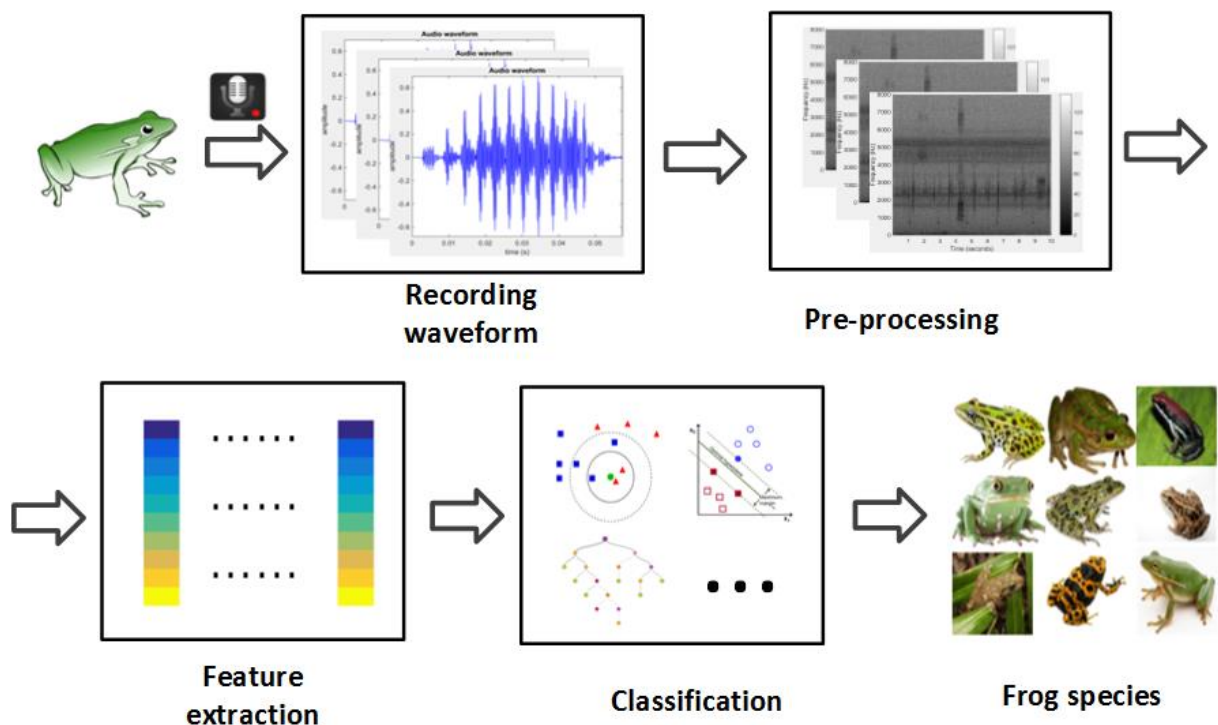


Figure 1.4: Flowchart of a frog call classification system

1.3 Research Challenges

Most datasets used in previous frog call classification studies assume that there is only one frog species in each individual recording. However, these resulting frog calls cannot reflect the characteristics of frog vocalisations in real-world situations, such as background noise, frog

chorus, and other vocalising animals. To develop a robust frog call classification system for environmental recordings, two main challenges have been identified.

Challenge 1: Most previous work studied frog call classification using high SNR recordings, but the classification performance of different studies varied a lot with a relatively low classification accuracy. The first challenge of this thesis is to build an enhanced feature representation to further improve the classification performance using high SNR recordings.

Challenge 2: Since our work finally aims to classify frog calls in low SNR recordings, most features that can successfully classify high SNR recordings cannot perform well for low SNR recordings. Consequently, it is still a big challenge to develop robust acoustic features to classify frog species in low SNR recordings.

Challenge 3: Since most previous work assumed that each individual recording consists of only one frog species, a single-instance single-label (SISL) framework is suitable for classifying frog calls in those high SNR recordings Figure 1.5. However, as low SNR recordings often have different characteristics containing more than one frog species, the SISL framework is no longer suitable. Therefore, the last challenge of this thesis is to design a novel classification framework for studying frog vocalisations in low SNR recordings with overlapping vocalising frog species.

1.4 Research questions

The research questions are developed in order to solve the aforementioned challenges, which can be categorised into three parts.

1. How to improve the classification performance when addressing high SNR recordings?
2. How to develop robust acoustic features to classify frog calls in low SNR recordings?
3. How to employ suitable classification frameworks to classify multiple simultaneous vocalising frog species in low SNR recordings?

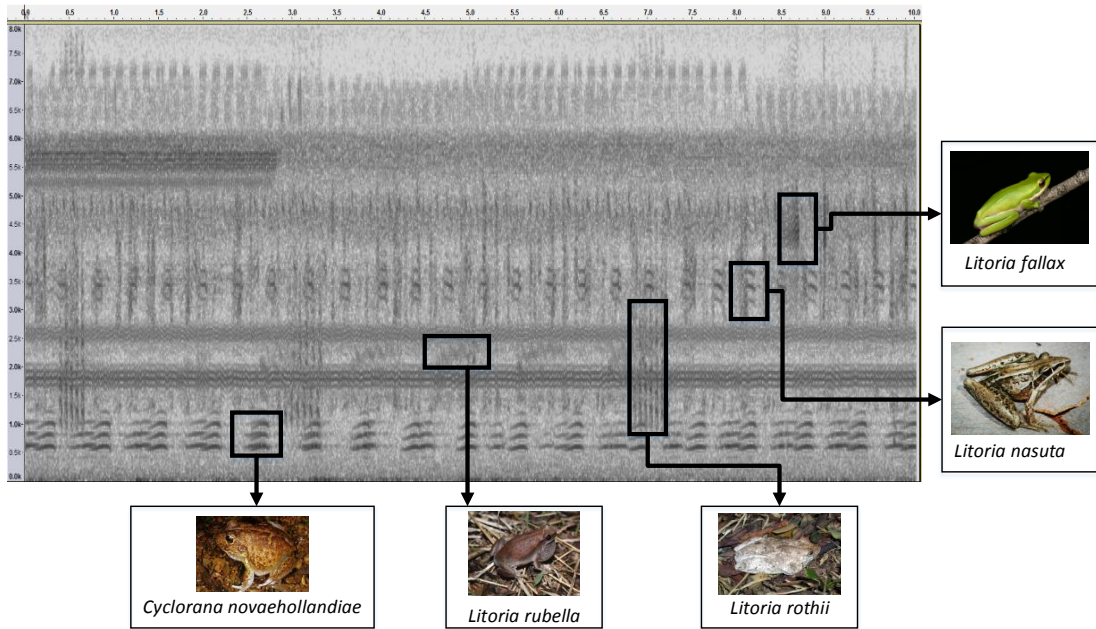


Figure 1.5: An example of collected recording with multiple simultaneously vocalising frog species. Five frog species exist in this 10-second recording: *Cyclorana novaehollandiae*, *Litoria rubella*, *Litoria nasuta*, *Litoria rothii*, and *Litoria fallax*.

1.5 Aims and objectives

This thesis aims to investigate techniques for robust and effective classification of frog species in acoustic data for environmental monitoring. For high SNR recordings, we need to improve the classification performance. As for the low SNR recordings, we plan to design novel frameworks to classify multiple simultaneously vocalising frog species. With our classification results, ecologists can then make decisions on how to protect and improve the health of frog populations. The specific research objectives are listed below.

1. To improve the current representation schemes for modelling frog calls in high SNR recordings
2. To develop robust feature extraction methods for frog call classification in low SNR recordings
3. To investigate machine learning techniques (MIML learning and ML learning) to tackle the frog call classification problem in low SNR recordings

1.6 Significance and contributions

Due to the development of sensor techniques, acoustic sensors have been widely deployed in the field for surveying vocalising animals. Different from recordings collected in the constrained environment, recordings collected in the field often have low SNR and consist of multiple simultaneous vocalising frog species. In this dissertation, firstly the high SNR recordings are investigated to further improve the classification performance of frog recordings with high SNR. Then, those features that can be used for studying frog calls in high SNR recordings are developed or adapted for analysing low SNR recordings for further analysis. Since field recordings often consist of multiple simultaneous vocalising frog species, both MIML and ML learning are used for the classification of those low SNR field recordings. Meanwhile, the frog calling activity can also be monitored based on the MIML and ML classification results. With the frog call classification framework developed, ecologists can then monitor frogs by collecting audio data. This will enable frog monitoring over large areas and long periods of time, and significantly reduce the expert labour cost for monitoring frog calling activity of a particular area. The monitoring result can also help reveal the importance of environmental protection, which can be achieved via studying the correlation between the frog calling activity and weather variables.

Below is a list of the publications arising from this PhD research.

Journal Articles

1. **Xie, Jie**, Towsey, Michael, Zhang, Jinglan, and Roe, Paul (2016) Adaptive frequency scaled wavelet packet decomposition for frog call classification. Ecological Informatics, 32, pp. 134-144.

This work corresponds to Chapter 4 in this thesis, which developed a novel spectral features for frog call classification.

2. Zhang Liang, Towsey Michael, **Xie Jie**, Zhang Jinglan, Roe Paul, Using multi-label classification for acoustic pattern detection and assisting bird species surveys, Applied Acoustics, Volume 110, September 2016, Pages 91-98.
3. **Xie, Jie**, Towsey, Michael, Zhang, Jinglan, and Roe, Paul, Frog call classification: a survey, Artificial Intelligence Review (**Under review**)

This work corresponds to Chapter 2 in this thesis, which reviewed the extant literature on frog call classification.

4. **Xie, Jie**, Towsey, Michael, Zhang, Jinglan, and Roe, Paul, Frog call classification based on enhanced features and machine learning algorithms, *Applied acoustics* (**Under review**)

This work corresponds to Chapter 3 in this thesis, which presented an enhanced feature representation for frog call classification using various machine learning algorithms.

Conference Papers

1. **Xie, Jie**, Towsey, Michael, Zhang, Jinglan, and Roe, Paul, Detecting frog calling activity based on acoustic event detection and multi-label learning, *International Conference on Computational Science* (Accepted)

This work corresponds to Chapter 5 in this thesis, which applied multiple-label learning for frog call classification.

2. **Xie, Jie**, Towsey, Michael, Zhang, Liang, Zhang, Jinglan, and Roe, Paul, Multiple-Instance Multiple-Label Learning for the Classification of Frog Calls With Acoustic Event Detection, *International Conference on Image and Signal Processing* (Accepted)

This work corresponds to Chapter 6 in this thesis, which applied multiple-instance multiple-label learning for frog call classification.

3. **Xie, Jie**, Towsey, Michael, Zhang, Liang, Zhang, Jinglan, and Roe, Paul, Feature Extraction Based on Bandpass Filtering for Frog Call Classification, *International Conference on Image and Signal Processing* (Accepted)

4. **Xie, Jie**, Towsey, Michael, Truskinger, Anthony, Eichinski, Philip, Zhang, Jinglan, and Roe, Paul (2015) Acoustic classification of Australian anurans using syllable features. In 2015 IEEE Tenth International Conference on Intelligent Sensors, Sensor Networks and Information Processing (ISSNIP), IEEE, Singapore, pp. 1-6.

5. **Xie, Jie**, Towsey, Michael, Yasumiba, Kiyomi, Zhang, Jinglan, and Roe, Paul (2015) Detection of anuran calling activity in long field recordings for bio-acoustic monitoring. In 2015 IEEE Tenth International Conference on Intelligent Sensors, Sensor Networks and Information Processing (ISSNIP), IEEE, Singapore, pp. 1-6.

6. **Xie, Jie**, Towsey, Michael, Zhang, Jinglan, and Roe, Paul (2015) Image processing and classification procedure for the analysis of Australian frog vocalisations. In Proceedings of the 2nd International Workshop on Environmental Multimedia Retrieval, ACM, Shanghai, China, pp. 15-20.
7. **Xie, Jie**, Towsey, Michael, Zhang, Jinglan, Dong, Xueyan, and Roe, Paul (2015) Application of image processing techniques for frog call classification. In IEEE International Conference on Image Processing (ICIP 2015), 27-30 September 2015, Quebec City, Canada.
8. **Xie, Jie**, Towsey, Michael, Eichinski, Philip, Zhang, Jinglan, and Roe, Paul (2015) Acoustic feature extraction using perceptual wavelet packet decomposition for frog call classification. In 2015 IEEE 11th International Conference on e-Science (e-Science), IEEE, Munich, Germany, pp. 237-242.
9. **Xie, Jie**, Zhang, Jinglan and Roe, Paul, Discovering acoustic feature extraction and selection algorithms for frog vocalization monitoring with machine learning techniques, 2015 Annual Conference of the Ecological Society of Australia. (Abstract accepted for poster presentation)
10. **Xie, Jie**, Zhang, Jinglan, and Roe, Paul (2015) Acoustic features for hierarchical classification of Australian frog calls. In 10th International Conference on Information, Communications and Signal Processing, 2-4 December 2015, Singapore.
11. Dong, Xueyan, **Xie, Jie**, Towsey, Michael, Zhang, Jinglan, and Roe, Paul (2015) Generalised features for bird vocalisation retrieval in acoustic recordings. In IEEE International Workshop on Multimedia Signal Processing, 19-21 October 2015, Xiamen, China.

1.7 Thesis structure

This thesis is organised in the manner outlined in Figure 1.6

Detailed description of each chapter is shown below:

- Chapter 1 provides a brief introduction to the problem of "Acoustic classification of

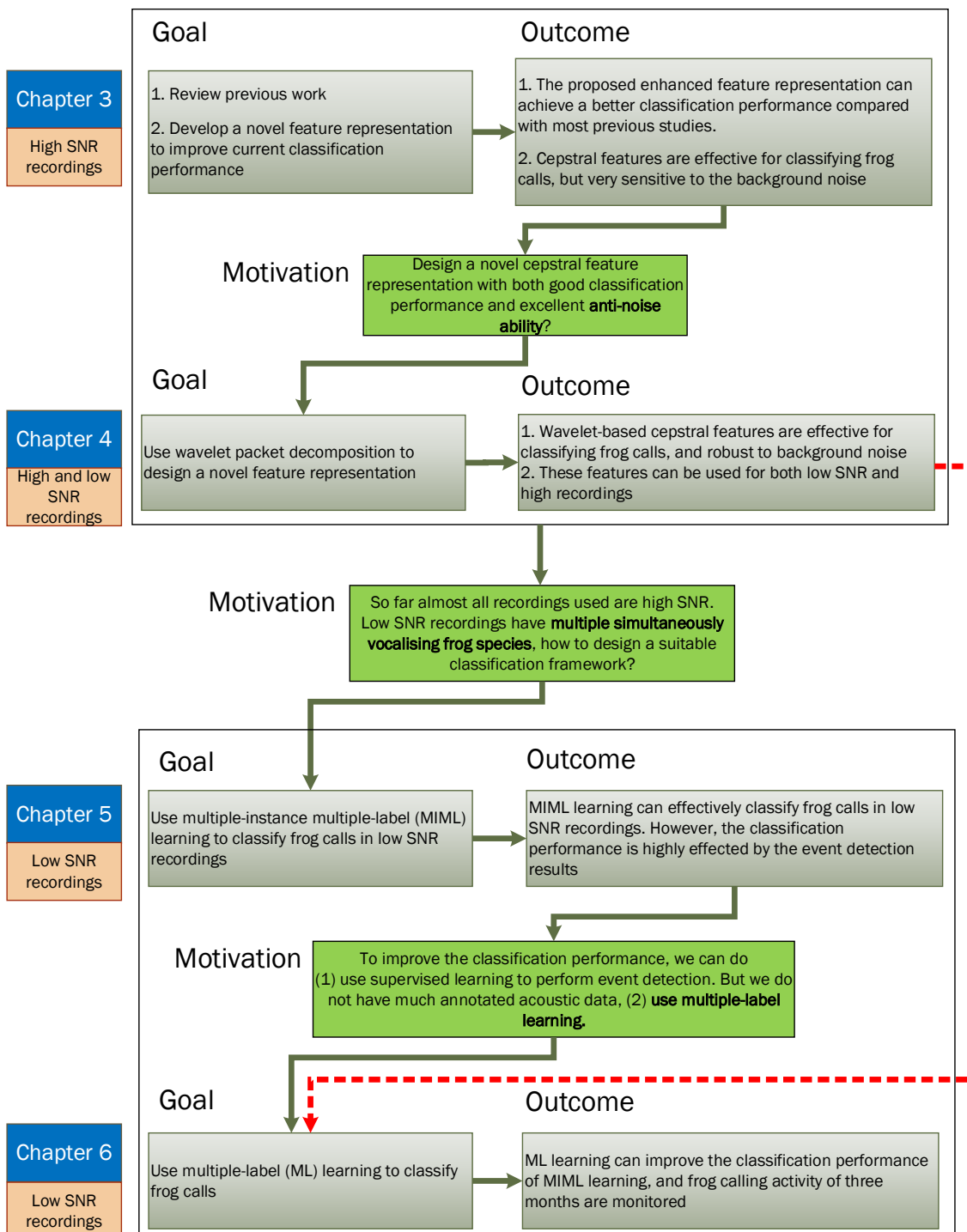


Figure 1.6: Structure of the four main chapters of this thesis

Australian frogs for ecosystem surveys". The background and motivation are first discussed. Then five basic concepts related to frog call classification are presented to lay the foundation for this research: environmental audio data, audio data analysis, frog call structure, acoustic event and background noise, and frog call classification system. Next,

research problems and questions, aims and objectives, significance and contributions are presented based on those five basic concepts. To be specific, there are three main objectives in this thesis. The remaining chapters are organised in the order of addressing those three objectives.

- Chapter 2 reviews the significant and latest literature in the field. The discussion divides the frog call classification system into three parts: signal pre-processing, feature extraction and classification. In addition, there are reviews for evaluation methods and previous experimental results. This chapter intends to provide the reader with a foundation for the research problem and necessary information about the state-of-the-art developments in the field. Furthermore, the research gap in current literature is identified, leading to the direction for the following research.
- Chapter 3 presents an enhanced feature representation for frog call classification in high SNR recordings. An enhanced feature representation is constructed via the combination of temporal, perceptual, and cepstral features. Five machine learning algorithms are evaluated with our proposed feature representation. This chapter aims to (1) review previous features used for frog call classification and develop a better feature representation; (2) explore those previous features and study which can be adapted from high SNR recordings to low SNR recordings.
- Chapter 4 discusses wavelet analysis for frog call classification. According to the conclusion from Chapter 3, it is found that a cepstral feature can achieve higher classification accuracy compared with temporal and perceptual features but it is very sensitive to the background noise. Consequently, in this research, a novel cepstral feature representation has been designed with wavelet packet decomposition that has both high classification performance and a good anti-noise ability. It is because this research will move to low SNR recordings from high SNR recordings, rather than only focusing on the low SNR recordings.
- Chapter 5 discusses the use of multiple-instance multiple-label framework for frog call classification. To cope with low SNR recordings with multiple simultaneously vocalising frog species, the traditional single-instance single-label classification framework is no longer suitable. Therefore, this research tries to adopt other classification frameworks such as MIML learning and ML learning. MIML learning is presented in this chapter. A

MIML classification framework is adopted for studying frogs. Frog syllables are detected using a supervised learning algorithm, which needs lots of annotated data. However, in this study there is a lack of those annotated frog recordings. An unsupervised learning method is developed to segment syllables, which is named *acoustic event detection (AED)*. Then, three MIML learning classifiers are evaluated with extracted features from each syllable after applying a bagging algorithm. The classification performance is highly affected by the results of AED. Although our AED methods achieves better results compared with previous AED methods, the results still need to be further improved.

- Chapter 6 discusses the multiple-label learning method for frog call classification. Since Chapter 5 shows that classification performance is highly affected by the AED results, the AED results still need to be improved. This chapter uses ML learning to study low SNR recordings with multiple simultaneously vocalising frog species, where AED is not necessary for the classification. In contrast, AED is used to predict the frog abundance. The cepstral feature representation proposed in Chapter 4 is used, where a simple but effective method is used to modify it. Both the results of AED and ML classification are applied to field recordings over three months.
- Chapter 7 summarises and concludes the thesis, and identifies the achievements.

Chapter 2

Literature review

This chapter reviews the extant literature on frog call classification. It aims to give a quantitative and detailed analysis of related techniques used in frog call classification. To the best of our knowledge, previous studies have not used multiple-instance multiple-label (MIML) learning or multiple-label (ML) learning for frog call classification, therefore we focus on the studies of single-instance single-label (SISL) classification of frog calls. For MIML and ML learning, some papers that have studied birds are reviewed.

2.1 Overview

Over the past decade, frog biodiversity has rapidly declined because of frogs' sensitivity to habitat loss and degradation, introduced invasive species, and environmental pollution [Dudgen et al., 2006]. On the one hand, frog biodiversity is rapidly declining, and on the other hand frogs are greatly valuable to the environment. Firstly, frogs are an integral part of the food web, and the decline of their population can result in negative impacts through the whole ecosystem. Secondly, frogs are famous indicator species for environment health. Finally, frogs are very useful in medical research that benefits humans¹. The rapid biodiversity decline and great importance of frogs make it necessary for frog biodiversity monitoring to increase.

To monitor the change of frog biodiversity and optimise frog protection policies, many researchers have shown interest in studying frogs. Compared to counting frogs by visual observation, hearing the vocalisations of frogs is much easier. Consequently, frog vocalisations

¹<http://www.savethefrogs.com/why-frogs>

are often used for monitoring frogs. There are two approaches for acoustic frog monitoring. The traditional field survey methods require ecologists to physically visit sites to collect acoustic data, which is both time-consuming and costly. In contrast, recent advances in acoustic sensor techniques have greatly extended the spatio-temporal scale for acoustic monitoring of frog biodiversity [Wimmer et al., 2013]. The large volumes of acoustic data collected this way make it essential to develop new automated methods of analysis.

Over the last few years, many researchers have described automated methods for detecting and classifying frog calls [Camacho et al., 2011, Chen et al., 2012, Gingras and Fitch, 2013, Han et al., 2011, Huang et al., 2014, 2009, 2008]. However, there is no paper that summarises those methods. In this work, we present a comprehensive survey of frog call classification to provide other researchers with basic information, current methods and trends in this field.

Three parts play important roles in the performance and precision of frog call classification: signal pre-processing, feature extraction, and classification. In this survey, these three important parts of frog call classification are presented as shown in Figure 1.4.

Signal pre-processing consists of signal processing, noise reduction and syllable segmentation. Signal processing here denotes changing a signal from one-dimension (audio data) into two-dimensional representation (image). Noise reduction is essential to improve the classification performance. Since the elementary acoustic unit for frog call classification is the syllable, which is a continuous vocalisation emitted by an individual, segmenting continuous recordings of frog calls into individual syllables is necessary.

Previous studies have developed various methods for feature extraction [Camacho et al., 2011, Chen et al., 2012, Gingras and Fitch, 2013, Han et al., 2011, Huang et al., 2014, 2009, 2008]. Here we review and analyse all the used features: time domain and frequency domain features, time-frequency features, cepstral features, and other features. After feature extraction, numerous classifiers have been proposed for frog call classification. A summary of those classifiers is given in section 2.4.

It is worth noting that most previous researchers used different databases for their experiments because frog call research is often related to geographical regions [Jang et al., 2011]. Consequently, there is still a lack of uniformity in the way classification methods are evaluated and assessed. This survey is not meant to compare all previous frog call classification methods and find the best one, but to assemble all the methods in order to provide a direction for the

classification of frog calls. To be specific, this research mainly surveyed different features used for frog call classification because most studies focus on new features rather than new signal processing techniques, syllable segmentation methods, or classifiers.

The remainder of this survey is organised as follows: In section 2.2, signal pre-processing is presented in its three parts: signal processing, noise reduction, and syllable segmentation. In section 2.3, different acoustic features are investigated for frog call classification. In section 2.4, numerous classifiers are studied for frog call classification. In section 2.6, experimental results of state-of-the-art research are discussed. Finally, section 2.7 discusses research gaps and 2.8 sums up this chapter.

2.2 Signal pre-processing

Frog call recordings are often collected using a battery-powered acoustic sensor (stored in a weather proof metal box) with an external microphone. After signal acquisition, signal pre-processing is the first step for a frog call classification system. It often consists of signal processing, noise reduction, and syllable segmentation. The research gap in each part of signal pre-processing is described below.

2.2.1 Signal processing

Signal processing often denotes the transformation of frog calls from one-dimension (recording waveform) to two dimensions (time-frequency representation). Two main techniques used for frog signal processing are short-time Fourier transform (STFT) [Colonna et al., 2015, Huang et al., 2014, 2009, Noda et al., 2016], wavelet packet decomposition [Yen and Fu, 2002], and discrete wavelet transform [Colonna et al., 2012b]. STFT is the most widely used technique among them for its flexible implementation and better applicability. Given one frog call $x(n)$, its fast Fourier transform can be expressed as

$$X(k) = \sum_{n=0}^{L-1} x(n)w(n)e^{-j2\pi kn/L}, 0 \leq k \leq L - 1 \quad (2.1)$$

where $X(k)$ is the frequency domain signal (spectrum) and denotes each frame of the spectrogram, and $w(n)$ is the window function. The waveform, spectrum and spectrogram of one

individual syllable for *Mixophyes fasciolatus* is illustrated in Fig. 2.1. Here three representations are consistent with features in three domains: the time domain, frequency domain and time-frequency domain.

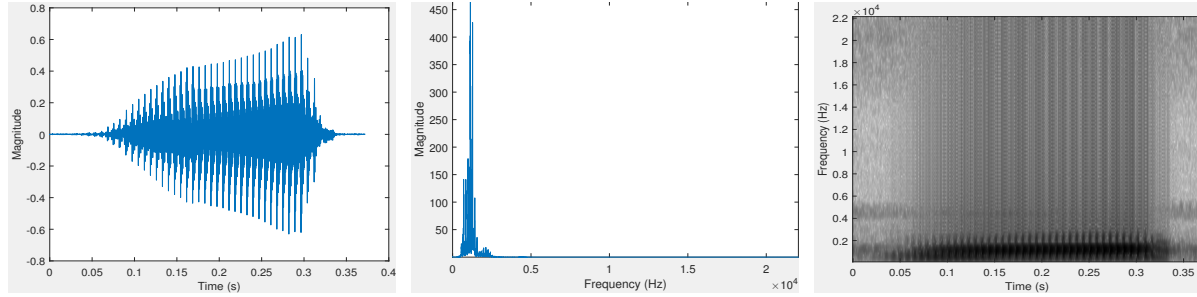


Figure 2.1: Waveform, spectrum and spectrogram of one frog syllable for *Mixophyes fasciolatus*. The window function, size and overlap are Hamming window, 128 samples and 85%, respectively

2.2.2 Noise reduction

Noise reduction is an optional process for frog call classification. Huang et al. [2014] applied a de-noise filter for noise reduction. The wavelet threshold function in the one-dimensional signal was used as the filter kernel function. Bedoya et al. [2014] introduced a spectral noise gating method for noise reduction. Specifically, the selected frequency band spectrum of the frogs' call to be detected was estimated and suppressed. While the aforementioned noise reduction methods can remove some background noise, some of the desired signals will be suppressed. Noise reduction methods are therefore selectively used based on signal-to-noise ratio of the acoustic data and the research problem.

2.2.3 Syllable segmentation

For frog calls, the basic elementary acoustic unit is a syllable, which is a continuous frog vocalisation emitted by an individual frog [Huang et al., 2009]. The precision of syllable segmentation will directly affect the classification performance, since features used for frog call classification are calculated based on each syllable. Frog syllable segmentation methods in previous studies are summarised and listed in Table 2.1. All previous methods cannot address recordings with simultaneous vocalising frog calls. Meanwhile, those methods that used the time domain feature for segmentation, cannot address recordings with low signal-to-noise ratio.

Table 2.1: Summary of related work for frog syllable segmentation. Here, E denotes energy, ZCR denotes zero-crossing rate.

Authors	Features for segmentation	Procedure
Han et al. [2011]	Spectral entropy	Manual
Jaafar and Ramli [2013a]	E and ZCR	Sequential
Huang et al. [2009]	Amplitude	Non-sequential
Chen et al. [2012]	Spectrogram	Non-sequential
Colonna et al. [2015]	Incremental E and Incremental ZCR	Sequential and real time

2.3 Acoustic features for frog call classification

Developing effective acoustic features that show greater variation between rather than within species is important for achieving robust classification results [Fox, 2008]. For frog call classification, acoustic features can be classified into four categories: time domain and frequency domain features, time-frequency domain features, cepstral features, and other features.

2.3.1 Time domain and frequency domain features for frog call classification

Time domain features for frog call classification have been explored for a long time [Camacho et al., 2011, Chen et al., 2012, Dayou et al., 2011, Huang et al., 2014, 2009, 2008]. Time domain features are often combined with frequency domain features for frog call classification.

Huang et al. [2009] used spectral centroid, signal bandwidth, and threshold-crossing rate for frog call classification with a k-nearest neighbour classifier (K-NN) and support vector machines (SVM). In another work, Huang et al. [2014] combined spectral centroid, signal bandwidth, spectral roll-off, threshold-crossing rate, spectral flatness, and average energy to classify frog calls using neural networks. Another paper published by [Huang et al., 2008] used spectral centroid, signal bandwidth, spectral roll-off, and threshold-crossing rate for frog call classification. Dayou et al. [2011] combined Shannon entropy, Rényi entropy and Tsallis entropy for frog call classification. Based on this work, Han et al. [2011] improved the classification accuracy by replacing Tsallis entropy with spectral centroid. To classify anurans into four genera, a three-parameter model was proposed based on advertisement calls,¹ which used mean values for dominant frequency, coefficients of variation of root-mean square energy, and

¹an advertisement call is produced by a male frog in order to attract females during the breeding season and to warn other rival males of his presence.

spectral flux [Gingras and Fitch, 2013]. With this model, three classifiers were employed for classification: K-NN, a multivariate Gaussian distribution model and a Gaussian Mixture Model (GMM) [Gingras and Fitch, 2013]. Chen et al. [2012] proposed a method based on syllable duration and a multi-stage average spectrum for frog call recognition. Their recognition stage was completed by the Euclidean distance-based similarity measure. Camacho et al. [2011] used the loudness, timbre and pitch to detect frogs with a multivariate ANOVA test.

2.3.2 Time-frequency features for frog call classification

For frog call classification, we often transform the one-dimensional signal into its two-dimensional time-frequency representation. Then, features based on the time-frequency representation can be calculated for classification. Acevedo et al. [2009] developed two feature sets for automated animal classification. The first was minimum and maximum frequencies, call duration, and maximum power; the second was minimum and maximum frequencies, call duration, and frequency of maximum power in eight segments of duration. With two feature sets, three classifiers were used for the classification: linear discriminant analysis(LDA), decision tree and SVM. Brandes [2008] proposed a method for classifying animals using duration, maximum frequency, and frequency bandwidth, and with Hidden Markov Model (HMM) used as the classifier. Yen and Fu [2002] combined wavelet packet feature extraction and two different dimensionality reduction algorithms to produce the final feature vectors. Then, they adopted a neural network classifier for classification. Grigg et al. [1996] developed a system to monitor the effect of the introduced Cane Toad on the frog population of Queensland. The classification was based on the local peaks in the spectrogram using Quinlan's machine learning system, C4.5. Brandes et al. [2006] proposed a method to classify frogs using central frequency, duration, and bandwidth with a Bayesian classifier. Croker and Kottege [2012] introduced a feature vector for detecting frogs with a similarity measure based on Euclidean distance. The feature vector consisted of dominant frequency, frequency difference between the lowest and dominant frequencies, frequency difference between the highest and dominant frequencies, time from the start of the sound to the peak volume, and time from the peak volume to the end of the sound.

2.3.3 Cepstral features for frog call classification

Cepstral features are also popular for frog call classification. These features include Linear Prediction Coefficients (LPCs) and Mel-frequency cepstral coefficients (MFCCs). Colombia and del Cauca [2009] introduced LPCs for frog call classification with a modified K-Means classifier. Jaafar et al. [2013a] introduced MFCCs and LPCs as features, and K-NN and SVM as classifiers for frog call identification. Yuan and Ramli [2012] also used MFCCs and LPCs as features, and K-NN as the classifier for frog sound identification. Lee et al. [2006] used the averaged MFCCs and LDA for the automatic recognition of animal sounds. Bedoya et al. [2014] combined MFCCs and a learning algorithm for multivariate data analysis (LAMDA) for frog call recognition. Vaca-Castano and Rodriguez [2010] proposed a method to identify animal species, which consisted of MFCCs, principal component analysis (PCA) and K-NN. Jaafar and Ramli [2013a], Jaafar et al. [2013b], Tan et al. [2014] published three papers about frog call classification with MFCCs, Δ MFCC and $\Delta\Delta$ MFCC calculated as features, and K-NN and SVM used as classifiers. Colonna et al. [2012a] introduced MFCCs for classifying anurans with a K-NN classifier. Noda et al. [2016] fused time domain features with cepstral features for frog call classification which achieved a better classification performance than using only cepstral features. Three classifiers were investigated for the classification: HMM, random forest, and SVM.

2.3.4 Other features for frog call classification

Besides time domain features, frequency domain features, time-frequency domain features and cepstral features, other features are also introduced to classify frog calls. Wei et al. [2012] proposed a distributed sparse approximation method based on ℓ_1 minimization for frog call classification. Dang et al. [2008] extracted the vocalisation waveform envelope as features, then classified calls by matching the extracted envelope with the original signal envelope. Kular et al. [2015] treated the sound signal of a frog call as a texture image. Then, texture visual words and MFCCs were calculated as the features for frog call classification.

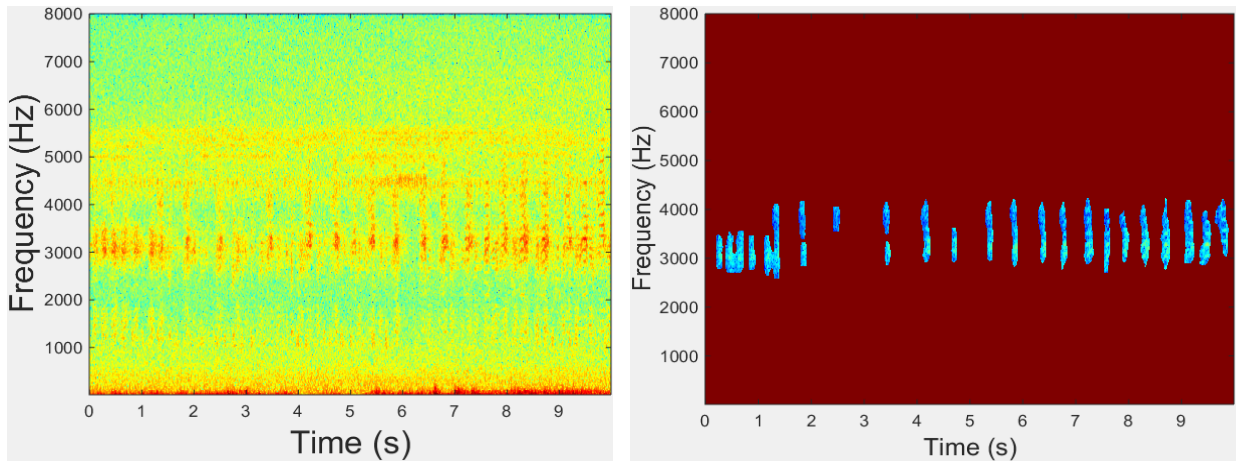


Figure 2.2: Original spectrogram and segmented events after applying acoustic event detection to the original spectrogram image.

2.4 Classifiers

For frog call classification, numerous pattern recognition methods have been used to construct the classifier, such as the Bayesian classifier [Brandes et al., 2006], k-nearest neighbour classifier (K-NN) [Colonna et al., 2012a, Dayou et al., 2011, Gingras and Fitch, 2013, Han et al., 2011, Huang et al., 2009, 2008, Jaafar and Ramli, 2013a, Jaafar et al., 2013a,b, Vaca-Castano and Rodriguez, 2010, Yuan and Ramli, 2012], support vector machine (SVM) [Acevedo et al., 2009, Gingras and Fitch, 2013, Huang et al., 2009, 2008, Jaafar et al., 2013a, Tan et al., 2014], hidden Markov model (HMM) [Brandes, 2008], Gaussian mixture model (GMM) [Gingras and Fitch, 2013, Huang et al., 2008], neural networks (NN) [Huang et al., 2014, Yen and Fu, 2002], decision tree (DT) [Acevedo et al., 2009, Grigg et al., 1996], one-way multivariate ANOVA [Camacho et al., 2011], and linear discriminant analysis (LDA) [Acevedo et al., 2009, Lee et al., 2006]. Besides classifiers, other methods for classifying frog species include those based on the similarity measure [Chen et al., 2012, Croker and Kottege, 2012, Dang et al., 2008] and those based on the clustering technique [Bedoya et al., 2014, Colombia and del Cauca, 2009, Wei et al., 2012]. The summary of those classifiers used in frog call classification is listed in Table 2.2. K-NN is the most commonly used classifier for its simplicity and easy application. However, the K-NN classifier is sensitive to the local structure of the data, as well as to the initial cluster centroids. Therefore, the K-NN classifier is often run multiple times based on different initial points. SVM is another classifier that is widely used for its good generalisation ability. However, the performance of SVM can be quite sensitive to the selection of the regularisation and kernel parameters, and it is possible to over-fit when tuning these

hyper-parameters. Therefore, selecting suitable parameters for SVM is very important and is realised by grid search in most previous studies [Hsu et al., 2003].

Table 2.2: A brief summary of classifiers used in previous studies.

Reference	Classifier	Reference	Classifier
Brandes et al. [2006]	Bayesian classifier	Acevedo et al. [2009]	Support vector machine
Huang et al. [2008]	K-nearest neighbour	Huang et al. [2009]	Support vector machine
Huang et al. [2009]	K-nearest neighbour	Tan et al. [2014]	Support vector machine
Han et al. [2011]	K-nearest neighbour	Gingras and Fitch [2013]	Support vector machine
Dayou et al. [2011]	K-nearest neighbour	Jaafar et al. [2013a]	Support vector machine
Jaafar and Ramli [2013a]	K-nearest neighbour	Gingras and Fitch [2013]	K-nearest neighbour
Brandes [2008]	Hidden Markov model	Jaafar et al. [2013b]	K-nearest neighbour
Huang et al. [2008]	Gaussian mixture model	Jaafar et al. [2013a]	K-nearest neighbour
Gingras and Fitch [2013]	Gaussian mixture model	Yuan and Ramli [2012]	K-nearest neighbour
Huang et al. [2014]	Neural networks	Vaca-Castano and Rodriguez [2010]	K-nearest neighbour
Yen and Fu [2002]	Neural networks	Grigg et al. [1996]	Decision tree
Acevedo et al. [2009]	Decision tree	Camacho et al. [2011]	One-way multivariate ANOVA
Colonna et al. [2012a]	K-nearest neighbour	Acevedo et al. [2009]	Linear discriminant analysis
Huang et al. [2008]	Support vector machine	Lee et al. [2006]	Linear discriminant analysis

2.5 MIML or ML learning for bioacoustic classification

To the best of this research's knowledge, there is still no paper that uses MIML or ML learning to focus on frog call classification. In contrast, some previous research has applied MIML or ML learning to study bird calls.

For MIML learning, [Briggs et al., 2012] introduced the MIML classifiers for acoustic classification of multiple simultaneous bird species. In their method, a supervised learning classifier (random forest) was first employed for segmenting acoustic events. Then features were extracted from each segmented acoustic event. Before putting features into classifiers, a bag generator was used to construct a bag-level feature. Lastly, three MIML classifiers were experimentally evaluated: MIML-SVM (support vector machines Based Multi-Instance Multi-Label Learning Algorithm), MIML-RBF(MIML Radial Basis Function), and MIML-kNN (k-Nearest Neighbor Based Multi-Instance Multi-Label Learning Algorithm). [Dufour et al., 2013] used Mel-filter cepstral coefficients and three MIML classifiers to classify birds. To be specific, Mel-filter cepstral coefficients were first calculated for each frame. Then two new feature vectors were computed to represent longer segments. Lastly, three MIML classifiers were experimentally evaluated: MIML-RBF, MIML-kNN, and M3MIML (Maximum Margin Method for Multi-instance Multi-label Learning).

For ML learning, several papers have been published in the Neural Information Processing Scaled for Bioacoustics (NIPS4B challenge), which classified birds, insects, and amphibians recordings, followed by pre-processing and segmentation, feature extraction, feature selection, and classification [Chen et al., 2013, Lasseck, 2013, Massaron, 2013, Mencia et al., 2013, Stowell and Plumbley, 2013]. [Lasseck, 2013] first pre-processed the recordings via the application of short-time Fourier transform, noise reduction and segmentation. Then, file-Statistics, segment-Statistics and segment-Probabilities are calculated as the features. Finally, for each sound class an ensemble of randomised decision trees is applied for the classification. [Stowell and Plumbley, 2013] used either MFCC statistics (52 dimensions), chirplet histograms (up to 20,000 dimensions), or both, as the features. Then, Random Forests was applied for multi-label classification. [Mencia et al., 2013] proposed an new feature extraction method via an unsupervised generation of an aleatory number of features, which included random patching, a Denoising Autoencoder unit and subsequent convolution. For the classification, a pairwise ensemble of SVMs, random decision trees and a single layer neural network were used. [Massaron, 2013] described an approach that involved building an ensemble of generalised linear models and a classification model by hinge loss and program based on stochastic gradient descent optimisation, and boosted trees ensembles. [Chen et al., 2013] first calculated prominent features from windowing MFCCs with overlap, and leveraged them to build an ensemble classifier which was a blend of different classifiers (Gradient Boosting Tree models, Random Forest models, Lasso and elastic-net regularized generalised linear model .etc).

2.6 Experiment results with state-of-the-art methods

2.6.1 Evaluation criteria

Accuracy is the most widely used statistical criterion for evaluating frog call classification. Other evaluation criteria such as precision, recall, sensitivity, specificity, F-measure, and ROC curves are also used. Before defining these evaluation criteria, we first define true positives (TP), true negatives (TN), false negatives (FN), and false positives (FP) as described by [Gordon et al., 2003] (1) TP: correctly recognised positives; (2) TN: correctly recognised negatives; (3) FN: positives recognised as negatives; (4) FP: negatives recognised as positives. Then, accuracy, precision, recall (sensitivity), and specificity can be defined as follows.

$$Accuracy = \frac{TP + TN}{TP + TN + FP + FN} \quad (2.2)$$

$$Precision = \frac{TP}{TP + FP} \quad (2.3)$$

$$Recall = \frac{TP}{TP + FN} \quad (2.4)$$

$$Specificity = \frac{TN}{FP + TN} \quad (2.5)$$

2.6.2 Previous experimental results

Table 2.3 shows the list of summarised frog call classification methods, together with the database they used and corresponding performance. From Table 2.3, we can find that few studies explored frog vocalisations using signal processing and machine learning techniques before 2010. Due to the decrease of frog biodiversity, advances in signal processing, machine learning techniques and acoustic sensors, the research in frogs has been increased in the last five years. In addition, few datasets are publicly shared with researchers. The classification performance of different studies varies a lot. One of the main reasons is the use of different datasets.

2.7 Research gap in current literature

In this section, the research gap of each part of a frog call classification system is discussed to give a direction for future work.

2.7.1 Database

One major problem for frog call classification is the lack of a universal database. The databases used are often related to geographical regions, since researchers from different countries focus on particular frog species in their specific area (Table 2.3). Therefore, it is difficult for

Table 2.3: A brief overview of frog call classification performance. The asterisk denotes that frog species are not the only animal species to be studied.

Database	Performance	Reference	Data source
3 frog species with 635 calls	Precision of 99%, recall of 92% Sensitivity of 0.85 with specificity of 0.92 when distinguishing <i>Miophytes literatus</i> calls from other species' call. Sensitivity of 0.88 with specificity of 0.82 against background noise	Camacho et al. [2011]	Collected from Costa Rica (unavailable)
1 frog species with 100 samples	50% true positive accuracy. over 50 false-negative for 4 animal types	Croker and Kotige [2012]	Recorded next to a running stream (unavailable)
17 animal types	NA	Brandoes et al. [2006]	Collected from NE Costa Rica (unavailable)
22 frog species	Best performance with averaged classification Accuracy of 72.18% and 0.76% for standard deviation.	Grigg et al. [1996]	Collected from Queensland, Australia (unavailable)
4 frog species with 66 samples	Accuracy of 88% for frogs	Yen and Fu [2002]	Unknown
10 frog species, 9 bird species, and 8 cricket species	Best true positive rate of 94.95% and 0.94% for false positive rate	Brandoes [2008]*	Collected from NE Costa Rica (unavailable)
9 frog species and 3 bird species with 10061 samples	Averaged classification accuracy of 90.00%	Acevedo et al. [2009]*	Collected from 14 montane sites in Puerto Rico
9 frog species with 90 syllables	Averaged classification accuracy of 98.00%	Dayou et al. [2011]	Obtained from http://www.Frogsaustralia.net.au/frogs
9 frog species with 54 syllables	Averaged classification accuracy of 95.86%	Han et al. [2011]	Obtained from http://www.Frogsaustralia.net.au/frogs
5 frog species with 727 syllables	Averaged classification accuracy of 95.86%	Huang et al. [2008]	Unknown
142 species belonging to four genera	Genus classification accuracy above 70%	Gingras and Fitch [2013]	obtained from commercially available compact discs (CDs) (available)
18 frog species with 960 syllables	Classification accuracy of 94.3%	Chen et al. [2012]	Recorded in a wild field located in the Shan-Ping forest ecological garden in Kaohsiung city, Taiwan (unavailable)
13 frog species with 1514 samples	Averaged recognition rate of 93.4%	Huang et al. [2014]	Unknown
5 frog species with 959 samples	Averaged classification accuracy of 90.03%	Huang et al. [2009]	Unknown
15 frog species with 286 samples	Averaged classification accuracy of 95.67%	Tan et al. [2014]	recorded at Sungai Sedim, in Kulim, Kedah, Malaysia
8 frog species with 160 samples	Averaged classification accuracy of 98.1%	Yuan and Ramli [2012]	Obtained from AmphibiaWeb (http://amphibiaweb.org/) (available)
10 frog species with 250 syllables	Averaged classification accuracy of 98.8%	Jaaifar et al. [2013a]	Internet database (http://learning.frogtheme.org/)
15 frog species with 386 syllables	Averaged classification accuracy of 85.78%	Jaaifar et al. [2013b]	IBM USM (http://www.frogwatch.org.au/?action=animalList) (available)
12 frog species with 291 syllables	Averaged classification accuracy of 97%	Jaaifar and Ramli [2013a]	Recorded from locations around Baling and Kulim, Kedah, Malaysia (unavailable)
12 frog species with 379 samples,	Averaged classification accuracy of 97%		Recorded from locations around Baling and Kulim, Kedah, Malaysia (unavailable)
10 bird species with 193 samples	Averaged classification accuracy of 86.6%	Vaca-Castano and Rodriguez [2010]	Recorded in Puerto Rico (http://www.amazon.com/Los-Anfibios-Reptiles-Puerto-Rico/dp/084770243X) (available)
13 frog species with 916 calls	Averaged classification accuracy of 100%, and 99.61% respectively for two database	Bedoya et al. [2014]	Provided by the Smithsonian Tropical Research Institute (STRI) and the Grupo Herpetológico de Antioquia (GHA) (unavailable)
30 frog species and 19 cricket calls	Averaged classification accuracy of 96.8% and 98.1%	Lee et al. [2006]	Derived from compact disk (unavailable)
15 frog species with 896 syllables	Precision of 99.00%	Coloma et al. [2015]	Obtained from Internet(http://bit.ly/1b8byE) (available)
10 frog species with 516 syllables	Averaged classification accuracy of 97.45%	Xie et al. [2013a]	Collected from compact disk (http://www.naturesound.com.au/) (available)
15 frog species with 436 syllables	Averaged classification accuracy of 74.73%	Xie et al. [2015c]	Collected from compact disk (http://www.naturesound.com.au/) (available)
9 frog species with 49 samples	Averaged classification accuracy of 97.60%	Coloma et al. [2012a]	Collected on the campus of the Federal University of Amazonas in Manaus, Brazil (unavailable)
3 frog species with 50 samples	Averaged classification accuracy of 90%	Dang et al. [2008]	Unknown
1564 syllables of 41 anurans,	98.8%, 96.9%, 95.48%, and 95.38% respectively	Noda et al. [2016]	AmphibiaWeb(41 anurans), 58 frogs from Cuba, 100 anurans from Brizil-Uruguay, and 199 anurans from all datasets (http://www.nihbs.com/) (available)
5201 syllables of 58 frogs,			
10905 syllables of 100 anurans,			
and 17671 syllables of 199 anurans			

researchers to compare their particular classification methods. Current studies often focus on the study of limited number of frog species (less than 100), but the number of known amphibian species is above 7000. To reach a high quality resolution, there still is a long way to go.

2.7.2 Signal pre-processing

Currently, short-time Fourier transform (STFT) is the most widely used technique for frog call classification. However, STFT has a trade-off between time and frequency resolution, which restricts the discriminability of features extracted from the spectrogram. In contrast, wavelet packet decomposition (WPD) has a better frequency domain resolution than STFT. The main disadvantage of WPD is the time dependence.

Noise reduction is an optional processing step in frog call classification. For some databases of studies shown in Table 2.3, frog calls have a high signal-to-noise ratio (SNR), where noise reduction is unnecessary. However, when studying recordings of low SNR, noise reduction is essential for improving the classification performance [Bedoya et al., 2014, Huang et al., 2014]. After noise reduction, both the accuracy of syllable segmentation and feature extraction can be relatively improved.

Frog syllable segmentation based on energy and zero-crossing rate cannot address recordings with low SNR. Meanwhile, this method cannot segment recordings with overlapping frog calls. Recent use of unsupervised learning algorithms opens a path for segmenting overlapping frog syllables with image processing techniques. However, like other unsupervised algorithms, this method has the disadvantage that not all segmented syllables are frog vocalisations [Potamitis, 2015]. Briggs et al used a supervised learning algorithm (Random Forest) for bird call segmentation. However, this method required lots of tagged acoustic data to train the classifier [Tjahja et al., 2015].

For syllable segmentation, time domain features are more sensitive to background noise than frequency domain features, because different frequency components can be separated by transforming the signal from time domain to frequency domain. But time domain features cannot segment those overlapping frog syllables, since time domain features have no ability to separate different frequency components. Compared to time domain features, the use of amplitude-frequency information provides a robust method to segment low SNR recordings. To address those overlapping frog syllables, image processing techniques can be a possible solution.

2.7.3 Acoustic features

Most previous studies directly transplant features developed for speech recognition to analyse frog calls, which might not be suitable. For example, MFCCs, which are based on the calculation of a non-linear Mel-scale, are designed for studying speech. However, the Mel-scale is designed for the perceptual scale of pitches judged by listeners rather than frogs. The direct use of speech features will therefore restrict classification performance.

Most frequency domain features are calculated by directly calculating the statistics over frames, which leads to the loss of temporal information. To add the temporal information of the feature set, time domain features can be combined with frequency domain features to achieve higher classification accuracy. Transforming audio data into its two-dimensional representation (such as a spectrogram) for quick visual analysis, has led to increasing attention being given to image processing techniques for automatically analysing animal calls. Image features are worth investigating for frog call classification. Sparse coding has been widely applied for feature extraction in other scaled bioacoustics studies [Glotin et al., 2013, Razik et al., 2015], which could be a potential direction for frog call classification.

2.7.4 Classifiers

Almost all previous studies assume that each recording has only one frog species, and then an SISL classification framework is adopted to classify frog calls. However, recent advances in acoustic sensor techniques have collected large volumes of acoustic data that have multiple simultaneously vocalising frog species, because different frog species tend to call together to make a frog chorus (Figure 1.5). Based on this characteristic of frog call recordings, the classification problem can be naturally framed as an MIML classification or an ML classification problem rather than an SISL classification. In previous studies, MIML learning and ML learning have been used to solve bioacoustic problems, but mainly focus on birds. In this thesis, MIML and ML learning will be investigated to study frog vocalisations.

2.8 Summary

The main objective of this survey is to provide a research direction for analysing acoustic signals, especially frog calls. With the use of signal processing and machine learning techniques, different frog species can be classified based on their vocalisations. To achieve this goal, three main parts of a frog call classification system are explained: signal pre-processing, feature extraction, and classification. For each part, current techniques used by different researchers are explored. For signal pre-processing, signal processing, noise reduction, and syllable segmentation are studied respectively. For feature extraction, acoustic features in different domains are explored. For classification, different single-instance single-label classifiers are investigated.

In general, frog call classification is still in its infancy as a field of study, and potential applications and unsolved problems are extending every day. For future work, it is worth further improving the accuracy and efficiency of noise reduction and syllable segmentation because they are critical processes for frog call classification. Since collected frog calls in the field often contain many background noises (birds, insects, rain, wind, human voices, etc.), it is necessary to design new noise reduction methods based on different environments. It is also necessary to develop accurate and efficient methods for syllable segmentation for its great influence in the frog call classification system performance. Currently, studies have focused on frequency domain features for classification. In the future, time domain features can be more incorporated for increasing the accuracy of frog call classification. For the classification frameworks, using MIML learning or ML learning for studying environmental recordings may be a productive research direction because of the characteristic of collected acoustic data. It is also worth making a uniform dataset that covers different frog species from different areas, since there is still no available uniform dataset of frog calls. Then researchers can evaluate their particular methods on a uniform platform.

Chapter 3

Frog call classification based on enhanced features and machine learning algorithms

3.1 Overview

This chapter presents an enhanced feature representation for frog call classification using various machine learning algorithms and explores whether a combination of three types of features discriminate a wider variety of species that may share similar characteristics in either temporal, perceptual or cepstral information but not all. In the literature, various feature representations have been developed for frog call classification. However, most features used in the prior work are based on either temporal features such as averaged energy and zero-crossing rate, perceptual features such spectral centroid and spectral flux, or cepstral features such as MFCCs.

This chapter aims to compare various feature representations with different machine learning techniques. Based on the classification performance, suggested features can then be adapted to study low-SNR recordings. This chapter directly addresses sub-research question (1): How to improve the classification performance when addressing high SNR recordings, and which of those features can be adapted from high SNR recordings to low SNR recordings?

The performance of the proposed method is evaluated based on twenty-four frog species, which are geographically well distributed through Queensland, Australia. Five feature representations are compared via five machine learning algorithms. Classification results demonstrate that a combination of temporal, spectral and cepstral features can achieve the best performance.

Compared with temporal and spectral features, cepstral features can achieve a robust classification accuracy, but are sensitive to the background noise. Therefore, in the next chapter, we aim to develop robust cepstral features that are not sensitive to the background noise.

3.2 Architecture of the classification system for frog calls

Our frog call classification system consists of six steps (Figure 3.1): data description, syllable segmentation, pre-processing, feature extraction, feature fusion, and classification. Detailed information of each step is shown in following subsections. Different from [Huang et al., 2009], pre-processing is directly applied to the segmented syllables rather than continuous recordings.

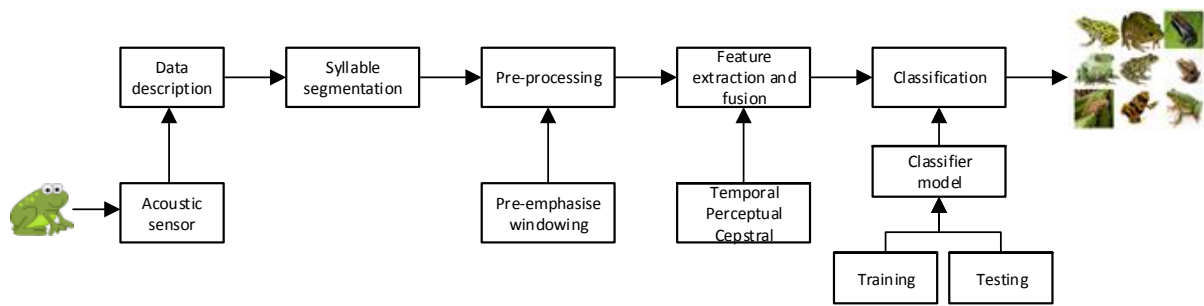


Figure 3.1: Flowchart of frog call classification system using enhanced features

3.2.1 Data description

In this study, twenty-four frog species, which are widespread in Queensland, Australia, are selected for experiments (Table 3.1). All the recordings are obtained from David Stewart's CD with a sample rate of 44.10 kHz and saved in MP3 format [Stewart, 1999]. Each recording includes one frog species with the duration ranging from eight to fifty-five seconds.

3.2.2 Syllable segmentation based on an adaptive end point detection

Each recording is made up of multiple continuous calls of one frog species. For frogs, one syllable is an elementary acoustic unit for classification, which is a continuous frog vocalisation emitted from an individual [Huang et al., 2009]. In this chapter, one method built on the Härmä's method is used to perform syllable segmentation for frog calls [Harma, 2003]. The syllable segmentation process is based on the spectrogram, which is generated by applying

Table 3.1: Summary of scientific name, common name, and corresponding code. Frog species name with asterisk means that it needs to be smoothed before segmentation

No.	Scientific-name	Common-name	Code
1	<i>Assa darlingtoni</i>	Pouched frog	ADI
2	<i>Crinia parinsignifera</i>	Eastern sign-bearing froglet	CPA
3	<i>Crinia signifera</i>	Common eastern froglet	CSA
4	<i>Limnodynastes convexiusculus</i>	Marbled frog	LCS
5	<i>Limnodynastes ornatus</i>	Ornate burrowing frog	LOS
6	<i>Limnodynastes tasmaniensis</i> *	Spotted grass frog	LTS
7	<i>Limnodynastes terraereginae</i>	Northern banjo frog	LTE
8	<i>Litoria caerulea</i>	Australian green tree frog	LCA
9	<i>Litoria chloris</i>	Red-eyed tree frog	LCS
10	<i>Litoria latopalmata</i>	Broad-palmed frog	LLA
11	<i>Litoria nasuta</i>	Striped rocket frog	LNA
12	<i>Litoria revelata</i>	Revealed tree frog	LEA
13	<i>Litoria rubella</i>	Desert tree frog	LRA
14	<i>Litoria tyleri</i>	Southern laughing tree frog	LTI
15	<i>Litoria verreauxii verreauxii</i>	Whistling tree frog	LVI
16	<i>Mixophyes fasciolatus</i>	Great barred frog	MFS
17	<i>Mixophyes fleayi</i>	Fleay's barred Frog	MFI
18	<i>Neobatrachus sudelli</i> *	Painted burrowing frog	NSI
19	<i>Philoria kundagungan</i>	Mountain frog	PKN
20	<i>Philoria sphagnicolus</i> *	Sphagnum frog	PSS
21	<i>Pseudophryne coriacea</i>	Red-backed toadlet	PCA
22	<i>Pseudophryne raveni</i> *	Copper-backed brood frog	PRI
23	<i>Uperoleia fusca</i> *	Dusky toadlet	UFA
24	<i>Uperoleia laevigata</i>	Smooth toadlet	ULA

short-time Fourier transform (STFT) to each recording. For STFT, the window function used is Hamming window with the size and overlap being 512 samples and 25%, respectively. The detail of the segmentation method is described in Figure 3.2, which is based on the iterative frequency-amplitude information of the spectrogram. This chapter focuses on the evaluation of fused features, but the accuracy of segmentation results can greatly affect the classification performance. To reduce the bias introduced by syllable segmentation, the segmented syllables are further filtered. First, those syllables whose length are smaller than 300 samples are removed. Then, those syllables whose averaged energy are smaller than 15% of the maximum energy and larger than 1.5 times the averaged energy are removed for each frog species experimentally

[Gingras and Fitch, 2013].

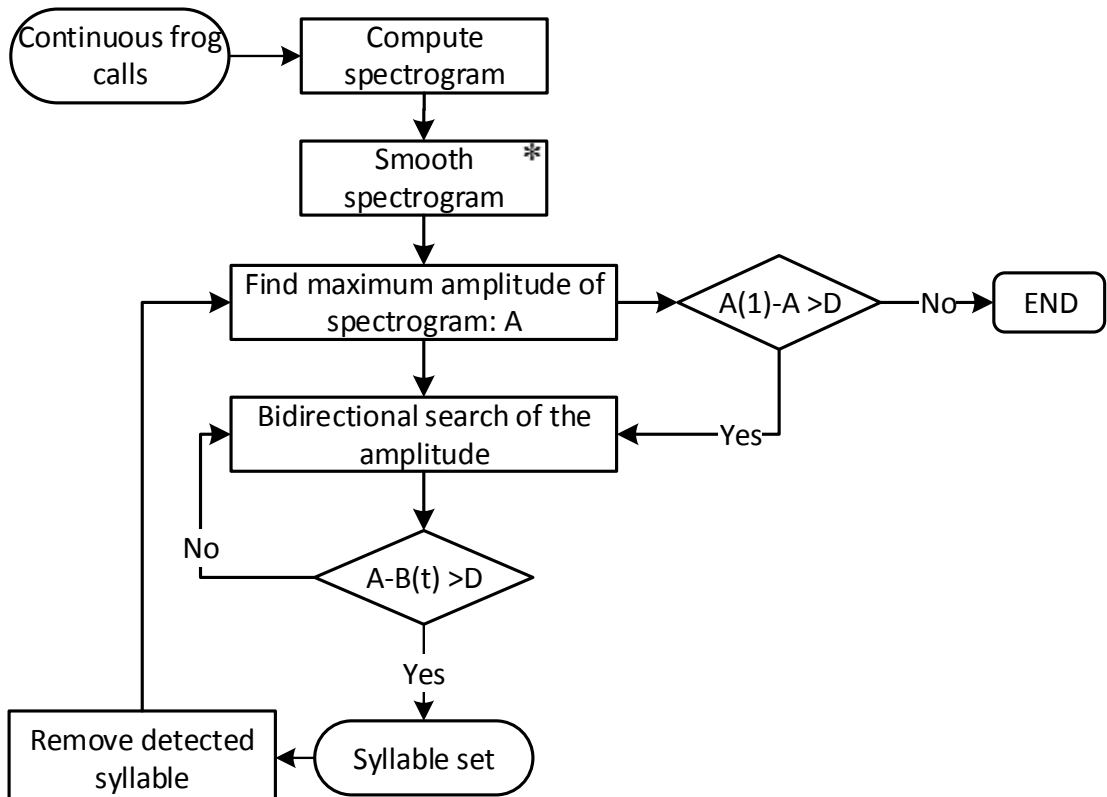


Figure 3.2: Segmentation method based on Härmä's algorithm. Here, D is the amplitude threshold for stopping criteria which is set at 20 dB experimentally, and the segmentation result is sensitive with this value. A is the maximum amplitude value of the spectrogram and we save the first maximum amplitude as $A(1)$, $B(t)$ is the amplitude of frame t . An asterisk denotes the optional processing step.

In this study, smoothing spectrogram is optionally applied to the spectrogram before the Härmä's algorithm, because some frog species have a large temporal gap within one syllable (see in Figure 3.3). As for the smoothing, a Gaussian filter (7×7) is applied to the spectrogram, where the size is set, taking into account a trade-off between connecting gaps within one syllable and separating adjacent syllables. The segmentation result after smoothing is shown in Figure 3.3. The distribution of syllable numbers after segmentation for all frog species is shown in Figure 3.4.

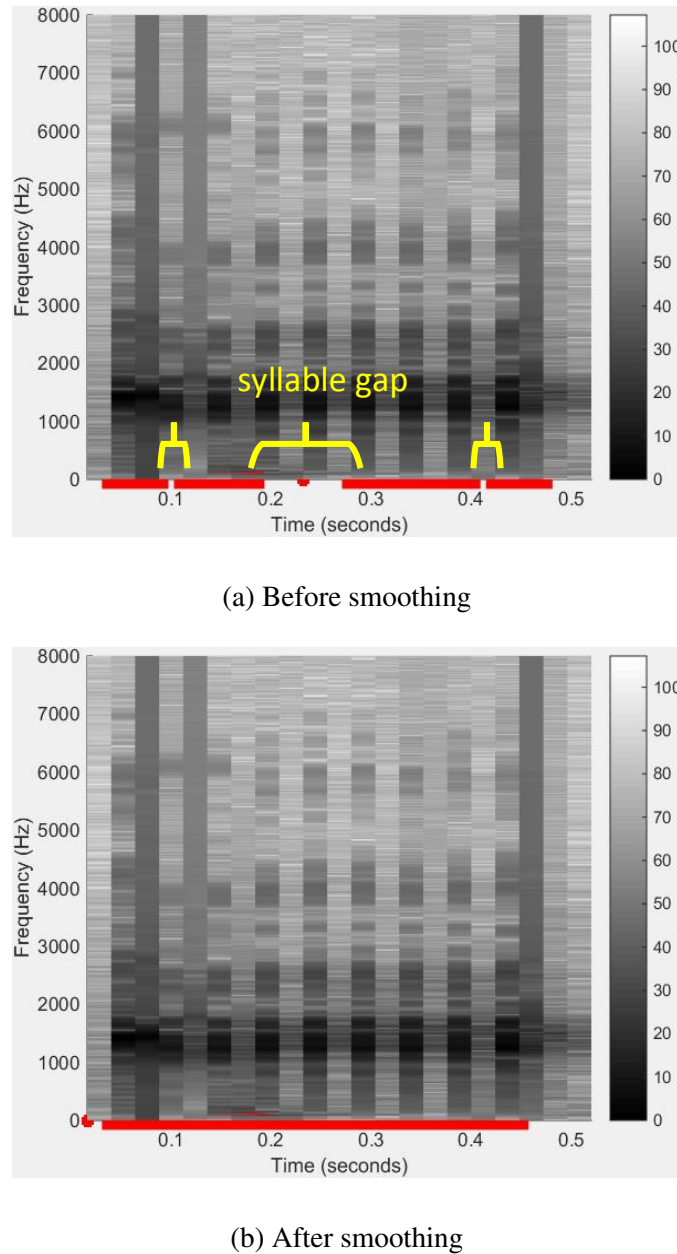


Figure 3.3: Syllable segmentation results are marked with a red line for *Neobatrachus sudelli* (one syllable).

3.2.3 Pre-processing

Since features play an important role in the classification performance, pre-processing is applied to each syllable to improve the accuracy of feature extraction. The pre-processing of each syllable consists of the following steps:

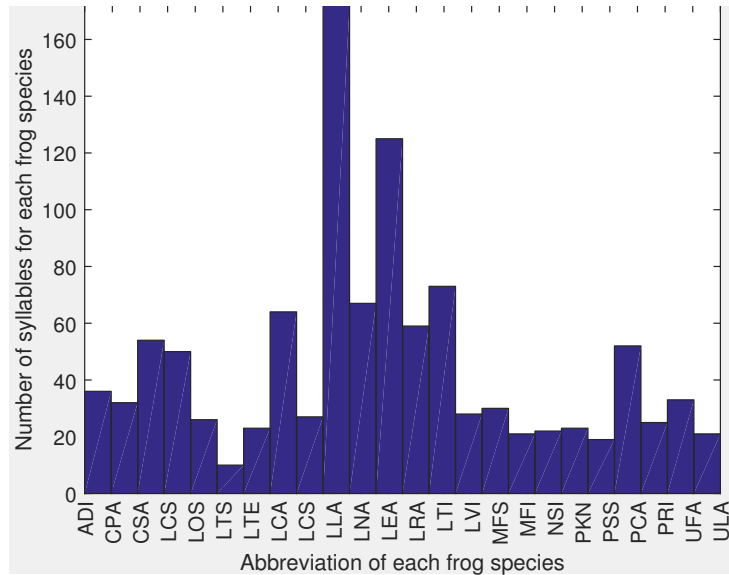


Figure 3.4: Distribution of syllable number for all frog species. The x-axis is the abbreviation of each frog species, and the corresponding scientific name can be found in Table 3.1.

Pre-emphasis

Some collected frog calls have low amplitude but in the high frequency, which will have an effect on feature extraction of the spectrum at the high frequency end. To enhance those high-frequency components and reduce the low-frequency components, a first-order high-pass filter with finite impulse response (FIR) is introduced and defined as follows:

$$y(n) = s(n) - \alpha s(n - 1) \quad (3.1)$$

where $s(n)$ is a syllable of frog call, $y(n)$ is the output of the high-pass filter, α denotes the cut-off frequency of the high-pass filter and is set at 0.97 here, n is the n-th sample of the syllable.

Windowing

After pre-emphasising, each syllable is segmented into overlapping frames with fixed length. A Hamming widow is used to minimise the maximum side-lobe in the frequency domain and get side-lobe suppression, which is defined as

$$w(n) = 0.54 - 0.46\cos\left(\frac{2n\pi}{L-1}\right), 0 \leq n \leq L-1 \quad (3.2)$$

where L is the length of the frame. Because window sizes have an effect on the classification results, different window sizes are optimised for different features in this study. The signal after windowing process is expressed as

$$x(n) = w(n)y(n) \quad (3.3)$$

3.2.4 Feature extraction

After pre-processing of each syllable, various parametric representations are used to represent the syllable. In the literature, a variety of parametric representations of frog calls can be found, such as LPC and MFCCs [Bedoya et al., 2014, Jaafar and Ramli, 2013b, Yuan and Ramli, 2012]. MFCCs achieved a better performance than LPC [Yuan and Ramli, 2012]. Different from the hybrid features used [Gingras and Fitch, 2013, Han et al., 2011, Huang et al., 2009], our enhanced feature consists of more features, such as oscillation rate [Xie et al., 2015b], to further improve the classification accuracy. In this study, temporal features include syllable duration, Shannon entropy, Rényi entropy, zero-crossing rate, averaged energy, and oscillation rate. Perceptual features contains spectral centroid, spectral flatness, spectral roll-off, signal bandwidth, spectral flux, and fundamental frequency. The MFCCs feature is used as a cepstral feature. The description of each feature is listed below.

(1) Syllable duration (Dr): Syllable duration [Xie et al., 2015b] is directly obtained from the bounds (time domain) of the segmentation results,

$$Dr = x(n_e) - x(n_s) \quad (3.4)$$

where n_e and n_s are the end and start location of one segmented syllable.

(2) Shannon entropy (Se): Shannon entropy is the expected information content of a sequence of a signal. It is often used to describe the average of all the information contents weighted by their probabilities p_i .

$$Se = - \sum_{i=1}^L p_i \log_2(p_i) \quad (3.5)$$

where L is the length of a frog syllable.

(3) Rényi entropy (Re): rényi entropy is calculated to obtain the different averaging of probabilities via the parameter α , and defined as

$$Re = \frac{1}{1 - \alpha} \log_2 \left(\sum_i^n p_i^\alpha \right) \quad (3.6)$$

where p_i is the probabilities of the occurrence $x(n)$ in the signal.

(3) Zero-crossing rate (Zcr): zero-crossing rate denotes the rate of signal change along a signal. When adjacent signals have different signs, a zero-crossing occurs. The mathematical expression of ZCR can be defined as

$$Zcr = \frac{1}{2} \sum_{n=0}^{L-1} [sgn(x(n)) - sgn(x(n+1))] \quad (3.7)$$

(4) Averaged energy (Ae): Averaged energy is defined as the sum of intensity of signal.

$$Ae = \frac{1}{L} \sum_{n=0}^{L-1} x(n)^2 \quad (3.8)$$

(5) Oscillation rate (Or): Oscillation rate is calculated in the frequency boundary around the fundamental frequency. First, the power within the frequency boundary is calculated. After normalising the power, the first and last 20% part of the power vector is discarded due to the uncertainty. Next, the autocorrelation is performed by the length of the vector. Furthermore, a discrete cosine transform is employed to the vector after mean subtraction, and the position of the highest frequency is achieved to calculate the oscillation rate.

(6) Spectral centroid (Sc): spectral centroid is the centre point of spectrum distribution. In terms of human audio perception, it is often associated with the brightness of the sound. With the magnitudes as the weight, it is calculated as the weighted mean of the frequencies.

$$Sc = \frac{\sum_{k=0}^{N-1} f_k X(k)}{\sum_{k=0}^{N-1} X(k)} \quad (3.9)$$

where $X(k)$ is the discrete Fourier transform (DFT) of the syllable signal of the k-th frame, N is the half size of DFT.

(7) Spectral flatness (Sf): spectral flatness provides a way to quantify the tonality of a sound. A higher spectral flatness indicates a similar amount of power of the spectrum in all spectral bands. Spectral flatness is measured by the ratio between the geometric mean and the arithmetic mean of the power spectrum and defined as

$$Sf = \frac{\sqrt{\frac{1}{N} \sum_{k=0}^{N-1} \ln X(k)}}{\frac{1}{N} \sum_{k=0}^{N-1} X(k)} \quad (3.10)$$

(8) Spectral roll-off (Sr): spectral roll-off is often used to measure the spectral shape, and defined as the frequency H . Here H is the value below which the θ of the magnitude distribution is concentrated,

$$\sum_k^H X(k) = \theta \sum_{k=1}^{N-1} X(k) \quad (3.11)$$

where θ is set at 0.85.

(9) Signal bandwidth (Bw): signal bandwidth can be used to represent the difference between the upper and lower cut-off frequencies.

$$Bw = \sqrt{\frac{\sum_{k=0}^{N-1} (k - Sc)^2 |x(n)|}{\sum_{k=0}^{N-1} X(k)}} \quad (3.12)$$

(10) Spectral flux (Sf): spectral flux is used to measure how quickly the power spectrum of a signal is changing. The spectral flux can be obtained via the power spectrum comparison between one frame and its previous one. The calculation of spectral flux is denoted as

$$Sf = \sum_{k=-\frac{N}{2}}^{\frac{N}{2}} H[|X(n, k)| - |X(n - 1, k)|] \quad (3.13)$$

where $H(x) = (x + |x|)/2$ is a half-wave rectifier function.

(11) Fundamental frequency: fundamental frequency is calculated via averaging peak intensity of all frames within one frog syllable. If the peak intensity value is higher than an empirically chosen or specified threshold, the frequency of that peak will be selected to calculate the fundamental frequency.

(12) Mel-frequency cepstral coefficients (MFCCs): MFCCs, which are obtained by applying cosine transform to a sub-band Mel-frequency spectrum within a short time, have been widely used in bird classification [Lee et al., 2006], speech/speaker recognition [Han et al., 2006], and frog identification [Bedoya et al., 2014]. In this study, MFCCs are calculated based on the method of [Lee et al., 2006].

Step 1: Band-pass filtering: The amplitude spectrum is then filtered using a set of triangular band-pass filters.

$$E_j = \sum_{k=0}^{N/2-1} \phi_j(k) A_k, 0 \leq j \leq J-1 \quad (3.14)$$

where J is the number of filters, ϕ_j is the j^{th} filter, and A_k is the amplitude of $X(k)$.

$$A_k = |X[k]|^2, 0 \leq k \leq N/2 \quad (3.15)$$

Step 2: Discrete cosine transform: MFCCs for the i^{th} frame are computed by performing DCT on the logarithm of E_j .

$$C_m^j = \sum_{j=0}^{J-1} \cos\left(m \frac{\pi}{J}(j + 0.5)\right) \log_{10}(E_j), 0 \leq m \leq L-1 \quad (3.16)$$

where L is the number of MFCCs.

In this study, the filter bank consists of 40 triangular filters, that is $J = 40$. The length of MFCCs of each frame is 12 ($L=12$). After calculating MFCCs from each frame, the averaged MFCCs of all frames within one syllable are calculated.

$$f_m = \frac{\sum_{i=1}^K (C_m^i)}{K}, 0 \leq m \leq L-1 \quad (3.17)$$

where f_m is the m^{th} MFCCs, K is the number of frames within the syllable.

For all perceptual features and Zcr , the mean values are calculated to characterise the frog

syllable. Then, the L-dimensional MFCC vectors are fused with the other 11 feature vectors to form the enhanced temporal, perceptual and cepstral (TemPerCep) features.

After the formulation of feature vectors, normalisation is conducted as follows

$$v_i = \frac{v_i - \mu_i}{\sigma_i} \quad (3.18)$$

where μ_i and σ_i are the mean and standard deviation computed for each feature vector i .

Let F_1 represent temporal features with length L_1 , F_2 and F_3 represent perceptual features and cepstral features with length L_2 and L_3 , respectively. The enhanced procedure is performed as

$$F_H = w_1 F_1 \oplus w_2 F_2 \oplus w_3 F_3 \quad (3.19)$$

where w_1 , w_2 , and w_3 are the weights, \oplus is the concatenation operation.

3.2.5 Classifier description

In this chapter we report the results for five classification algorithms: 1) Linear discriminant analysis (LDA), 2) K-nearest neighbour, 3) Support vector machines, 4) Random forest, 5) Artificial neural network. Five feature vectors, linear predictive coding, MFCCs, enhanced temporal feature and MFCC (*TemCep*), enhanced temporal and perceptual features (*TemPer*), enhanced temporal, perceptual features, and MFCC (*TemCepPer*), are fed into each classifier respectively to test their classification performance.

Linear discriminant analysis

After transforming the feature vector into low-dimensional space, the classification accuracy can be improved for linear discriminant analysis (LDA). In LDA, the goal is to find an optimal transformation matrix to transform the feature vector from an n-dimensional space to a d-dimensional space. A linear mapping, which maximises the Fisher criterion J_F , is used to obtain the transformation matrix as follows.

$$J_F(A) = \text{tr}((A^T S_w A)^{-1} (A^T S_B A)) \quad (3.20)$$

where S_w and S_B are the within-class scatter matrix and between-class scatter matrix, respectively. The within-class scatter matrix and between-class scatter matrix are respectively defined as

$$S_W = \sum_{j=1}^C \sum_{i=1}^{N_j} (F_i^j - \mu_j)(F_i^j - \mu_j)^T \quad (3.21)$$

$$S_B = \sum_{j=1}^C (\mu_i - \mu)(\mu_i - \mu)^T \quad (3.22)$$

where F_i^j is the i-th feature vector of frog species j , μ_j is the mean vector of species j , C is the number of frog species, and N_j is the number of feature vectors in species j , μ is the mean vector of all frog species.

The optimisation of the transform matrix can be determined via finding the eigenvectors of $S_W^{-1}S_B$.

$$A_{opt} = \text{argmax} \frac{\text{tr}(A^T S_B A)}{A^T S_W A} \quad (3.23)$$

In the recognition stage, the feature vector is first transformed into a lower-dimensional space via A_{opt} derived by LDA. Then, the distance between the feature vector of the test syllable and the feature vector representing this species is calculated. The one with minimum distance is regarded as the identified species.

K-nearest neighbour

For the K-NN classifier, the distance between an input frog feature vector and all stored feature vectors is first calculated. Then K closest vectors are selected to determine the species of the input feature vector by majority voting. For example, the Euclidean distance between an input instance i (frog feature vector) and one stored instance j is calculated as

$$d(i, j) = \sqrt{\sum_{c=1}^n (F_{i,c} - F_{j,c})^2} \quad (3.24)$$

Then the species of this input instance i can be predicted from the selected k nearest neighbours.

If

$$\frac{1}{k_1} \sum_{j \in S_1} d(i, j(S_1)) \leq \frac{2}{k_2} \sum_{j \in S_2} d(i, j(S_2)) \quad (3.25)$$

where $k = k_1 + k_2$, k_1 is the number of frog species S_1 , k_2 is the number of frog species S_2 . Here the input instance i will be classified as frog species S_2 . Following prior work ([Han et al., 2011, Xie et al., 2015b]), the distance function used for K-NN is the Euclidean function, and k is set at 1.

Support vector machines

Due to the high accuracy and superior generalisation properties, support vector machines (SVM) have been widely used for classifying animal sounds [Huang et al., 2009] [Acevedo et al., 2009]. In this study, the feature set obtained is first selected as training data. Then, the pairs $(F_l^n, L_l^n), l = 1, 2, \dots, C_l$ are constructed using the selected training data, where C_l is the number of frog instances in the training data, F_l^n is the feature vector obtained from the l -th frog instance in the training data, L_l^n is the frog species label. Furthermore, the decision function for the classification problem based on SVM [Cortes and Vapnik, 1995] is defined by the training data as follows.

$$f(v) = \operatorname{sgn}\left(\sum_{sv} \alpha_l^n L_l^n K(v, v_l^n) + b_l^n\right) \quad (3.26)$$

where $K(., .)$ is the kernel function, α_l^n is the Lagrange multiplier, and b_l^n is the constant value. In this work, the Gaussian kernel is selected as the kernel function. Parameters α and v are selected independently for each feature vector by grid search using cross-validation [Hsu et al., 2003].

Random forest

Random forest (RF) is a tree-based algorithm, which builds a specified number of classification trees without pruning. The nodes are split on a random drawing of m features from the entire feature set M . A bootstrapped random sample from the training set is used to build each tree. The advantage of RF is its ability to generate a metric to rank predictors based on their relative

contribution to the model's predictive accuracy [Bao and Cui, 2005]. The prediction is defined as follows.

$$Pred = \frac{1}{K} \sum_{n=1}^K T_i \quad (3.27)$$

where T_i is the n-th tree response of the RF. In this work, the number of trees K is set at 300 trees to characterise frog calls. As for the predictor variables m , it is set at \sqrt{N} , where N is the feature dimension in a syllable.

Artificial neural network

Artificial neural network (ANN) is a non-linear, adaptive, machine learning tool with great capabilities for learning, generalisation, non-linear approximation, and classification. An ANN architecture often consists of many interconnected neurons organised in successive layers: pattern layer, summation layer, and decision layer. The neuron in class is often computed by a Gaussian function. Then, the summation layer uses summation units to memorise the class conditional probability density functions of each class through a combination of Gaussian densities. Lastly, the decision layer unit classifies the pattern in accordance with the Bayesian decision rule based on the output of all summation layer neurons as follows.

$$D(F) = argmax p_i(F), i = 1, \dots, N \quad (3.28)$$

where i is the species index, N is the total number of frog species.

$$p_i(F) = \sum_{j=1}^{m_i} \beta_{ij} \phi_{ij}(F) \quad (3.29)$$

where m_i is the number of Gaussian components, β_{ij} and $\phi_{ij}(F)$ can be represented as follows.

$$\sum_{j=1}^{m_i} \beta_{ij} = 1 \quad (3.30)$$

$$\phi_{ij}(F) = \frac{1}{(2\pi)^{(d/2)} \sigma^d} \exp\left[-\frac{(F - \mu_{ij})^T (F - \mu_{ij})}{2\sigma^2}\right] \quad (3.31)$$

where $i = 1, \dots, N$, $j = 1, \dots, m_i$, d denotes the dimension of the input vector F , σ is the smoothing parameter, μ_{ij} is the mean vector and the central of the classification. In this study,

one ANN classifier named multiple perception layer (MLP) is used to classify frog calls.

3.3 Experiment results

In this experiment, all the dataset have been divided as 50% of the training set and 50% the testing set. For the testing phase, each machine learning algorithm is used to learn a model to classify frog calls with 5-fold cross validation. The performance of the proposed frog call classification system is evaluated by quantitatively expressed detection metrics, such as average accuracy, precision, and specificity. The definition of accuracy, precision, and specificity can be defined as

$$Sensitivity = \frac{TP}{TP + FN} \quad (3.32)$$

$$Specificity = \frac{TN}{TN + FP} \quad (3.33)$$

$$Accuracy = \frac{TP + TN}{TP + TN + FP + FN} \quad (3.34)$$

where TP is true positive, FP is false positive, TN is true negative, and FN is false negative.

3.3.1 Effects of different machine learning techniques

Figure 3.5 shows the frog call classification performance with different machine learning techniques. The high classification results in term of the accuracy, sensitivity and specificity measure of different classifiers indicates good classification performance. It can be observed that RF achieves the best classification performance, while the classification performance of LDA is the lowest. Meanwhile, the classification performances of SVM and MLP are very good, which might be that the features and classifiers are quite suitable. It can be seen from Figure 3.5 that frog call classification with different machine learning techniques can achieve good performance with our enhanced feature representation, because the classification accuracy is very high. It can also be noted that RF can be highly recommended for classification of frog calls due to the highest classification accuracy.

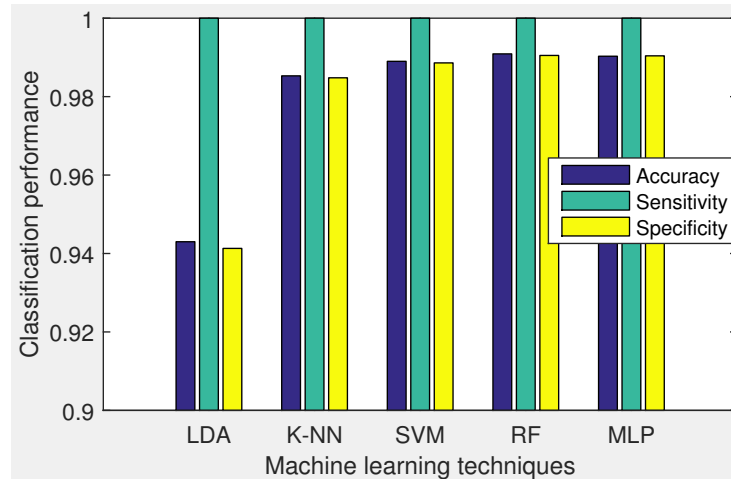


Figure 3.5: Results of different classifiers

3.3.2 Effects of different feature sets

Figure 3.6 illustrates the classification accuracy with different feature sets: LPC feature, MFCCs (*Cep*), temporal features and MFCCs (*TempCep*), temporal features and perceptual features (*TemPer*), and temporal features, perceptual features and MFCCs (*TemPerCep*). It can be seen that cepstral features (*Cep*, *TempCep*, *TemPerCep*) have a more stable performance than LPC and perceptual features. It is evident that our proposed enhanced feature (*TemPerCep*) shows outstanding performance of all proposed feature representations of all the machine learning techniques. The reason for the high classification accuracy is that frog calls are of short duration and cover a small spectral band. Our proposed enhanced feature, *TemPerCep*, can better characterise the content of frog calls. Although the classification performance of *TemPerCep* is not significantly higher than other feature representations, the difference does show that our proposed feature set is suitable and effective for the classification of frog calls.

3.3.3 Effects of different window size for MFCCs and perceptual features

As we know, the window size has an effect on the MFCCs and perceptual features. Therefore, a different window size will lead to a different classification performance (Figure 3.7 and Figure 3.8). The window size used for the test is 32, 64, 128, 256, because the syllable length of some frog species is less than 512 samples. It is found that the best classification performance for MFCCs is achieved with window size of 64 samples. For *TemPer*, the window size of 64 obtains the best classification performance. It also can be observed that SVM and RF achieve the best classification performance. Moreover, different window sizes of MFCCs have a larger

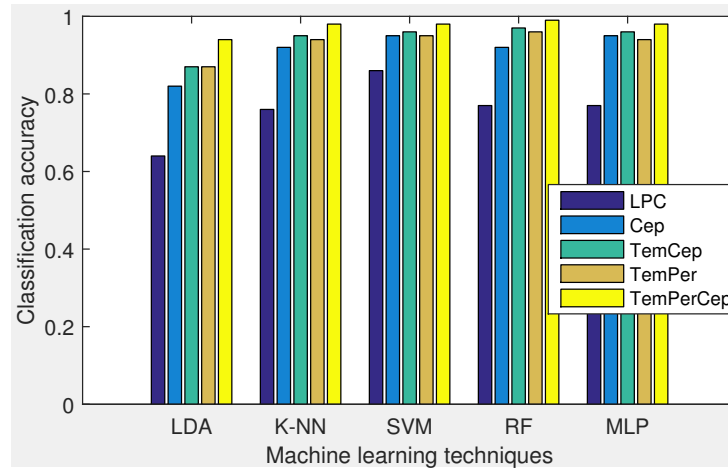


Figure 3.6: Classification results with different feature sets

variation than *TemPer* features, which might be because temporal features have a high weight in *TemPer* for the classification task.

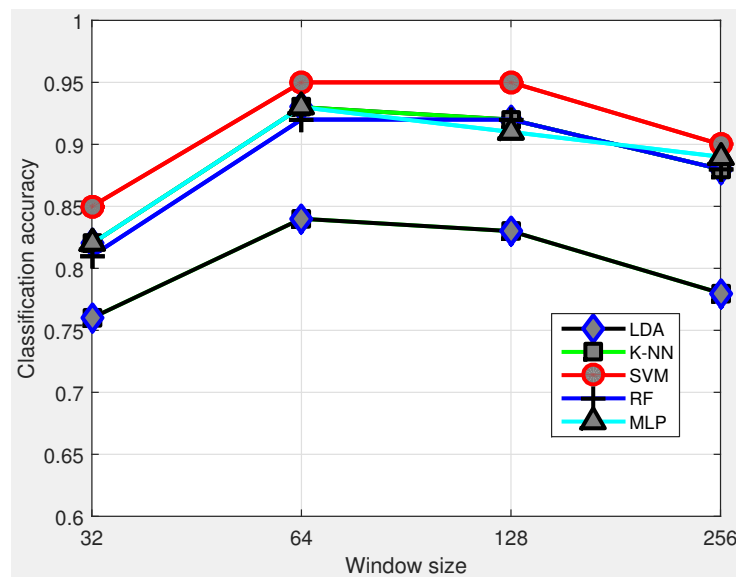


Figure 3.7: Classification results of MFCCs with different window size

3.3.4 Effects of noise

To further evaluate the robustness of our proposed feature set, white noise with different signal-to-noise (SNR) of 40 dB, 30 dB, 20 dB, 10 dB, 0dB, and -10 dB is added to the frog calls. Because this chapter focuses on the evaluation of features rather than the segmentation method, the artificial noise is added after syllable segmentation. Since SVM has shown a good performance for frog call classification in 3.3.1, we only use SVM to test the effects of different levels of artificial noise. The classification results of different levels of noise contamination are shown

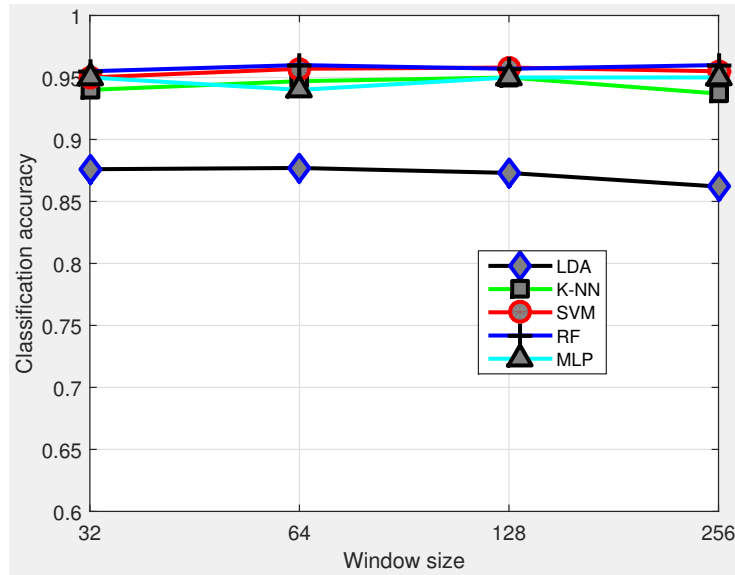


Figure 3.8: Classification results of TemPer with different window size

in Figure 3.9. It is found from Figure 3.9, that MFCCs (Cep) are very sensitive to background noise, compared with other feature representations. Comparing *TemCep* with *TemPer*, it can be observed that perceptual features have a better anti-noise ability than the cepstral feature. It is also found that LPC has a good anti-noise ability when SNR is larger than 10, but the classification accuracy quickly decreases when SNR is smaller than 10.

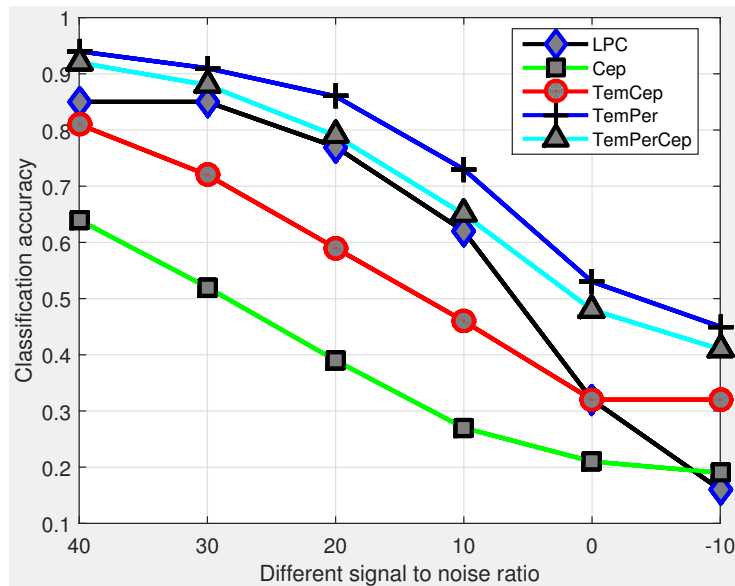


Figure 3.9: Sensitivity for different features for different levels of noise contamination

3.4 Discussion

Table 3.2 shows the classification performance of previous methods. Since previous studies often used different datasets to perform the classification task, this research implemented all those features and applied them to the used dataset with the same classifier (SVM). Compared with those previous methods, this proposed enhanced feature representation significantly outperforms other methods. Therefore, it can be concluded that the results of this research stand above the current classification performance. From the table, we can also observe that MFCCs is the most popular feature that has been used for frog call classification. Among all used machine learning techniques, SVM shows the superior performance and is widely used for the classification task. It can be found that the classification accuracy of *TemPerCep* does not show significant improvement when compared with MFCCs. However, combining temporal and perceptual features with cepstral features greatly improves the anti-noise ability of MFCCs.

Table 3.2: Comparision with previous used feature representations

Ref.	Feature	Accuracy
[Juan Mayor, 2009, Yuan and Ramli, 2012]	LPCs	93.5%
[Bedoya et al., 2014, Jaafar and Ramli, 2013b, Lee et al., 2006, Xie et al., 2015b]	MFCCs	94.9%
[Han et al., 2011]	Spectral centroid, Shannon entropy, Rényi entropy	75.6%
[Xie et al., 2015b]	Syllable duration, dominant frequency, oscillation rate, frequency modulation, energy modulation	92.3%
[Huang et al., 2014]	Spectral centroid, signal bandwidth, spectral roll-off, threshold-crossing rate, spectral flatness, and average energy	95.8%
Our feature representation	<i>TemPerCep</i>	99.1%

3.5 Summary and limitations

In this chapter, a novel enhanced feature representation was proposed to classify frog calls with various machine learning techniques. After segmenting continuous recordings into individual syllables, a variety of acoustic features are extracted from each syllable. Then, different features are fused to form different feature representations. Finally, various machine learning techniques are used to classify frog calls with different feature representations. Our proposed enhanced feature representation shows the best classification accuracy and has good anti-noise ability. Meanwhile, the SVM and RF outperform the traditional LDA and K-NN classifiers. Therefore, it is suitable to combine *TemPerCep* with SVM or RF to build a frog call classification system.

Ecologists can apply the proposed classification system to long-term frog recordings. Then, the long-term change of frog species richness can be reflected by the classification results.

Since the MFCCs feature shows a good classification performance, but a bad anti-noise ability, we can modify MFCCs to improve the anti-noise ability. After transforming frog audio data into its spectrogram representation, the visual inspection motivates us to use image processing techniques for studying frog calls. Also, a wider variety of frog audio data from different geographical and environmental conditions will be tested in future experiments.

Chapter 4

Adaptive frequency scaled wavelet packet decomposition for frog call classification

4.1 Overview

This chapter presents a novel cepstral feature representation based on adaptive frequency scaled wavelet packet decomposition. Following the conclusion of Chapter 3 that cepstral features can achieve a good classification accuracy, but are sensitive to background noise, the goal of this chapter is to develop a novel cepstral feature representation with a good anti-noise ability.

Since both high and low SNR recordings are studied in this research, developing feature representations with a good anti-noise ability is important for dealing with low SNR recordings. Different from most previous studies that extracted features via the Fourier transform, wavelet packet decomposition is employed in this chapter for feature extraction. The classification performance is evaluated with two different datasets from Queensland, Australia (18 frog species from commercial recordings (high SNR) and field recordings of eight frog species from James Cook University recordings (low SNR)). This chapter answers research question 2: How to improve the performance of developed features for frog call classification in low SNR recordings?

Although low SNR recordings are used in this research, the classification task is regarded as a single-instance single-label learning problem. However, most individual low SNR recordings have more than one frog species. In the next two chapters, we will focus on the classification of multiple simultaneously vocalising frog species in one individual recording.

4.2 Method

The architecture of the proposed classification method consists of five modules: syllable segmentation, syllable feature extraction, adaptive frequency scale generation, WPD feature extraction and classification (see Figure 4.1). Each module is described in the following sections.

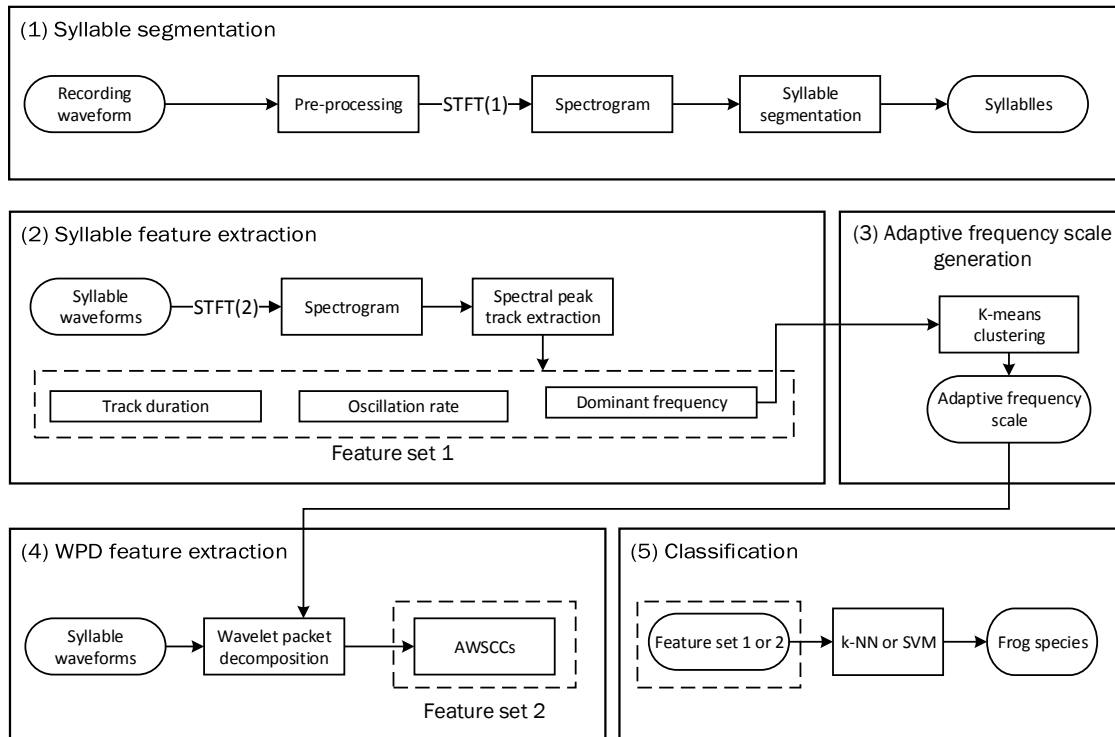


Figure 4.1: Block diagram of the frog call classification system. The line of dashes indicates the extracted feature set. AWSCCs is the abbreviation of *adaptive wavelet packet decomposition sub-band cepstral coefficients*. STFT is short-time Fourier transform. For STFT(1), the window function, size and overlap are Kaiser window, 512 samples and 25%. For STFT(2), the window function, size and overlap are Hamming window, 128 samples and 90%. In this diagram, two feature sets are extracted, the description of other feature sets is shown in Figure 4.6.

4.2.1 Sound recording and pre-processing

Two datasets obtained from a commercial recording [Stewart, 1999] and James Cook University (JCU) were selected for this chapter. Recordings, which were collected from the CD, are two-channel, sampled at 44.10 kHz and saved in MP3 format. All recordings were obtained with a directional microphone and have a high signal to noise ratio (SNR). Each recording includes one frog species, and has a duration ranging from twenty-one to fifty-four seconds. The calls of eighteen frog species recorded in Queensland, Australia were used to develop the detailed

methodology described in Figure 4.1. To reduce the subsequent computational burden, all the recordings selected from the CD were re-sampled at 16 kHz per second, mixed to mono, and saved in WAV format.

The JCU recordings were obtained from Kiyomi dam (S 19° 22' 16.0'', E 146° 27' 31.3'') BG Creek dam (S 19° 27' 1.23'', E 146° 24' 5.65'') and Stony Creek dam (S 19° 24' 07.0'', E 146° 25 51.3) in Townsville, using Song Meter (SM2) [Xie, 2016]. The recordings were stored on 16 GB SD cards in 64 kbps MP3 mono format and have a low SNR compared with the commercial recording. The sample rate is 16.00 kHz. All the JCU recordings started around sunset, finished around sunrise every day and have 12 hour duration.

4.2.2 Spectrogram analysis for validation set

In this chapter, three syllables for each frog species are set aside and used as a *reference data set*. For the commercial recording, three parameters including syllable duration, dominant frequency, and oscillation rate, are manually calculated for those three syllables of each species and averaged, as listed in Table 4.1. The reference data set is excluded from the data used in the testing stage.

Table 4.1: Parameters of 18 frog species averaged of three randomly selected syllable samples in the commercial recording. These selected samples make the *reference data set*.

No.	Scientific name	Abbreviation	Syllable duration (millisecond)	Peak frequency (Hz)	Oscillation rate (cycle/second)
1	Assa darlingtoni	ADI	80	3200	160
2	Crinia parinsignifera	CPA	250	4300	350
3	Litoria caerulea	LCA	500	500	50
4	Litoria chloris	LCS	800	1700	220
5	Litoria fallax	LFX	430	4700	70
6	Litoria gracilenta	LGA	1400	2700	100
7	Litoria latopalmata	LLA	30	1400	2100
8	Litoria nasuta	LNA	100	2800	160
9	Litoria revelata	LRA	160	4100	70
10	Litoria rubella	LUA	500	2900	60
11	Litoria verreauxii verreauxii	LVV	270	3100	125
12	Mixophyes fasciolatus	MFS	200	1200	140
13	Mixophyes fleayi	MFI	50	1000	140
14	Philoria kundagungan	PKN	170	430	95
15	Pseudophryne coriacea	PCA	300	2400	80
16	Pseudophryne raveni	PRI	370	2500	45
17	Rheobatrachus silus	RSS	510	1500	60
18	Uperoleia laevigata	ULA	450	2400	150

For the JCU recordings², the corresponding parameters are described in Table 4.2. Compared with the commercial recordings from the CD, peak frequency shows a smaller variation than syllable duration and oscillation rate.

Table 4.2: Parameters of eight frog species obtained by averaging three randomly selected syllable samples from recordings of James Cook University. NA indicates there is no oscillation structure in the spectrogram for the background noise and frog chorus. Since syllable durations of *Rhinella marina* (Common name: Canetoad) are very different from each other, we manually set the duration of Canetoad using the maximum duration of other frog species, which is 500 milliseconds.

No.	Scientific name	Abbreviation	Syllable duration (millisecond)	Peak frequency (Hz)	Oscillation rate (cycles/second)
1	<i>Rhinella marina</i>	CTD	500	680	12
2	<i>Cyclorana novaehollandiae</i>	CNE	350	600	NA
3	<i>Limnodynastes terraereginae</i>	LTE	80	630	NA
4	<i>Litoria fallax</i>	LFX	120	4100	50
5	<i>Litoria nasuta</i>	LNA	100	2700	NA
6	<i>Litoria rothii</i>	LRI	350	1150	15
7	<i>Litoria rubella</i>	LUA	500	2400	NA
8	<i>Uperoleia mimula</i>	UMA	120	2400	40

4.2.3 Syllable segmentation

For frog calls, an elementary acoustic unit for classification is the syllable, which is a continuous vocalisation emitted from an individual [Huang et al., 2009]. Each commercial recording consists of multiple continuous calls of one frog species. Therefore, it is necessary to segment each call into individual syllables. This syllable segmentation process is applied to the spectrogram, which is generated by applying short-time Fourier transform (STFT) to each recording. For STFT, the window function is the Hamming window with the size and overlap of 512 samples and 25%, respectively.

To further improve the segmentation result, the averaged energy of which is less than 15% of the maximum energy, are removed [Gingras and Fitch, 2013]. The distribution of syllable numbers after segmentation for all frog species is shown in Figure 4.2.

For the JCU recordings, bandpass filtering is applied to each recording before using the Härmä's method [Harma, 2003]. A bandpass filter is first used to filter specific frog species, because different frog species tend to call simultaneously. The filtering is

²<https://www.ecosounds.org/>

$$S'(t, f) = \begin{cases} S(t, f) & F_{lower} \leq f \leq F_{upper} \\ 0 & \text{otherwise} \end{cases}$$

Here, $S'(t, f)$ is the filtered spectrogram, the F_{lower} and F_{upper} are lower and upper cutoff frequency and calculated as

$$\begin{aligned} F_{upper} &= F_{peak} + \beta \\ F_{lower} &= F_{peak} - \beta \end{aligned} \tag{4.1}$$

where F_{peak} is the peak frequency (Table 4.2), β is a threshold for determining the frequency bandwidth and set at 300 Hz based on the *reference data set*.

After bandpass filtering, noise reduction is essential for improving the segmentation result for the low signal to noise ratio in JCU recordings. Here, we use the method of Towsey et al. [2012] for noise reduction. Finally, we use the Härmä's method to detect individual syllables (Figure 4.3).

For *Canetoad*, the durations of different calls are very different, therefore, we manually selected 30 syllables, the combined duration of which is 500 ms.

For the JCU recordings, eight frog species were used for the experiment. After syllable segmentation of continuous recordings, for each frog species, we randomly selected 30 syllables from segmentation results for subsequent analysis.

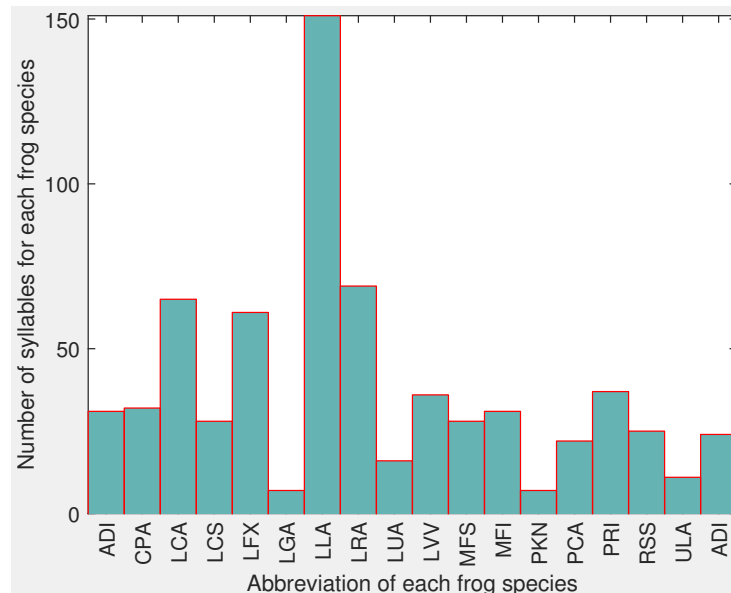


Figure 4.2: Distribution of syllable number for all frog species. The x-axis is the abbreviation of each frog species, and the corresponding scientific name can be found in Table 4.1.

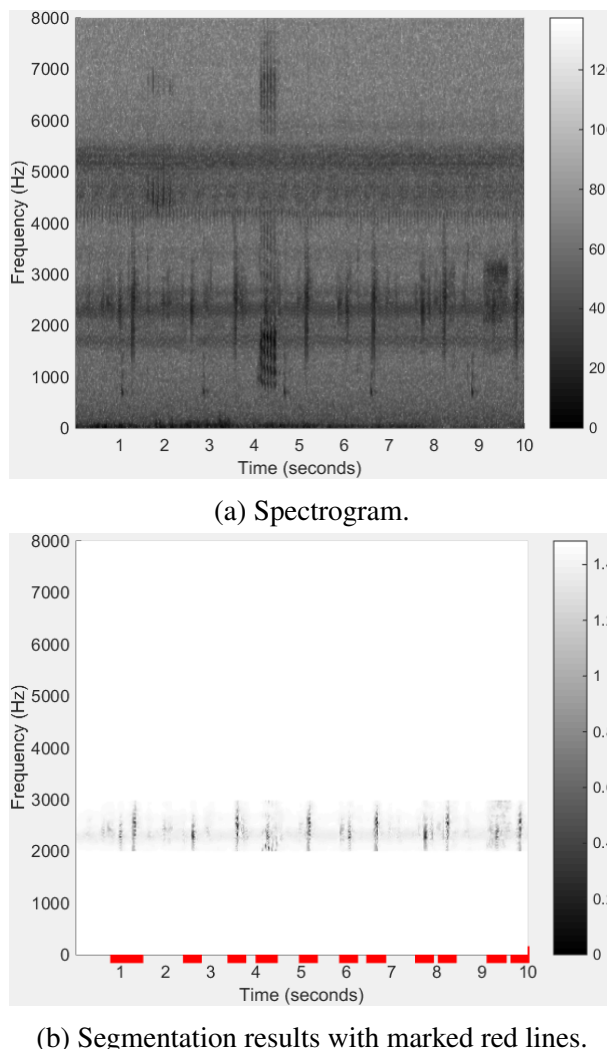


Figure 4.3: Segmentation results for *Uperolela mimula* using bandpass filtering, noise reduction and Härmä's method. The red line in (b) indicates the start and stop location of each segmented syllable.

4.2.4 Spectral peak track extraction

Spectral peak tracks (SPT) (also called frequency tracks) have been explored for studying birds [Heller and Pinezich, 2008, Jancovic and Kokuer, 2015] and whales [Roch et al., 2011]. In this chapter, the spectral peak track is used to represent the trace of a frog advertisement call, because frogs that are genetically related share more similar advertisement calls than distantly related frogs [Gingras and Fitch, 2013]. The reasons for using SPT are (1) to isolate the desired frog calls from the background noise; (2) to extract corresponding SPT features. Here, the SPT method is reported in [Xie et al., 2015b].

For the SPT extraction algorithm, seven parameters need to be set (Table 4.3). The process for determining those parameters is explained in Section 3.

Table 4.3: Parameters used for spectral peak extraction

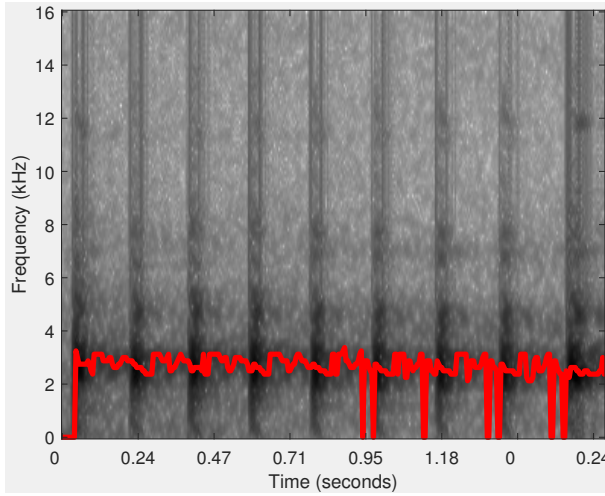
Parameter	Description
I (dB)	Minimum intensity threshold for peak selection
T_c (s)	Maximum time domain interval for peak connection
T_s (s)	Minimum time interval for stopping growing tracks
f_c (Hz)	Maximum frequency domain interval for peak connection
d_{min} (s)	Minimum track duration
d_{max} (s)	Maximum track duration
β (0~1)	Minimum density value

Before applying the SPT extraction algorithm, each syllable is transformed to a spectrogram with the following parameter settings (Hamming window, frame size is 128 samples, and window overlap is 90%). For the generated spectrogram, the maximum intensity (real peak) is selected from each frame with a minimum required intensity, I . Then, the time and frequency domain intervals between two successive peaks are calculated. If the time and frequency intervals are smaller than T_c and f_c respectively, one initial track (SPT_1) will be generated. After that, linear regression is applied to the generated track for calculating the position of the next predicted peak. Based on peaks $p_1(t_1, f_1)$ and $p_2(t_2, f_2)$ within the initial track (SPT_1), a and b in Equation (4.2) can be solved.

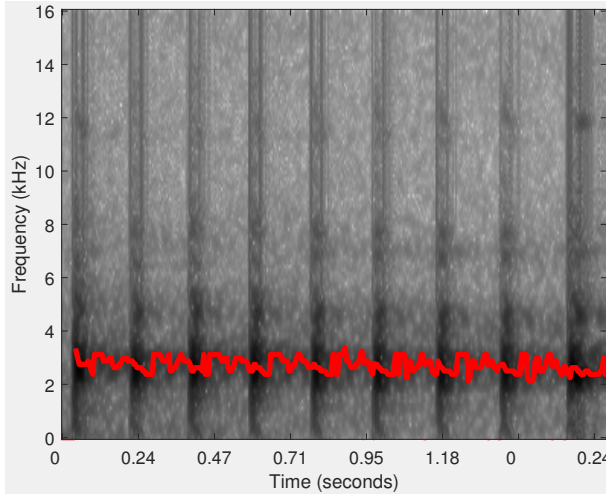
$$f = at + b \quad (4.2)$$

Based on a and b , the predicted peak \hat{p}_n of the following frame t_n can be calculated. Next, the time and frequency domain intervals between predicted peak (\hat{p}_n) and the real peak of the successive frame are recalculated. If the time and frequency intervals are smaller than T_c and f_c respectively, the real peak will be added to the initial track. After each peak is added to the initial track, linear regression is repeated to recalculate the next predicted peak using at most the last 10 included peaks. This iterative process continues until T_s is no longer satisfied. When no more peaks will be added to one track, the next step is to compare the duration and density of the track with d_{min} , d_{max} , and β . If all conditions are satisfied, then the track will be saved to the track list. The SPT results for *Neobatrachus sudelli* are shown in Figure 4.4. During the process of track extraction, time domain gaps are generated where the intensity threshold I is not reached. These gaps can be filled by predicting the correct frequency bin using linear

regression, as illustrated in Figure 4.4.



(a) selected peaks below the intensity threshold I are set to zero.



(b) spectral peak track with predicted peaks using linear regression.

Figure 4.4: Spectral peak track extraction results for *Neobatrachus sudelli*. By filling the gaps within the track, the dominant frequency can be more accurately calculated.

4.2.5 Syllable SPT features

After SPT extraction, each SPT is expressed in the following format: (1) track start time t_s ; (2) track stop time t_e ; (3) frequency bin index for each of the peaks within the track f_t ($t_s \leq t \leq t_e$). Then, syllable features including track duration, dominant frequency, and oscillation rate are calculated based on the SPT.

a) Track duration (second): Track duration (D_t) is directly obtained from the bounds of the

track.

$$D_t = (t_e - t_s) * r_x \quad (4.3)$$

where r_x is the time domain resolution in unit second per frame.

b) Dominant frequency (Hz): Dominant frequency (\bar{f}) is calculated by averaging the frequency of all peaks within one track

$$\bar{f} = \sum_{t=t_s}^{t_e} f_t / (t_e - t_s + 1) * r_y \quad (4.4)$$

where r_y is the frequency domain resolution with unit frequency per bin, f_t is the frequency bin index of peak t .

c) Oscillation rate (Hz): Oscillation rate (O_r) represents the number of pulses per second. The algorithm for extracting oscillation rate is introduced and summarised as follows. First, the frequency domain boundary is defined based on the dominant frequency, and the power within the boundary is calculated. Then, the power vector is normalised, and the first and last 20% part of the vector is discarded, because of the uncertainty in the start and end of the syllables. Next, the autocorrelation with the length of the vector is calculated. Furthermore, a discrete cosine transform (DCT) is applied to the vector after subtracting the mean, and the position of the highest frequency (P_f) is achieved. Finally, the oscillation rate is defined as

$$O_r = \frac{P_f}{L_{dct}} * r_x * \gamma \quad (4.5)$$

where P_f is the position of the highest frequency values of the DCT result, L_{dct} is the length for applying DCT to the power vector, and is experientially set as 0.2 second in this chapter.

4.2.6 Wavelet packet decomposition

Wavelet packet decomposition (WPD) is a powerful tool for the analysis of non-stationary signals, which includes multiple bases and different basis [Selin et al., 2007]. With WPD, an original acoustic signal can be split into two frequency bands such as lower and higher frequency band. Then, both lower and higher frequency bands can be further continuously decomposed into two sub-bands, which produce a complete wavelet packet tree [Farooq and Datta, 2001]. Due to its ability for analysing a non-stationary signal, WPD has been used to

analyse acoustic signals [Ren et al., 2008, Selin et al., 2007]. Here, WPD is used to obtain features for frog call classification.

4.2.7 WPD based on an adaptive frequency scale

To obtain robust features for frog call classification, the frequency scale used for WPD is crucial. In prior work [Biswas et al., 2014, Litvin and Cohen, 2011, Zhang and Li, 2015], different frequency scales have already been proposed for WPD. Bark-scaled WPD was proposed by Litvin and Cohen to separate blind source from a single channel audio source [Litvin and Cohen, 2011]. Biswas et al. [2014] used features based on ERB-scaled (Equivalent rectangular bandwidth) WPD for Hindi consonant recognition. Zhang and Li [2015] developed a method based on Mel-scaled WPD for bird sound detection with the SVMs classifier. However, most frequency scales used for WPD are developed for studying speech rather than frogs. Therefore, finding a suitable frequency scale for frogs to perform the WPD is important for obtaining features with strong discriminatory power. In this chapter, an adaptive frequency scale for WPD for frog calls is proposed, based on the dominant frequency of frog species to be classified. Specifically, the k-means clustering algorithm is used to cluster the dominant frequency of all syllables. Then, the centroids of the clustering result are used to generate the frequency scale. Here, the value of k for the k-means clustering algorithm is the same as the number of frog species to be classified, the distance function used is *city block* [Melter, 1987].

Based on the obtained frequency scale, an adaptive frequency scaled WPD method is proposed, which is described in Algorithm 1. The wavelet packet tree used for classifying 18 frog species is shown in Figure 4.5.

4.2.8 Feature extraction based on adaptive frequency scaled WPD

In previous studies [Bedoya et al., 2014, Xie et al., 2015b], Mel-frequency cepstral coefficients (MFCCs) have been used for studying bioacoustic data, and used as the baseline for feature comparison in this chapter. Besides MFCCs, another feature set called Mel-scaled wavelet packet decomposition sub-band cepstral coefficients (MWSCCs) is also included in the comparison experiment [Zhang and Li, 2015], because it shows better performance than MFCCs for bird detection in a complex environment. In this chapter, we propose a novel feature set named *adaptive frequency scale wavelet packet decomposition sub-band cepstral*

Algorithm 1: Adaptive frequency scale for WPD

Data: $c_i (i = 1, 2, \dots, K)$, f_s , where K is the number of frog species to be classified, c_i is the centroid of the clustering results, $f_s = sr/2$ where sr is the sample rate of the audio recordings, which is 16 kHz here.

Result: Adaptive wavelet packet tree

begin

Step 1: Sort the centroid $c_i (i = 1, 2, \dots, K)$, and calculate the difference between the consecutive vectors of c , sort the difference and save it as $d_j (j = 1, 2, \dots, K - 1)$

Step 2: Calculate the decomposition level L based on the following rule

$$f_s / \min(d) \leq 2^{L-1}$$

where L is the minimum integer that satisfies that equation.

Step 3: Perform the wavelet packet decomposition

for $l = 1 : L$ **do**

1. Calculate the frequency resolution of level 1

for $i = 1 : K$ **do**

1: Put the c_i into the right frequency band

2: Count the number of c_i in each band (n)

if $n \geq 2$ **then**

| perform further decomposition to that particular node

else

| stop decomposition

coefficients (AWSCCs) for frog call classification. The extraction procedure of AWSCCs is similar to MWSCCs. However, the frequency scale used for our AWSCCs is based on an adaptive frequency scale rather than the Mel-scale for MWSCCs. Meanwhile, after performing DCT, temporal feature integration is used for calculating the statistics of feature vectors which generates different statistical types of AWSCCs. (see in Figure 4.6).

After syllable segmentation, the signal of one syllable is represented as $y(n)$, $n = 1, \dots, N$, where N is the length of one syllable of frog calls. Based on the $y(n)$, steps for AWSCCs extraction are described as follows:

- 1). Add Hamming window to the signal $y(n)$.

$$x(n) = w(n)y(n) \quad (4.6)$$

where $w(L)$ is the Hamming window function and defined as $w(n) = 0.54 - 0.46\cos(\frac{2n\pi}{L-1})$, L is the length of Hamming window and set as 128 samples here.

- 2). Perform wavelet packet decomposition spaced in adaptive frequency scale as described in

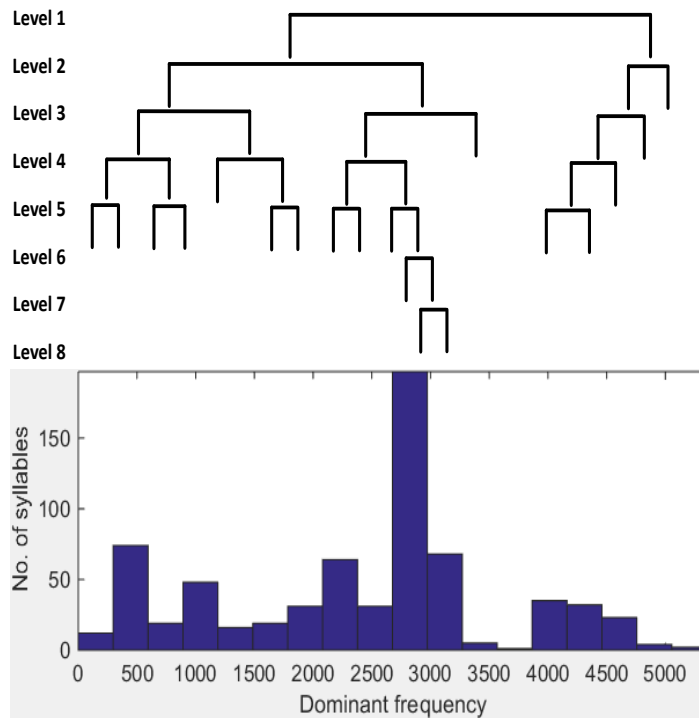


Figure 4.5: Adaptive wavelet packet tree for classifying twenty frog species. The upper image is the wavelet packet tree; the lower image is the histogram of dominant frequency for twenty frog species.

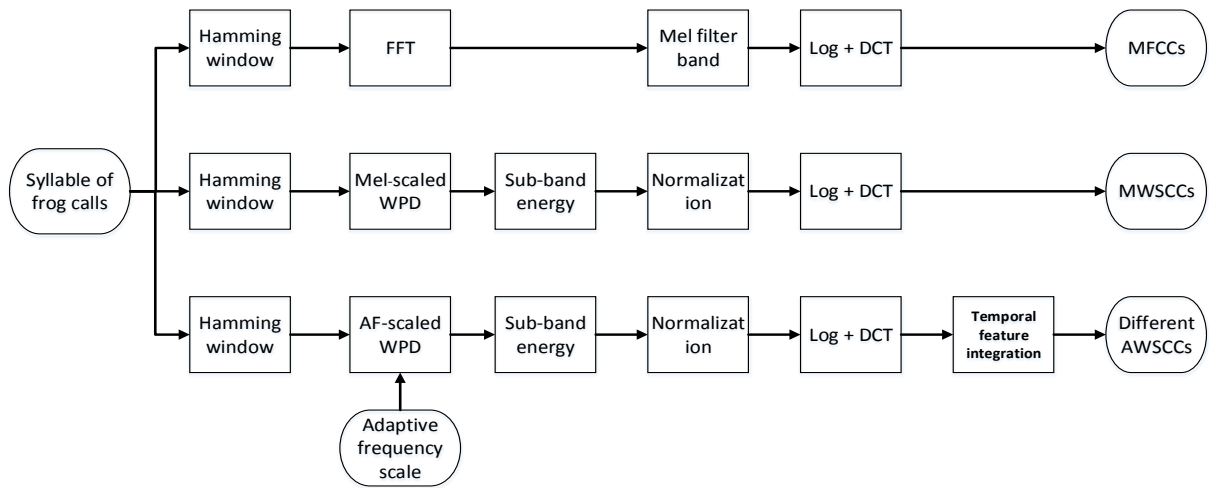


Figure 4.6: Description of three feature extraction methods including MFCCs, MWSCCs, and different statistical types of AWSCCs.

Section 2.7.

$$WP(i, j) = \sum_{i=1}^M x(n)\psi_{(a,b)}(n) \quad (4.7)$$

where $WP(i, j)$ is the wavelet coefficients of the decomposition, i is the sub-band index, j

is the index of wavelet coefficients, $\psi_{(a,b)}(n)$ is the wavelet base function, and we use 'Db 4' experimentally. Here, a and b are the scale and shift parameters, respectively. 'Db 4' represents the Daubechies wavelet transform which has four scaling and wavelet function coefficients.

3). Calculate the total energy of each sub-band.

$$WP_i = \sum_{j=1}^{M_i} [WP(i, j)]^2 \quad (4.8)$$

where $i = 1, 2, \dots, T$, and T is the total number of sub-band, and $j = 1, 2, \dots, M_i$, M_i is the total number of wavelet coefficients.

4). Normalise the energy of each sub-band.

$$SE_i = \frac{WP_i}{M_i} \quad (4.9)$$

where $i = 1, 2, \dots, T$.

5). Perform DCT on the logarithm sub-band energy for dimension reduction and obtain the feature AWSCCs.

$$AWSCCs(d) = \sum_{i=1}^T \log SE_i \cos\left(\frac{d(i - 0.5)}{T}\pi\right) \quad (4.10)$$

where $d = 1, 2, \dots, d'$, $1 \leq d' \leq T$, here d' is the dimension of AWSCCs, and set as 12 here. To keep the feature dimension consistency, the dimensions for MFCCs and MWSCCs are also set as 12 in this chapter, and the detailed steps for extraction can be found in [Bedoya et al., 2014] and [Zhang and Li, 2015].

6). Temporal feature integration

Here, the statistics of all feature vectors over each windowed signal are calculated, which include sum, average, standard deviation, and skewness. With randomly selected five instances for each frog species, the classification accuracy of averaged AWSCCs is higher than other statistics of AWSCCs. Therefore, only averaged AWSCCs are used in the subsequent experiment. To capture the dynamic information of the frog calls, the delta-AWSCCs are also calculated based on the averaged AWSCCs.

4.2.9 Classification

In this chapter, the k-nearest neighbour (k-NN) and support vector machine (SVM) classification algorithms are used for frog call classification. The input parameters for each classifier are syllable features (SFs), MFCCs, MWSCCs, and different AWSCCs, and the output is the frog species.

k-nearest neighbours

For the k-NN classifier, an object is classified to the class of the majority of its k nearest neighbours [Huang et al., 2009]. Specifically, frog feature vectors are stored with species labels in the training phase. For the test phase, the distances between an input frog feature vector and all stored vectors are calculated. Then, k closest vectors are used for selecting the most frequent vector as the label. For example, the Euclidean distance between an input feature vector $f_{i,c}$ and one stored feature vector $f_{j,c}$ is calculated as

$$d(i, j) = \sqrt{\sum_{c=1}^n (f_{i,c} - f_{j,c})^2} \quad (4.11)$$

where i and j are indices of the feature vector, n means the dimension of the feature vector. Next, k nearest neighbours of the feature vector i are selected based on the Euclidean distance for selecting the most frequent vector as the label. If the following equation is satisfied

$$\frac{1}{k_1} \sum_{j \in s_1} d(i, j(s_1)) \leq \frac{1}{k_2} \sum_{j \in s_2} d(i, j(s_2)) \quad (4.12)$$

where $k = k_1 + k_2$, k_1 is the number of frog species s_1 , k_2 is the number of frog species s_2 . Here, the input feature vector i will be classified as frog species s_2 .

Support vector machines

Due to the high accuracy and superior generalisation properties, support vector machines have been widely used for classifying animal sounds [Acevedo et al., 2009, Huang et al., 2009]. In this chapter, the feature set obtained is first selected as training data. Then, the pairs (v_l^n, L_l^n) , $l = 1, 2, \dots, C_l$ are constructed using the selected training data, where C_l is the number of frog

instances in the training data, v_l^n is the feature vector obtained from the l -th frog instance in the training data, L_l^n is the frog species label. Furthermore, the decision function for the classification problem based on SVM [Cortes and Vapnik, 1995] is defined by the training data as follows:

$$f(v) = \operatorname{sgn}(\sum_{sv} \alpha_l^n L_l^n K(v, v_l^n) + b_l^n) \quad (4.13)$$

where $K(., .)$ is the kernel function, α_l^n is the Lagrange multiplier, and b_l^n is the constant value.

4.3 Experiment result and discussion

Several experiments are described for evaluating our proposed frog call classification system. First, the parameter tuning is discussed based on the reference data set. Then, the comparisons between all proposed features are studied. Finally, the classification results under different SNR are described.

4.3.1 Parameter tuning

There are five modules for parameter tuning: syllable segmentation, spectral peak track, feature extraction, and classification (Figure 5.1).

For syllable segmentation, the window size and overlap are 512 samples and 25%, however, the intensity threshold is 10 dB and 5 dB for the commercial recordings and the JCU recordings respectively.

In the spectral peak track determination, there are seven parameters (see in Table 4.3). The parameter settings are shown in Table 4.4.

With a random parameter setting start, an iterative loop is performed for a fixed range of each parameter as seen in Table 4.1 to optimise those parameters.

For feature extraction, the window size and overlap are the same for MFCCs, MWSCCs, and AWSCCs using Hamming window, which are 128 samples and 90%, respectively. The dimensions of MFCCs, MWSCCs and AWSCCs are 12. For SFs and delta-AWSCCs, the dimensions are 3 and 24, respectively.

Table 4.4: Parameter setting for calculating spectral peak track.

Parameter	Commercial recordings	JCU recordings
I (dB)	3	3
T_c (s)	0.005	0.1
T_s (s)	0.05	0.2
f_c (Hz)	800	800
d_{min} (s)	0.01	0.05
d_{max} (s)	2	2
β (0~1)	0.8	0.6

Following prior work [Han et al., 2011, Huang et al., 2009, Xie et al., 2015b], the distance function used for k-NN is the Euclidean distance, and k is set as 3. As for the SVM classifier, the Gaussian kernel is used. Parameters α and v are selected independently for each feature set by grid-search using cross validation [Hsu et al., 2003].

4.3.2 Feature evaluation

All experiments are carried out in Matlab R2014b. Performance statistics are estimated with ten-fold cross validation. Totally, five feature sets including SFs, MFCCs, MWSCCs, and averaged AWSCCs, and delta-AWSCCs, are fed to two classifiers, which are the k-NN and SVM classifiers. Both k-NN and SVM classifiers are run ten times for evaluating the feature robustness. Due to the non-uniform distribution of the number of syllables for different frog species in the commercial recordings, a weighted classification accuracy is define as follows

$$weighted\ Acc = \sum_{i=1}^N Acc(i) * \frac{n_i}{N} \quad (4.14)$$

where n_i is the number of syllables for frog species i , N is the number of syllables for all frog species, Acc is the classification accuracy for that particular frog species.

4.3.3 Comparison between different feature sets

The classification accuracy comparison for 18 frog species using five feature sets and two classifiers is shown in Table 4.5.

Table 4.5: Weighted classification accuracy (mean and standard deviation) comparison for five feature sets with two classifiers.

Feature set	Classification accuracy (%)	
	k-NN	SVM
SFs	82.2 ± 11.2	84.2 ± 10.5
MFCCs	90.8 ± 8.6	92.8 ± 11.0
MWSCCs	95.0 ± 7.7	97.6 ± 5.7
Averaged AWSCCs	98.8 ± 4.2	99.0 ± 3.6
Delta-AWSCCs	99.2 ± 2.1	99.6 ± 1.8

In this experiment, the best classification accuracy is 99.6%, which is achieved by the delta-AWSCCs with the SVM classifier. Compared with the average AWSCCs, the delta-AWSCCs achieved a slightly better performance. One may conjecture that the delta-AWSCCs can capture the dynamic information of the frog calls. For MWSCCs, the averaged classification accuracy of both classifiers is about 2% lower than that of averaged AWSCCs and delta-AWSCCs with 96.3%. The improvement shows that the proposed adaptive frequency scale can capture more information about frog calls than the Mel-scale (Figure 4.7).

As for SFs and MFCCs, the averaged classification accuracy is much lower than AWSCCs, which is 83.2% and 91.8%, respectively. To explore the reason for the improvement of the proposed feature, the frog call classification accuracy of all frog species is shown in Table 4.6. However, only the features that use the SVM classifier are shown, because averaged accuracy of the k-NN classifier (93.2%) is lower than the SVM classifier (94.64%).

Table 4.6 lists the classification accuracy of all 18 frog species with five features. It can be seen from the table that delta-AWSCCs have an accuracy greater than 95% for all frog species. Compared with averaged AWSCCs, the classification accuracy of *Pseudophryne coriacea* (PCA) and *Litoria verreauxii verreauxii* (LVV) are improved to 100%; it might be that the delta-AWSCCs include the dynamic information of frog calls. For *Litoria revelata* (LRA), both the classification accuracy of averaged AWSCCs and delta-AWSCCs are lower than 100%; this is because the dominant frequency is quite similar with multiple frog species including *Assa darlingtoni* (ADI), *Litoria nasuta* (LNA) and *Litoria verreauxii verreauxii* (LVV). However, the classification of *Litoria revelata* (LRA) is 100% using Mel-scale based techniques, because the Mel-scale has a better frequency resolution for *Litoria chloris* (LCS) within its dominant

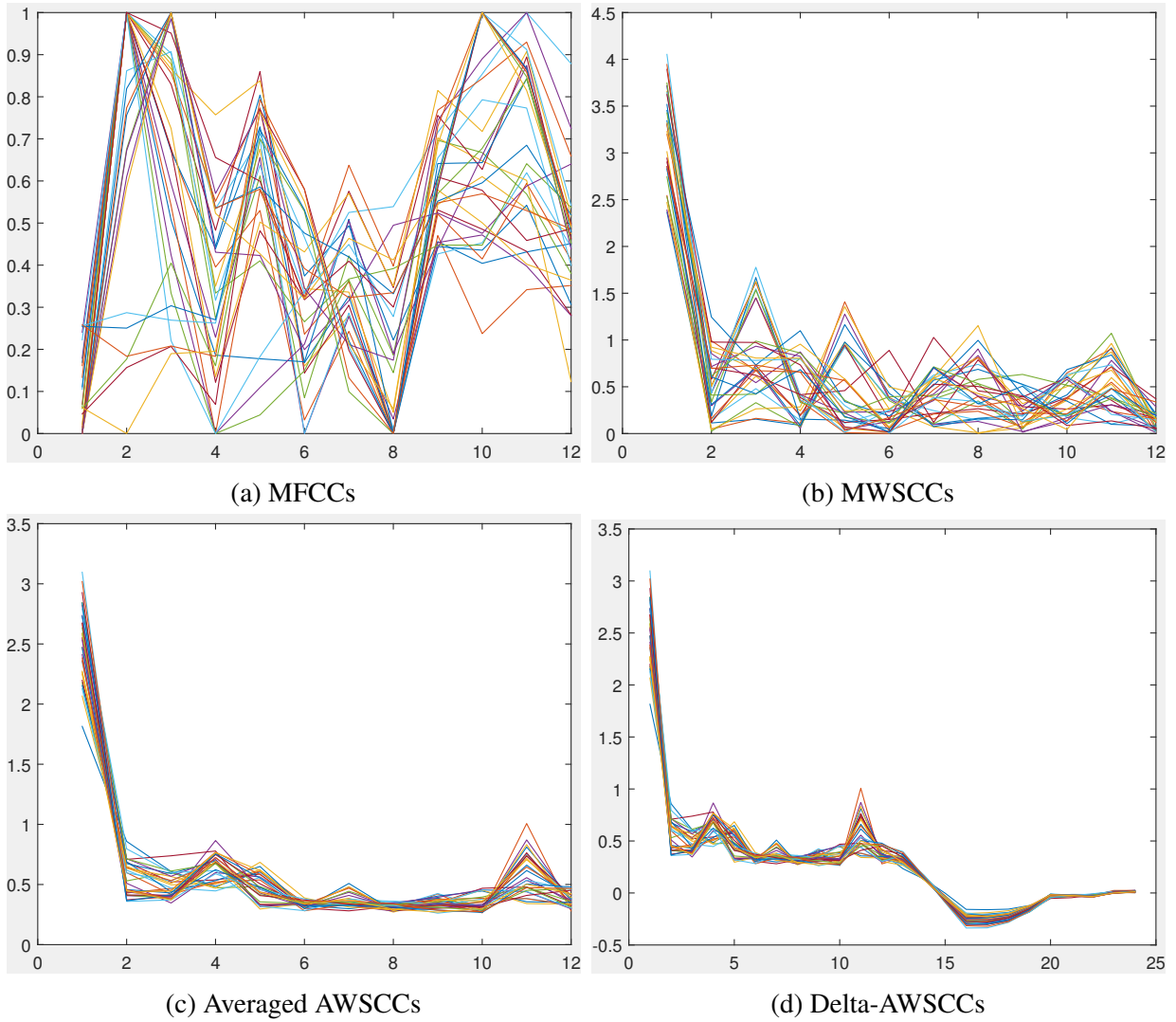


Figure 4.7: The feature vectors for 31 syllables of the single species, *Assa darlingtoni*. The x-axis is the feature index and y-axis is the feature value. Note that the feature vectors for averaged AWSCCs (c) and delta-AWSCCs (d) are more highly correlated than for the other two methods (a) and (b).

frequency range. In Table 4.8, the classification accuracy of SFs and MFCCs is lower than the other three features, at only 84.2% and 92.8%, respectively.

The statistical significance of the results is shown in Table 4.7. The classification accuracy of average AWSCCs is not significantly lower than the delta-AWSCCs. However, the classification accuracy of MWSCCs, MFCCs and SFs is significantly lower than delta-AWSCCs.

Since our wavelet packet tree for feature extraction is obtained based on the frog species to be classified, two more experiments are used for further evaluation. The first experiment is to classify first ten frog species (No.1-10); the second is to classify the first fourteen frog species (No.1-14) (see Table 4.1). The wavelet packet tree for classifying ten and fourteen frog species

Table 4.6: Classification accuracy of five features for the classification of twenty-four frog species using the SVM classifier. Here, Avg AWSCCs means the averaged AWSCCs.

Code	Classification accuracy (%)				
	SFs	MFCCs	MelCCs	Avg AWSCCs	Delta-AWSCCs
ADI	76.7 ± 15.3	80.0 ± 22.1	83.3 ± 16.7	100.0 ± 0.0	100.0 ± 0.0
CPA	86.7 ± 16.3	100.0 ± 0.0	93.3 ± 13.3	100.0 ± 0.0	100.0 ± 0.0
LCA	93.3 ± 15.3	100.0 ± 0.0	100.0 ± 0.0	100.0 ± 0.0	100.0 ± 0.0
LCS	70.0 ± 23.3	63.3 ± 27.7	96.7 ± 10.0	93.3 ± 13.3	96.7 ± 10.0
LFX	91.7 ± 8.3	93.3 ± 8.2	93.3 ± 8.2	100.0 ± 0.0	100.0 ± 0.0
LGA	30.0 ± 45.8	100.0 ± 0.0	100.0 ± 0.0	100.0 ± 0.0	100.0 ± 0.0
LLA	92.7 ± 8.1	98.7 ± 2.7	98.0 ± 4.3	100.0 ± 0.0	100.0 ± 0.0
LNA	78.6 ± 14.6	94.3 ± 9.5	95.7 ± 9.1	100.0 ± 0.0	100.0 ± 0.0
LRA	40.0 ± 30.0	10.0 ± 20.0	100.0 ± 0.0	90.0 ± 20.0	98.2 ± 6.5
LUA	60.0 ± 20.0	100.0 ± 0.0	86.7 ± 22.1	100.0 ± 0.0	100.0 ± 0.0
LVV	100.0 ± 0.0	96.7 ± 10.0	80.0 ± 22.1	93.3 ± 13.3	100.0 ± 0.0
MFS	90.0 ± 15.3	76.7 ± 21.3	90.0 ± 15.3	100.0 ± 0.0	100.0 ± 0.0
MFI	90.0 ± 30.0	100.0 ± 0.0	100.0 ± 0.0	100.0 ± 0.0	100.0 ± 0.0
PKN	90.0 ± 20.0	100.0 ± 0.0	100.0 ± 0.0	100.0 ± 0.0	100.0 ± 0.0
PCA	72.5 ± 20.8	77.5 ± 20.8	95.0 ± 10.0	92.5 ± 11.5	100.0 ± 0.0
PRI	45.0 ± 35.0	80.0 ± 33.2	100.0 ± 0.0	100.0 ± 0.0	100.0 ± 0.0
RSS	50.0 ± 50.0	100.0 ± 0.0	100.0 ± 0.0	100.0 ± 0.0	100.0 ± 0.0
ULA	93.3 ± 13.3	100.0 ± 0.0	100.0 ± 0.0	100.0 ± 0.0	100.0 ± 0.0

Table 4.7: Paired statistical analysis of the results in Table 4.6. For the classification accuracy of each frog species, the paired Student t-test was conducted [Tanton, 2005].

Pairs	t-test results
Delta-AWSCCs - Avg AWSCCs	t=1.95 (not significant)
Delta-AWSCCs - MWSCCs	t=3.41 (significant at p <0.01, df =17)
Delta-AWSCCs - MFCCs	t=2.91 (significant at p <0.01, df =17)
Delta-AWSCCs - SFs	t=5.52 (significant at p <0.001, df =17)

is shown in Figure 4.8, which is different from the tree for classifying eighteen frog species. However, the Mel-scaled wavelet packet tree is the same for all experiments (see Figure 4.9). The classification results are shown in Table 4.8. Since the classification accuracy with averaged AWSCCs is very high for classifying ten and fourteen frog species, the delta-AWSCCs is not included in this experiment. Table 4.8 shows that averaged AWSCCs can achieve the highest classification accuracy for classifying different numbers of frog species. Since the averaged AWSCCs is adaptively extracted based on the data, more frog species do not cause a large decrease in the classification accuracy.

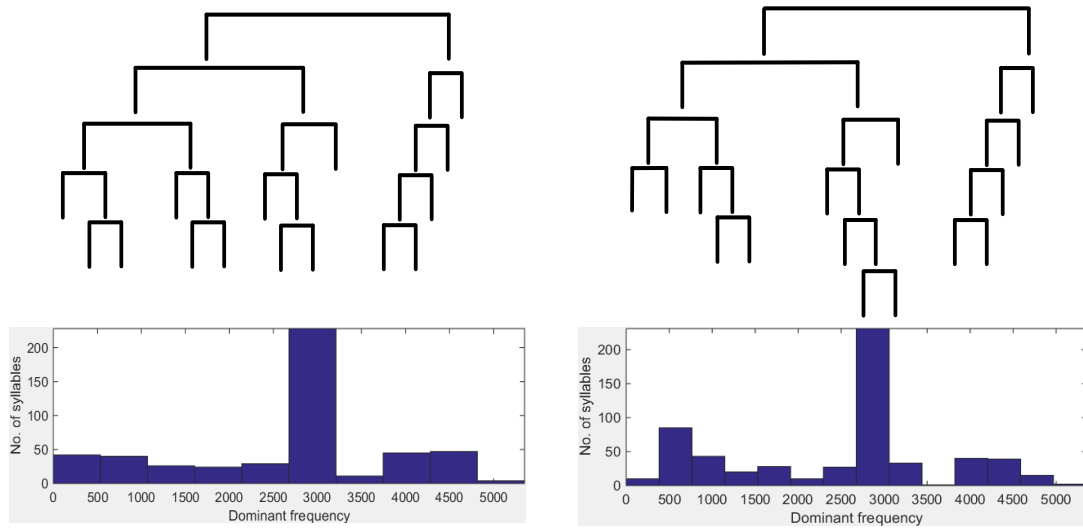


Figure 4.8: Wavelet packet tree based on adaptive frequency scale for classifying ten and fifteen frog species.

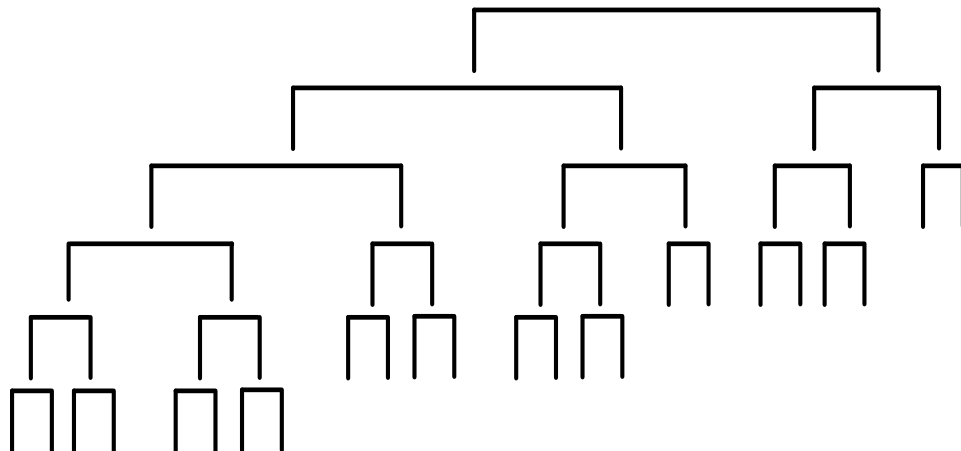


Figure 4.9: Mel-scaled wavelet packet tree for frog call classification.

Table 4.8: Classification accuracy (%) for classifying different number of frog species with four feature sets.

Features	SFs	MFCCs	MWSCCs	Averaged AWSCCs
18 frog species	84.2 ± 10.5	92.8 ± 11.0	97.6 ± 5.7	99.0 ± 4.6
14 frog species	89.6 ± 9.7	94.4 ± 8.5	99.2 ± 2.6	100.0 ± 0.0
10 frog species	94.6 ± 8.7	95.8 ± 8.6	100.0 ± 0.0	100.0 ± 0.0

4.3.4 Comparison under different SNRs

To further evaluate the robustness of the proposed feature, a Gaussian noise signal, with SNR of 40 dB, 30 dB, 20 dB, and 10 dB, is added to the original signal. The noise is added

after syllable segmentation, because this chapter focuses on the development of novel features for classification rather than the segmentation method. The classification accuracy with five features under different SNRs is shown in Figure 4.10. Compared with MFCCs and MWSCCs, SFs has a stronger anti-noise performance, because the dominant frequency of SFs has a small variation under low SNR. Correspondingly, the adaptive frequency scale also has a small variation, because it is generated by means of applying the k-means clustering algorithm to the dominant frequency. Therefore, our proposed feature has a stronger anti-noise performance than other cepstral features (MFCCs and MWSCCs).

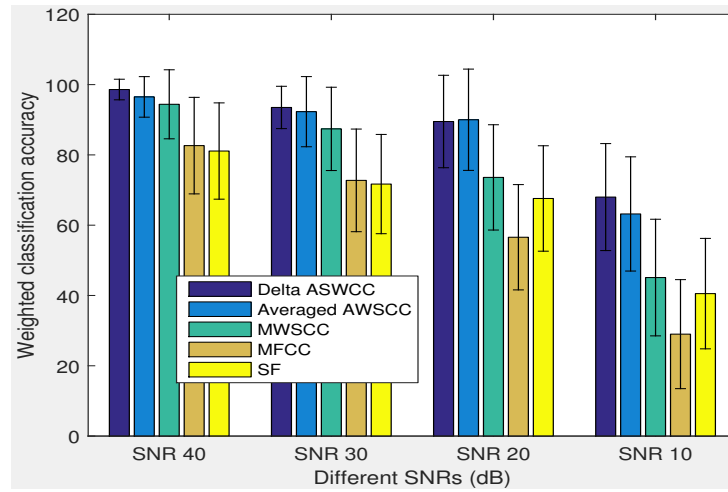


Figure 4.10: Sensitivity of five features for different levels of noise contamination.

4.3.5 Feature evaluation using the real world recordings

Table 4.9 shows the classification accuracy comparison using our proposed feature to classify eight frog species obtained from the JCU recordings. Since calls of some frog species in the JCU recordings do not have oscillation structure, SFs are not included for the comparison. Compared with other referred features, our proposed feature also achieves the best classification performance. Since the JCU recordings often have multiple calls from different frog species, spectral peak track occasionally can not capture the specific frog species (labelled species for that syllable), but other frog species to be classified; however, applying k-mean clustering to the dominant frequency calculated from the spectral peak track can reduce this deviation. Therefore, the frequency scale used for the WPD can be accurately achieved, which still leads to a high classification accuracy with the proposed feature.

Table 4.9: Classification accuracy using the JCU recordings.

Feature set	Classification accuracy (%)	
	k-NN	SVM
MFCCs	67.5 ± 13.2	70.8 ± 14.1
MWSCCs	90.4 ± 9.2	91.6 ± 8.7
Averaged AWSCCs	94.1 ± 6.3	94.5 ± 5.8
Delta-AWSCCs	97.0 ± 5.2	97.4 ± 5.4

4.4 Summary and limitations

In this chapter, a novel feature extraction method for frog call classification is developed using the adaptive frequency scaled wavelet packet decomposition. With segmented syllables, spectral peak track is first extracted from each syllable. Then, track duration, dominant frequency, and oscillation rate are calculated based on each track. Next, a k-means clustering algorithm is applied to the dominant frequency, which generates the frequency scale for WPD. Finally, a new feature set, AWSCCs, is calculated. Since the feature extraction method is developed based on the data itself, the wavelet packet tree varies according to the frog species to be classified. Compared with the Mel-scaled WPD tree, the proposed adaptive wavelet packet tree can better fit the dominant frequency distribution of the frog species to be classified. With the proposed frequency scale, the call characteristics of those frog species to be classified can be enhanced, while the background noise and calls from other animals will be suppressed. Therefore, the proposed feature sets can achieve a higher accuracy for the classification of frog calls than others. Meanwhile, since the frequency scale is calculated based on the dominant frequency of those frog species to be classified, our proposed wavelet tree structure is more accurate and efficient in classifying the frog calls when compared with Mel-scale (Figure 4.8 and Figure 4.9).

The feature extraction algorithm is designed for classifying frog calls. For frog calls, the typical structure in a spectrogram is frequency contour (named spectral peak track in this chapter) which is within a given frequency range starting at a given time [Mellinger et al., 2011]. For other organisms that have similar frequency contour structures such as the whistles of dolphins, and chirps of birds [Chen and Maher, 2006], spectral peak tracks can also be extracted from the spectrograms of their calls. Based on those spectral peak tracks, dominant frequency can be calculated. For the subsequent analysis, the features can be calculated using the same process as described in this chapter. For those organisms without clear frequency

contour structure, this proposed method can also be used by enhancing the frequency contour structure, which can be realised by applying a small window size and a large window overlap to the recording waveform.

The oscillation rate is calculated based on the spectrogram, which is generated by applying STFT to the waveform. However, when the temporal gap is smaller than the window size used for STFT, the oscillation structure will disappear. Therefore, finding new techniques for translating the 1-D signal to 2-D signal is our future direction. Since the frequency scale is generated based on the dominant frequency, this technique can be applied to other organisms that have clear frequency contour structure. Modifying this algorithm to those organisms without a clear frequency contour structure needs to be solved. This research also plans to include additional experiments that test a wider variety of audio data from different geographical and environment conditions. Other animal calls such as birds, insects, and whales can also be studied. Furthermore, the idea of developing new features based on the data itself will be explored.

Chapter 5

Multiple-instance multiple-label learning for the classification of frog calls with acoustic event detection

5.1 Overview

This chapter presents a method for the classification of simultaneously vocalising frog species in low signal-to-noise ratio (SNR) recordings. In Chapters 3 and 4, frog call classification is solved using a signal-instance single-label (SISL) framework, which cannot reflect the nature of automatically collected environmental recordings. Most automatically collected field recordings have low SNR and consist of multiple simultaneous animal vocal activities including frogs, birds, crickets, and so on. This character of environmental acoustic recordings makes the multiple-instance multiple-label (MIML) learning a suitable classification framework. To be specific, individual frog syllables in one audio clip are regarded as *multiple instance*, and the frog species included in that audio clip denote *multiple labels*. The key part of this MIML classification framework for studying frog calls is to detect individual syllables in environmental recordings with multiple simultaneously vocalising frog species. After syllable detection, standard acoustic features and MIML classifiers can be used to perform the MIML classification.

To evaluate our proposed MIML classification framework, a representative sample of 342 10-second recordings was exported from the database and split into training and testing sets. The performance is evaluated based on the MIML learning measures. Experimental results demonstrate that the MIML classification framework can be successfully adopted to classify

multiple simultaneously vocalising frog species in low SNR recordings.

5.2 Materials and methods

Our frog call classification system consists of four steps: signal processing, acoustic event detection, feature extraction, and classification (Fig. 5.1). Detailed description of each step is listed in the following sections.

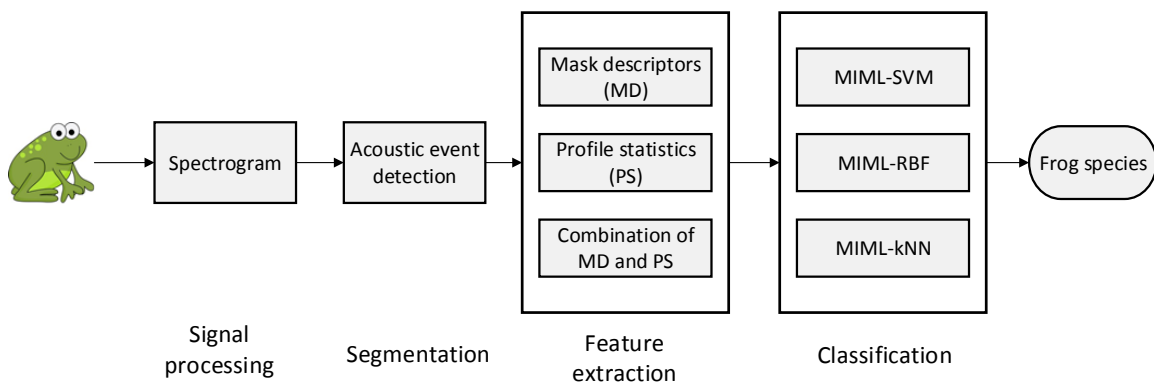


Figure 5.1: Flowchart of a frog call classification system using MIML learning

5.2.1 Materials

Digital recordings in this chapter were obtained with a battery-powered, weather-proof acoustic sensors. Recordings were two-channel, sampled at 22.05 kHz and saved in WAV format. In this chapter, a representative sample of 342 10-second recordings was selected to train and evaluate our proposed algorithm for predicting which frog species are present in a 10-second recording. All those examples were collected between February 2014 to April 2014, because it is the breeding season for frogs in Queensland, Australia with high calling activities. All the 10-second recordings were manually labelled by an ecologist with eight frog species: Cane-toad (CAD) ($F_0=560$ Hz), Cyclorana novaehollandiae (CNE) ($F_0=610$ Hz), Limnodynastes terraereginae (LTE) ($F_0=610$ Hz), Litoria fallax (LFX) ($F_0=4000$ Hz), Litoria nasuta (LNA) ($F_0=2800$ Hz), Litoria rothii (LRI) ($F_0=1800$ Hz), Litoria rubella (LRA) ($F_0=2300$ Hz), and Uperolela mimula (UMA) ($F_0=2400$ Hz). Here, F_0 is the averaged dominant frequency for each frog species. Each recording includes between 1 and 5 species. Following the prior work of Briggs et al. [2012], we assume that recordings without frog vocalisations can be filtered out during the acoustic event detection process.

5.2.2 Signal processing

All the recordings were first re-sampled at 16 kHz and mixed to mono. A spectrogram was then generated by applying short-time Fourier transform (STFT) to each recording. Specifically, each recording was divided into frames of 512 samples with 50% frame overlap. A fast Fourier transform was then performed on each frame with a Hamming window, which yielded amplitude values for 256 frequency bins, each spanning 31.25 Hz. The final decibel values (S) were generated as

$$S_{tf} = 20 * \log_{10}(A_{tf}) \quad (5.1)$$

where A denotes the amplitude value, $t = 0, \dots, T - 1$ and $f = 0, \dots, F - 1$ represent time and frequency index, T and F are 256 frequency bins and 625 frames, respectively.

5.2.3 Acoustic event detection for syllable segmentation

The aim of acoustic event detection (AED) is to detect a specified acoustic event in audio data. In this chapter, we use AED for frog syllable segmentation. Since all the recordings are collected from the field, there are many overlapping vocal activities from different sources. Traditional methods for frog syllable segmentation are based on time domain information Huang et al. [2009], Somervuo et al. [2004], which cannot address those recordings. Here, we modified the AED method developed by Towsey et al. Towsey et al. [2012] for syllable segmentation. The detail of our AED method is described as follows:

Step 1: Wiener filtering

A 2-dimensional Wiener filter is applied to the spectrogram image over a 5×5 time-frequency grid for reduce the background graininess, where the filter size is selected after the consideration of trade-off between removing the background graininess and blurring the acoustic events.

$$\hat{S}_{tf} = \mu + \frac{(\sigma^2 - \nu^2)}{\sigma^2} (S_{tf} - \nu) \quad (5.2)$$

where μ and σ^2 are local mean and variance, respectively; ν^2 is the noise variance estimated by averaging all local variances.

Step 2: Spectral subtraction

Wiener filtering can successfully remove the graininess, but some noises, such as wind, insect,

motor engine that cover the whole recording can not be addressed using Wiener filtering. Here, a modified spectral subtraction method is employed to deal with those noises.

Algorithm 2: Modified Spectral Subtraction

Data: \hat{S}_{tf} , spectrogram after Wiener filtering.
Result: $\hat{S}'_{tf} = \hat{S}_{tf}$, noise reduced spectrogram.
begin

- Construct** an array of the modal noise values for all frequency bins;
- for** $f \in F$ **do**
 - 1. calculate the histogram of the intensity value over each frequency bin
 - 2. smooth the histogram array with a moving average window of size 7
 - 3. regard the modal noise intensity at the position of maximal bin in the left-side of the histogram
- Smooth** the array with a moving average filter with window of size 5;
- for** $f \in F$ **do**
 - 1. subtract the modal noise intensity
 - 2. truncated negative decibel values to zero

Step 3: Adaptive thresholding

After noise reduction, the next step is to convert a noise reduced spectrogram \hat{S}'_{tf} into the binary spectrogram S'_{tf}^b for the event detection. Here, an adaptive thresholding method named *Otsu thresholding* Otsu [1975] is employed to find an optimal threshold.

$$\phi_b^2(k) = w_1(k)w_2(k)[\mu_1(k) - \mu_2(k)]^2 \quad (5.3)$$

where $w_1(k) = \sum_0^k p(j)$ is calculated from the histogram as k , $p(j) = n(j)/N$ are the values of the normalised gray level histogram, $n(j)$ is the number of values in level j , N is the total number of values over the whole spectrogram image, $\mu_1(k) = [\sum_0^k p(j)x(j)]/w_1$, $x(j)$ is the value at the center of the j th histogram bin. Then, the threshold, T_0 , is calculated as

$$T_0 = (\phi_{b1}^2(k) + \phi_{b2}^2(k))/2 \quad (5.4)$$

Step 4: Events filtering using dominant frequency and event area

Since not all detected events correspond to frog vocalisations, to further remove those events that are not from the listed frog species in section 5.2.1, dominant frequency (F_0) and area of the event (Ar) are used for filtering.

Step 5: Region growing

Algorithm 3: Event filtering based on dominant frequency and event area

Data: S_{tf}^b , spectrogram; $t_s(n)$, $t_e(n)$, $f_l(n)$, $f_h(n)$, location of each acoustic event n ; $F_0(i)$, dominant frequency of frog species i .

Result: \tilde{S}_{tf} , spectrogram after events filtering.

begin

Calculate the area of each acoustic event n .

$$Area(n) = (t_e(n) - t_s(n)) * (f_h(n) - f_l(n))$$

for $n \in N_{e1}$ **do**

if $Ar(n) \geq Ar_l$ **then**

split event n into small events

where Ar_l is set as 3000 pixels.

Filter events using dominant frequency $f_d(n) = \sum_{t=t_s(n)}^{t_e(n)} F(t)/t_e(n) - t_s(n)$

where $F(t)$ is the peak frequency of each frame within the event area

for $n \in N_{e2}$ **do**

for $i \in I$ **do**

if $f_d(n) \geq F_0(i) + \theta$; $f_d(n) \leq F_0(i) - \theta$ **then**
 style="padding-left: 3em;"> $f_d(n) = 0$;

where θ is frequency range and set as 300 Hz.

Remove small acoustic events except frequency band between θ_l and θ_h

for $n \in N_{e2}$ **do**

if $Ar(n) \leq Ar_s$ **then**
 style="padding-left: 2em;">remove event n

where Ar_s is set as 300 pixels, θ_l and θ_h are set as 300 Hz and 800 Hz, respectively.

Because the area of LTE is smaller than Ar_s .

A region growing algorithm is used to obtain the contour of the particular acoustic event Mallawaarachchi et al. [2008]. To get the accurate boundary of each acoustic event and improve the discrimination of extracted features, a 2-dimensional region growing algorithm is applied to obtain the accurate event shape within each segmented event. First, a maximal intensity value within the event area is selected as the seed point. Then, the neighbourhood pixels of the seed(s) above the threshold are located and assigned to the output image, and new added pixels are used as seeds for further processing. Finally, when all the pixels that satisfy the criteria are added to the output image, the recursive algorithm will stop and get the final results (Figure 5.3). Here, the threshold value is empirically set as 5 dB.

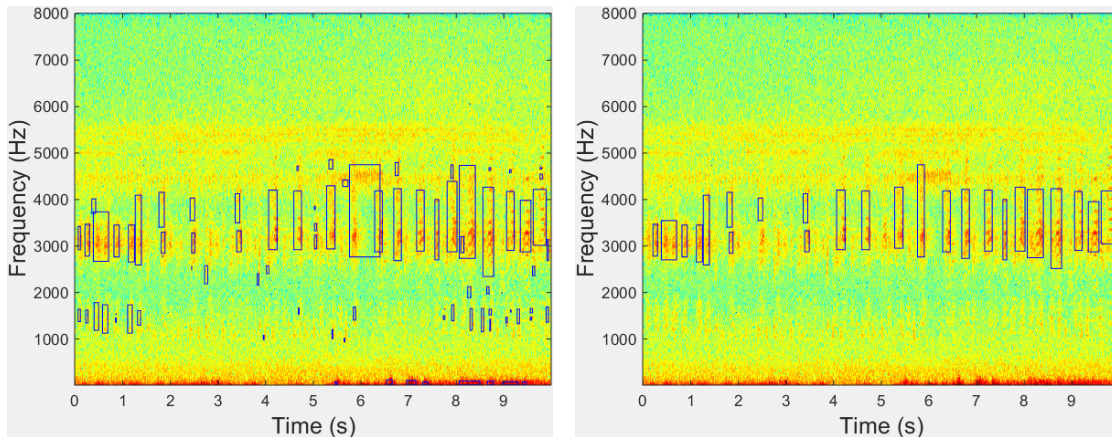


Figure 5.2: Acoustic event detection results before (Left) and after (Right) event filtering based on dominant frequency. Here, blue rectangle means the time and frequency boundary of each detected event.

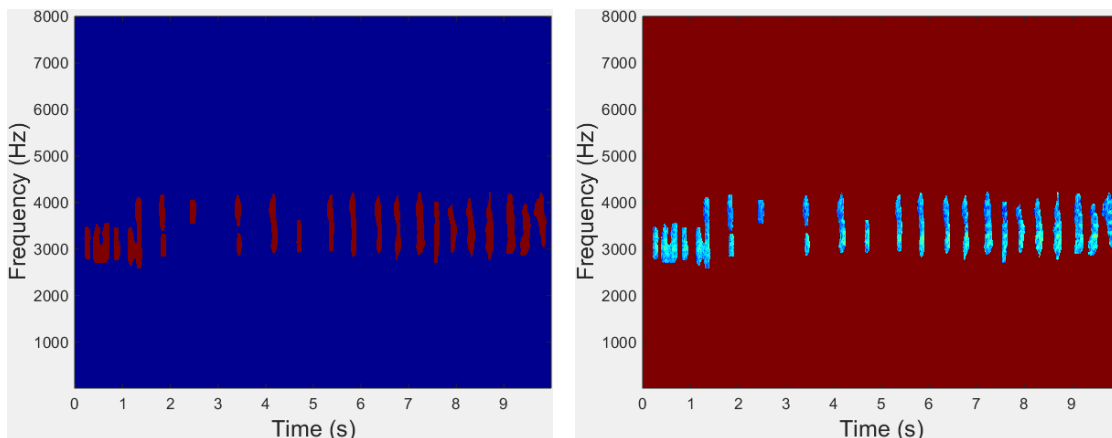


Figure 5.3: Acoustic event detection results after region growing. Left: binary segmentation results; Right: segmented frog syllables.

5.2.4 Feature extraction

Based on acoustic event detection results, two feature representations are first calculated to describe each event (syllable): mask descriptors and profile statistics Briggs et al. [2012]. Here, we exclude *histogram of orientation (HOG)* from our feature set, because the previous studies have already demonstrated its lowest classification accuracy Briggs et al. [2012], Ruiz-Munoz et al. [2015]. For mask descriptors, it is used to describe the syllable shape including minimum frequency, maximum frequency, bandwidth, duration, area, perimeter, non-compactness, rectangularity. For profile statistics, there are time-Gini, frequency-Gini, frequency-mean, frequency-variance, frequency-skewness, frequency-kurtosis, frequency-max, time-max, mask-mean, and mask standard deviation. The third feature set consists of all features.

5.2.5 Multiple-instance multiple-label classifiers

After feature extraction, three MIML algorithms are evaluated for the classification of multiple simultaneous vocalising frog species: MIML-SVM, MIML-RBF, and MIML-kNN. With the form of event-level distance measure, the MIML problem can be reduced to a single-instance multiple-label problem by associating each event with an event-level feature Briggs et al. [2012]. Here, the maximal and average Hausdorff distances between two syllables are used by MIML-SVM and MIML-RBF, separately. For MIML-kNN, the nearest neighbour is used to assign syllable-level features.

5.3 Experiment results

5.3.1 Parameter tuning

There are three modules, the parameters of which need to be discussed: signal processing, acoustic event detection, and classification. For signal processing, the window size and overlap are 512 samples and 50%, respectively. During the process of acoustic event detection, four thresholds for event filtering need to be determined, which are small and large area threshold, and frequency boundary for events filtering. All those thresholds were determined empirically by applying various combinations of thresholds to a small number of randomly selected 10-second clips. For MIML-SVM classifiers, the parameters used are (C, γ, r) and set as $(0.1,$

0.6, 0.2) experimentally. For MIML-RBF, the parameters are (r, μ) and set as (0.1, 0.6). For MIML-kNN, the number of references (k) and citers (k') are 10 and 20, respectively.

5.3.2 Classification

In this chapter, all the algorithms were programmed in Matlab 2014b. Each MIML algorithm is evaluated with five-fold cross-validation on the collection of 342 species-labelled recordings. Five evaluation rules are used for comparing the performance with the combination of three feature representations and three ML algorithms: Hamming loss, Rank loss, Average precision, One error, Example based F1, and Micro F1 [Madjarov et al., 2012, Zhou et al., 2008]. The value range of all five evaluation rules is between 0 to 1. The definition of each evaluation rule is described as follows:

1) Hamming loss is defined as the fraction of labels that are incorrectly predicted for an instance and the normalised Hamming loss which is normalised over instances is reported. This metric is defined as

$$hammingLoss = \frac{1}{N} \sum_{i=1}^N \frac{1}{Q} |h(x_i) \Delta y_i| \quad (5.5)$$

where Δ denotes the symmetric difference between two instances, N is the number of instances and Q is the total number of possible labels. y_i denotes the ground truth of instance x_i , and $h(x_i)$ denotes the predictions for the same instance.

2) Ranking loss evaluates the average fraction of label pairs that are reversely ordered for the particular instance given by

$$rankingLoss = \frac{1}{N} \sum_{i=1}^N \frac{|D_i|}{|y_i||\bar{y}_i|} \quad (5.6)$$

where $D_i = (\lambda_m, \lambda_n) | f(x_i, \lambda_m) \leq f(x_i, \lambda_n), (\lambda_m, \lambda_n) \in y_i \times \hat{y}_i$, while \bar{y} denotes the complementary set of y in L , and $L = \lambda_1, \lambda_2, \lambda_3, \dots, \lambda_Q$, λ represents the label.

3) Average precision is the average fraction of labels that are ranked higher than an actual label belonging to an instance.

$$precision = \frac{1}{N} \sum_{i=1}^N \frac{h(x_i) \cap y_i}{|y_i|} \quad (5.7)$$

4) One error evaluates how many times the top-ranked label is not in the set of relevant labels

of the instance. This evaluation metric is defined as

$$oneError = \frac{1}{N} \sum_{i=1}^N [[argmax_{\lambda \in y} f(x_i, \lambda)] \notin y_i] \quad (5.8)$$

5) Exampled based F_1 is the average of the harmonic mean of instance-precision and instance-recall for every instance. The instance-precision is defined for an instance as the size of the intersection of the set of its predicted labels and the set of its ground truth labels divided by the size of the set of its predicted labels. The instance-recall is defined for an instance as the size of the intersection of the set of its predicted labels and the set of its ground truth labels divided by the size of the set of its ground truth labels.

$$macroF_1 = \frac{1}{Q} \sum_{j=1}^Q \frac{2 \times p_j \times r_j}{p_j + r_j} \quad (5.9)$$

where p_j and r_j are the precision and recall for all $\lambda_h \in h(x_i)$ from $\lambda_j \in y_j$.

6) Micro F_1 is the harmonic mean of micro-precision and micro-recall, where micro-precision and micro-recall are the precision and the recall which are averaged over all instances and label pairs.

$$microF_1 = \frac{2 \times microPrecision \times microRecall}{microPrecision + microRecall} \quad (5.10)$$

The values for Hamming loss, rank loss, one-error, coverage, and micro-AUC range from 0 to 1. For Hamming loss, Rank loss, one-error and coverage, 0 denotes the perfect result, and 1 means the wrong prediction of all labels over every instance, whereas for micro-AUD, the values have the completely opposite meanings.

The $\frac{positive}{negative}$ is defined as $1 - hammingLoss$ and it is 0.818 for MIML-RBF with Mask descriptors (MD). MD and profile statistical (PS), and all features (AF) are put into the three classifiers, respectively. The accuracy measure for each MIML classifier is shown in Table 5.1. Here, the best classification accuracy is achieved using MIML-RBF with MD. For each classifier, the classification accuracy of MD is higher than PS and AF, which indicates that the event shape has a better discriminability than the event content. To give a concrete view of predictions, the results of five randomly selected recordings using MIML-RBF are shown in Table 5.2. From the table, we can see that recordings of No.1 and No.3 are accurately predicted.

Table 5.1: Accuracy measures for MIML classifiers with different feature representations. Here, \downarrow indicates the smaller the better, while \uparrow indicates the bigger the better.

Feature	Algorithm	Hamming loss \downarrow	Rank loss \downarrow	One-error \downarrow	Coverage \downarrow	Micro-AUC \uparrow
MD	MIML-SVM	0.253	0.186	0.308	3.147	0.745
MD	MIML-kNN	0.205	0.153	0.298	2.647	0.771
MD	MIML-RBF	0.182	0.132	0.223	2.352	0.828
PS	MIML-SVM	0.239	0.208	0.323	3.544	0.728
PS	MIML-kNN	0.211	0.153	0.298	2.647	0.777
PS	MIML-RBF	0.186	0.161	0.338	3.161	0.746
AF (MD+PS)	MIML-SVM	0.261	0.199	0.279	3.588	0.761
AF (MD+PS)	MIML-kNN	0.205	0.160	0.264	2.735	0.787
AF (MD+PS)	MIML-RBF	0.191	0.142	0.220	2.632	0.821

Table 5.2: Example predictions with MIML-RBF.

No.	Ground truth	Predicted labels
1	UMA	UMA
2	LNA, LRI, UMA	LNA, LRA, UMA
3	LNA, UMA	LNA, UMA
4	LNA, LFX, LRA	LNA, LFX, LRI, LRA
5	LNA, LFX, LRA	LNA, LRA

5.4 Discussion

Since most recordings used in this chapter consist of multiple simultaneously vocalising frog species, the traditional single-instance single-label classification framework is no longer suitable. A novel framework for the classification of multiple simultaneous vocalising frog species in environmental recordings is proposed, which is adopted from Briggs et al. [2012], a study on birds. Differently from that work, this research designs a new acoustic event detection method for syllable segmentation rather than using a supervised learning algorithm. It is because there is a lack of lots of annotated frog recordings. As for the classification results, our proposed framework can achieve an acceptable classification accuracy. All the features used in this study are calculated from the segmented syllables. The accuracy of the segmentation results will therefore directly affects the final classification performance.

5.5 Summary and limitations

In this chapter, we propose a novel framework for the classification of multiple simultaneous vocalising frog species in environmental recordings. To the best of our knowledge, this is the first study that focuses on the frog recordings using the MIML algorithm. Since frogs tend to call simultaneously, the MIML algorithm is more suitable for dealing with those recordings than single-instance single-label classification. After applying an acoustic event detection algorithm to 10-second recordings, frog syllables are segmented. Then, three feature representations, MD, PS, and AF, are calculated from those segmented syllables. Finally, three MIML classifiers are used for the classification of frog calls with the best true positive/negatives of 81.8%. Future work will focus on the study of novel features and MIML classifiers to further improve the classification performance. Current classification results are highly affected by the syllable segmentation results, and the use of AED can not accurately segment all the syllables. One solution is to prepare an annotated dataset and apply supervised learning algorithms for the segmentation task. Another is to use a different classification framework, which does not need the segmentation process.

Chapter 6

Detecting frog calling activity based on acoustic event detection and multi-label learning

6.1 Overview

This chapter describes the research conducted for detecting frog calling activity (frog abundance and frog species richness). Compared with Chapter 5, acoustic event detection is used to predict the present or absence of eight specific frog species. Here frog abundance is calculated based on the area and content of each segmented event. In Chapter 5, acoustic features are calculated based on the results of acoustic event detection (AED) to predict frog species richness, but the accuracy of AED results directly affect the multiple-label multiple-instance (MIML) classification performance. To reduce the bias introduced by AED, this research presents a global feature representation for the classification of recordings with simultaneous vocalising frog species. This feature representation regards all the frog species in each individual recording as a whole. Therefore, the classification process can be framed as multiple-label (ML) learning.

Compared with that described in Chapter 5, three global feature representations are calculated to classify each segmented recording: linear predictive coding (LPC), MFCCs and wavelet-based features. The wavelet-based features are similar with the features used in Chapter 4. The difference is that we divide *adaptive WPD sub-band cepstral coefficients* into three equal stages to capture more temporal information.

Furthermore, this proposed classification framework is conducted for a long-term analysis. The frog calling activity during the breeding season is calculated. Also, the correlation between

the frog calling activity and weather variables is studied for finding the relationship between frog calls and environments.

6.2 Materials and methods

The architecture of this frog calling activity detection system is shown in Figure 6.1. The system consists of three parts: frog abundance detection, frog species richness detection, and correlation analysis. Each part is discussed in detail in the following subsections.

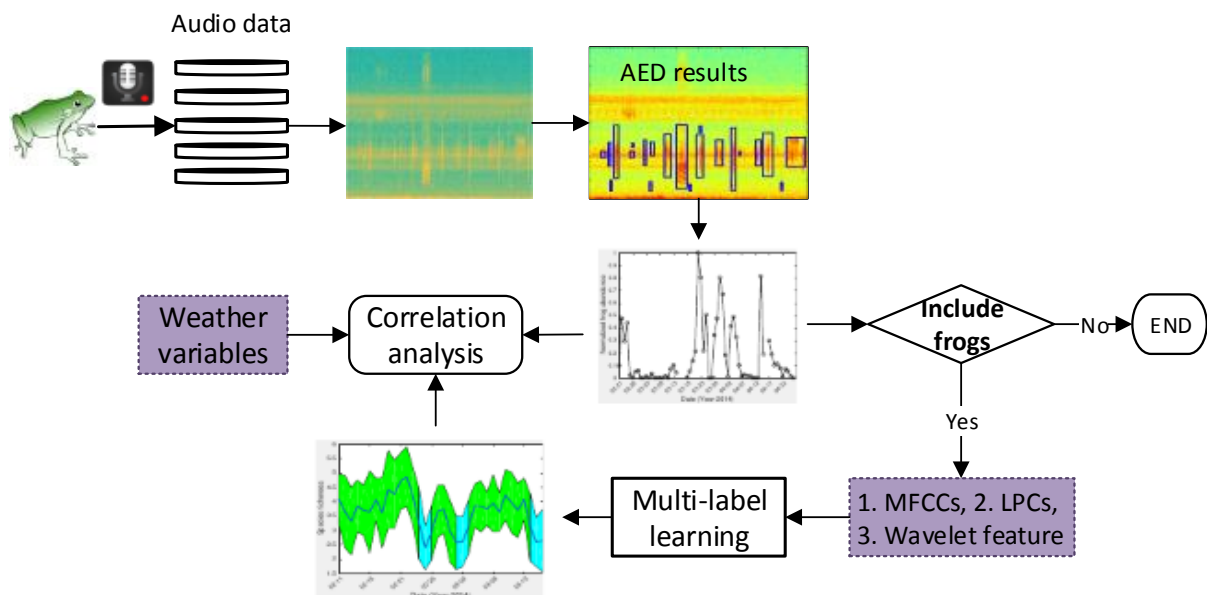


Figure 6.1: Flowchart of a frog call classification system using multi-label learning

6.2.1 Acquisition of frog call recordings

All recordings selected for this chapter were obtained from three sites in Queensland, Australia: *Kiyomi dam*, *Stony creek dam* and *BG creek dam*, using a battery-powered acoustic sensor (stored in a weather proof metal box) with an external microphone. The recordings were stored on 16 GB SD cards in 64 kbps MP3 mono format. All recordings were collected from February, 2014 to April, 2014, because it is the breeding season in Queensland when male frogs make calls to attract females for the purpose of reproducing. All recordings started around sunset, finished around sunrise every day and have 12 hour duration. This study sampled 10-second recordings every 10 minutes for those continuous recordings. There are 4170, 4908, and 1544 10-second recordings for *Kiyomi dam*, *Stony Creek dam* and *BG Creek dam* respectively, because of data

loss. A representative sample of 342 10-second recordings was selected to train and evaluate the proposed method. The ground truth of those 342 10-second recordings is generated by a frog expert, who manually tagged each recording with frog species.

We first manually inspected spectrograms of ten randomly selected call examples for each frog species. Two parameters, dominant frequency and syllable duration, were then measured and averaged, as listed in Table 6.1, which are used as prior information for subsequent analysis.

Table 6.1: Dominant frequency (F_0) and syllable duration (T_s) of eight frog species averaged for ten randomly selected syllables.

Frog species	Code	Dominant frequency (Hz)	Syllable duration(ms)
<i>Canetoad</i>	CAD	560	NA
<i>Cyclorana novaehollandiae</i>	CNE	610	400
<i>Limnodynastes terraereginae</i>	LTE	610	100
<i>Litoria fallax</i>	LFX	4000	280
<i>Litoria nasuta</i>	LNA	2800	160
<i>Litoria rothii</i>	LRI	1800	500
<i>Litoria rubella</i>	LRA	2300	580
<i>Uperolela mimula</i>	UMA	2400	120

6.2.2 Frog abundance monitoring

Frog abundance is monitored through the detection of acoustic events in a spectrogram image. Here, the spectrogram was generated by applying short-time Fourier transform (STFT) to each 10-second recording. Acoustic event detection, which consists of multiple image processing steps, is modified from our previous study [Xie et al., 2015d] and summarised as follows.

Step 1: Wiener filter

To de-noise and smooth the spectrogram, a 2-dimensional Wiener filter is applied to the spectrogram image over a 5×5 time-frequency grid, where the filter size is selected after the consideration of trade-off between removing the background graininess and blurring acoustic events.

$$\hat{S}_{tf} = \mu + \frac{(\sigma^2 - \nu^2)}{\sigma^2} (S_{tf} - \nu) \quad (6.1)$$

where μ and σ^2 are local mean and variance, respectively. ν^2 is the noise variance estimated by averaging all local variances.

Step 2: Spectral subtraction

After Wiener filtering, the graininess has been removed. However, some noises such as wind,

insect, and motor engine, which cover the whole recording, still remained. Here, a modified spectral subtraction is employed for dealing with those noises. Description of this algorithm can be found in our previous study Xie et al. [2016].

Step 3: Adaptive thresholding

Following noise reduction, the next step is to convert the noise reduced spectrogram \hat{S}'_{tf} into the binary spectrogram S^b_{tf} for events detection. Here, an adaptive thresholding method named *Otsu thresholding* Otsu [1975] is employed to find an optimal threshold.

$$\phi_b^2(k) = w_1(k)w_2(k)[\mu_1(k) - \mu_2(k)]^2 \quad (6.2)$$

where $w_1(k) = \sum_0^k p(j)$ is calculated from the histogram as k , $p(j) = n(j)/N$ are the values of the normalised gray level histogram, $n(j)$ is the number of values in level j , N is the total number of values over the whole spectrogram image, $\mu_1(k) = [\sum_0^k p(j)x(j)]/w_1$, $x(j)$ is the value at the centre of the j th histogram bin. Then, the threshold, T_0 , is calculated as

$$T_0 = (\phi_{b1}^2(k) + \phi_{b2}^2(k))/2 \quad (6.3)$$

Step 4: Events filtering using dominant frequency and event area

To further remove those events that do not belong to the frog species shown in Table 6.1, dominant frequency (F_0) and area (number of pixels) within the event boundary (Ar) are used for filtering. First, large acoustic events, whose area is larger than A_{large} , are separated into small events, because the area of frog calls to be classified in Table 6.1 is empirically smaller than A_{large} . Then, dominant frequency is used to filter the events. First, the averaged frequency is calculated by averaging the peak frequency within each acoustic event. Then, the event, the averaged frequency of which is not within allowed fluctuation in both sides of dominant frequency, is discarded. Finally, small acoustic events, the area of which are smaller than A_{small} , are filtered. Those events, with average frequency of between 300 Hz and 800 Hz, are not filtered out using A_{small} , because the area of LTE (averaged frequency is between 300 Hz and 800 Hz) is smaller than A_{small} . Figure 6.2 shows the acoustic event detection results.

To calculate frog abundance of each segmented recording, the frog abundance is calculated as follows.

$$F_{abun} = \sum_{n=1}^N A_{i,j}(n)^2 \quad (6.4)$$

Here, $A_{i,j}$ represents the decibel value of location (i, j) within each acoustic event n in the spectrogram.

6.2.3 Wavelet-based feature extraction for species richness analysis

Frog species richness is calculated by tagging each segmented recording. Since many segmented recordings consist of multiple frog species, one direct solution is to assign each recording with a set of labels (frog species) for explicitly expressing its semantics Zhang and Zhou [2014]. Therefore, multi-label learning is adopted to tag each segmented recording.

Extracting discriminating features, which maximise between-group (inter-specie) dissimilarity and minimise within-group (intra-specie) dissimilarity, is very important for achieving high classification performance Bedoya et al. [2014], Huang et al. [2009]. In this chapter, feature extraction is performed based on wavelet packet decomposition using a modified version of the method introduced in Chapter 4 and detailed below.

For feature extraction, constructing a suitable frequency scale for a wavelet packet (WP) tree based on the dominant frequency of each frog species is the first step, because different frog species tend to have different dominant frequencies Gingras and Fitch [2013]. In Chapter 4, k-means clustering was first applied to the extracted dominant frequencies of training data. Then, the frequency scale was built by sorting clustering centroids to construct the WP tree. In this chapter, the prior information on dominant frequency (F_0) obtained from Table 6.1 is directly used to construct the WP tree. We iteratively detect each WP tree sub-band node until the frequency range of each node includes more than one dominant frequency F_0 . Then, the WP tree of that particular sub-band node will be further split until each sub-band node has only one dominant frequency value or none. After constructing the frequency scale, adaptive frequency scaled wavelet packet decomposition is applied to each segmented recording for feature extraction.

For each 10-second recording, it is represented as $y(n)$, $n = 1, \dots, N$, where N is the length of each recording. Based on the $y(n)$, detailed description for WP-based feature extraction is listed as follows:

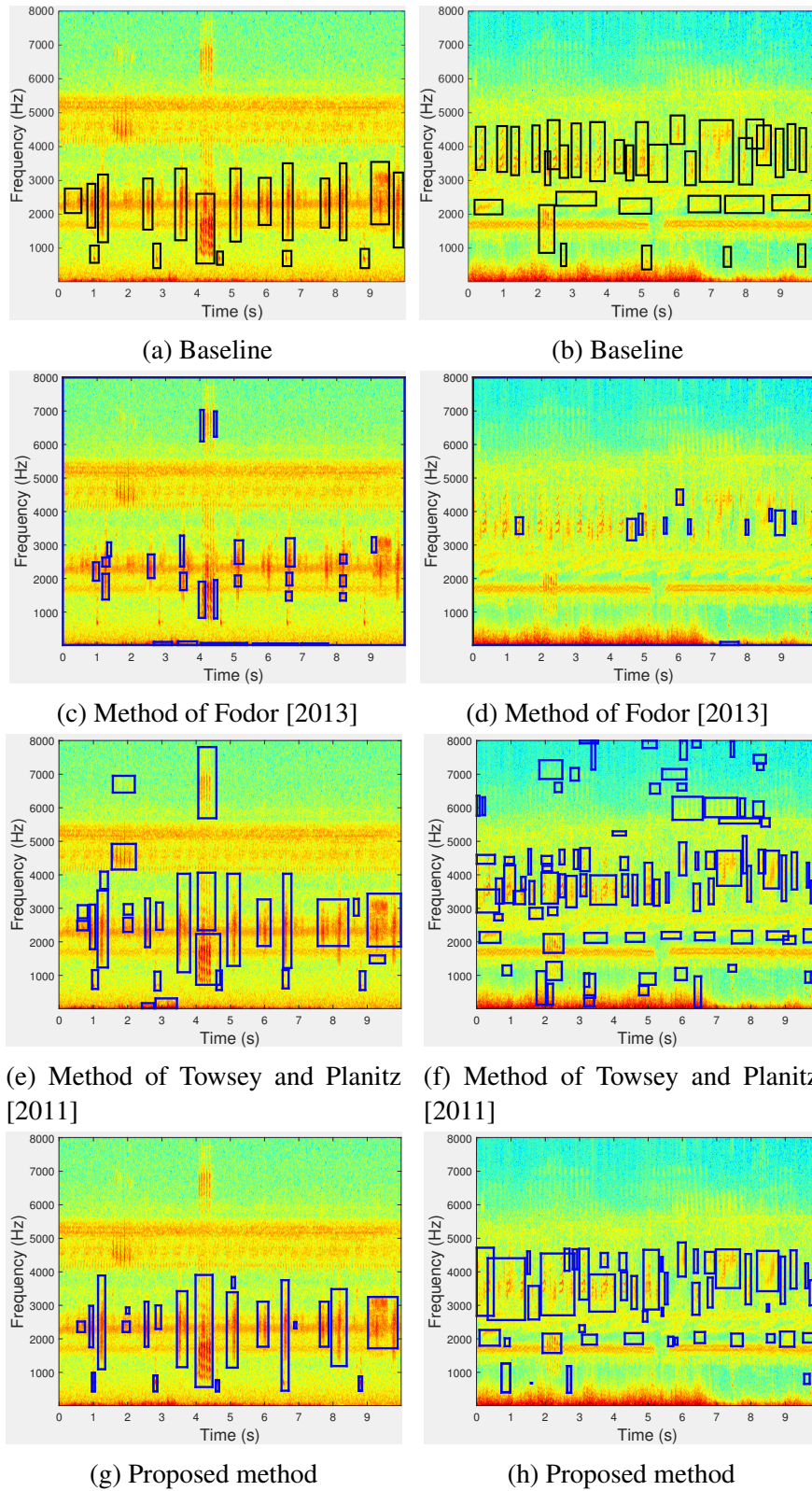


Figure 6.2: Acoustic event detection for frog abundance monitoring using different methods. For each row, different methods are applied to the same recordings. The baseline of the detection results is shown in the first row; detected frog calls are drawn using a blue rectangle. For each column, different methods are used for the same recording.

Step 1: Add a Hamming window to the signal $y(n)$ and perform wavelet packet decomposition spaced in adaptive frequency scale as described in [Xie et al., 2016].

$$WP(i, j) = \sum_{i=1}^M y(n)w(n)\psi_{(a,b)}(n) \quad (6.5)$$

where $w(L)$ is the Hamming window function, $WP(i, j)$ is the wavelet coefficients of the decomposition, i is the sub-band index, j is the index of wavelet coefficients, $\psi_{(a,b)}(n)$ is the wavelet base function, and 'db4' is used experimentally. Here, a and b are the scale and shift parameters, respectively.

Step 2: Calculate the total energy of each sub-band.

$$WP_i = \sum_{j=1}^{M_i} [WP(i, j)]^2 \quad (6.6)$$

where $i = 1, 2, \dots, T$, and T is the total number of sub-band, and $j = 1, 2, \dots, M_i$, M_i is the total number of wavelet coefficients.

Step 3: Normalise the energy of each sub-band.

$$SE_i = \frac{WP_i}{M_i} \quad (6.7)$$

where $i = 1, 2, \dots, T$.

Step 4: Perform discrete cosine transform on the logarithm sub-band energy for dimension reduction and obtain the WP-based feature.

$$WP_{base}(d) = \sum_{i=1}^T \log SE_i \cos\left(\frac{d(i - 0.5)}{T}\pi\right) \quad (6.8)$$

where $d = 1, 2, \dots, d'$, $1 \leq d' \leq T$, here d' is the dimension of WP-based feature, and set as 12.

Differently from that described in Chapter 4, the recording is first segmented into frames using a Hamming window. Then, all frames are divided into three equal parts, and the WP-feature within each part is averaged, respectively, because different frog species within similar frequency bands may exist in one 10-second recording, segmenting each recording into small parts might be able to keep the information of different frog species in the same frequency band. Besides the WP-based feature, two other acoustic features, linear predictive coefficients (LPCs)

and Mel-frequency Cepstral coefficients (MFCCs), are calculated for the comparison.

6.2.4 Multi-label classification for species richness analysis

Since many segmented recordings consist of calls from multiple frog species, frog call classification can be framed as a multi-label classification problem. However, previous studies have not adopted multi-label learning to classify frog calls. Therefore, it is worth investigating different multi-label learning algorithms for the classification of multiple vocalising frog species. In this chapter, four multi-label learning algorithms, whose base classifier is a C4.5 decision tree, are employed: binary relevance (BR), classifier chains (CC), random k-labEL Pruned Sets (RAKEL and RAKEL1) Zhang and Zhou [2014]. The default parameter settings of those four multi-label learning algorithms are used. The trained classifier, which achieves the best classification performance, is then used to tag the rest recordings. After tagging each 10-second recording, frog species richness is lastly calculated as follows.

$$F_{rich} = \frac{\sum_{k=1}^K f_{rich}(k)}{K} \quad (6.9)$$

where $f_{rich}(k)$ is the number of frog species of each tagged 10-second recording, K is the number of 10-second recording for each day.

6.3 Experiment results

6.3.1 Experiment setup

Each 10-second recording is divided into frames of 512 samples and 50% frame overlap for STFT. A_{large} and A_{small} , which are used for area filtering in acoustic event detection, are empirically set at 3000 pixels and 300 pixels, respectively. Allowed fluctuations in both sides of dominant frequency are 300 Hz for dominant frequency filtering. For WP-based feature, window size and overlap are 512 samples and 50%, the window function is a Hamming window. All algorithms were programmed in Matlab 2014b except multi-label learning, which was implemented in Meka 1.7.7⁴.

⁴<http://meka.sourceforge.net/>

6.3.2 Frog abundance detection

Figure 6.3 shows the frog abundance result of three selected sites through the whole frog breeding season. It can be found that the frog abundance of the same site changes a great deal over time. In the *Kiyomi dam*, frog abundance is relatively high from February 21 to February 25. However, frog abundance is quite low in two periods, which are February 26 to March 11 and April 07 to April 12. The highest abundance of this site is achieved on March 22. However, the highest abundance for *Stony Creek dam* and *BG Creek dam* is obtained in February, which shows that frog abundance of different sites often varies a lot for different environments. Recordings of 47 days of all three sites have no frog calls. In the subsequent analysis, only those recordings that consist of frog calls are used for frog species richness analysis.

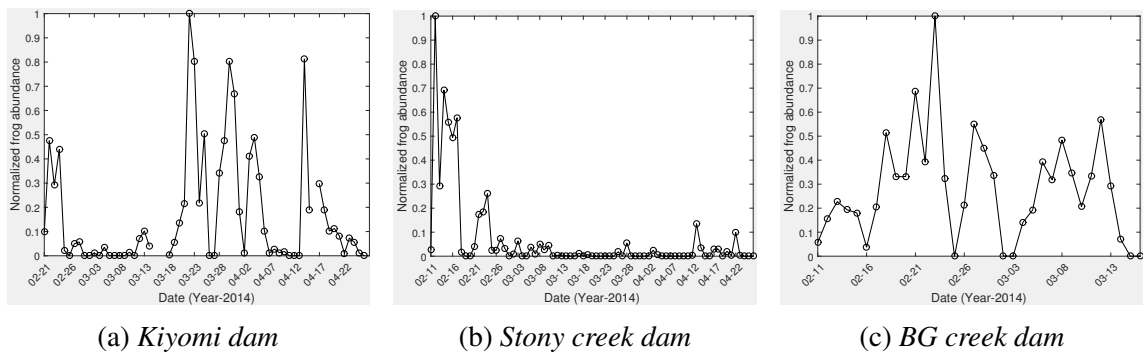


Figure 6.3: Frog abundance detection of different sites: *Kiyomi dam*, *Stony Creek dam* and *BG Creek dam*. For *Kiyomi dam*, three days do not record any acoustic data and then there is no value in those particular days. All the frog abundance value is normalised to [0 1].

6.3.3 Frog species richness analysis

Different multi-label learning algorithms are applied on 342 selected recordings to compare different feature sets. Then, five evaluation rules are used to compare the performance with the combination of four feature sets and four multi-label algorithms: Hamming loss, Rank loss, One error, Example based F1, and Micro F1 Madjarov et al. [2012], Zhang and Zhou [2014]. Experiment results are shown in Table 6.2.

The combination of multi-stage WP-based feature+LPCs and the RAKEL1 method achieves the best performance. Therefore, this combination is used for the testing data. Figure 6.4 shows the frog species richness of the three selected sites. For all the three sites, the variation of

Table 6.2: Classification results based on four feature sets and four multi-label learning algorithms. Here the methods for multi-label algorithms are in accordance to the name in the *Meka* software. The base classifier of all methods is decision tree. For a metric, the best value is in bold. Here, ↓ indicates the smaller the better, while ↑ indicates the bigger the better.

Features	Method	Hamming loss ↓	Rank loss ↓	One error ↓	Exampled based F1 ↑	Micro F1 ↑
MFCCs+LPCs	BR	0.155 ± 0.015	0.171 ± 0.037	0.246 ± 0.063	0.699 ± 0.03	0.749 ± 0.024
	CC	0.147 ± 0.018	0.147 ± 0.02	0.199 ± 0.042	0.722 ± 0.035	0.756 ± 0.029
	RAKEL	0.167 ± 0.038	0.122 ± 0.026	0.194 ± 0.063	0.721 ± 0.044	0.752 ± 0.041
	RAKEL1	0.134 ± 0.012	0.099 ± 0.025	0.147 ± 0.056	0.74 ± 0.044	0.783 ± 0.022
Multi-stage MFCCs + LPCs	BR	0.155 ± 0.016	0.169 ± 0.035	0.249 ± 0.064	0.7 ± 0.03	0.75 ± 0.024
	CC	0.147 ± 0.018	0.147 ± 0.021	0.199 ± 0.042	0.722 ± 0.034	0.756 ± 0.028
	RAKEL	0.166 ± 0.035	0.124 ± 0.027	0.194 ± 0.069	0.724 ± 0.048	0.754 ± 0.04
	RAKEL1	0.134 ± 0.013	0.101 ± 0.026	0.15 ± 0.063	0.737 ± 0.05	0.783 ± 0.023
WP-based feature + LPCs	BR	0.148 ± 0.025	0.139 ± 0.033	0.254 ± 0.063	0.708 ± 0.046	0.762 ± 0.036
	CC	0.168 ± 0.031	0.168 ± 0.045	0.272 ± 0.061	0.684 ± 0.054	0.723 ± 0.048
	RAKEL	0.155 ± 0.023	0.103 ± 0.022	0.178 ± 0.031	0.729 ± 0.032	0.763 ± 0.030
	RAKEL1	0.14 ± 0.027	0.094 ± 0.018	0.193 ± 0.063	0.727 ± 0.053	0.773 ± 0.042
Multi-stage WP-based feature + LPCs	BR	0.153 ± 0.014	0.147 ± 0.022	0.266 ± 0.037	0.689 ± 0.035	0.75 ± 0.025
	CC	0.142 ± 0.029	0.146 ± 0.023	0.254 ± 0.094	0.714 ± 0.042	0.764 ± 0.045
	RAKEL	0.154 ± 0.022	0.11 ± 0.012	0.196 ± 0.062	0.739 ± 0.022	0.768 ± 0.025
	RAKEL1	0.131 ± 0.012	0.09 ± 0.014	0.173 ± 0.03	0.743 ± 0.026	0.787 ± 0.018

species richness is not high, which shows that species richness of the same area is relatively stable. However, frog species richness of *BG Creek dam* has a smaller variation over the time than *Kiyomi dam* and *Stony Creek dam*. The comparison of the species richness for the three sites is shown in Figure 6.5. In contrast to other sites, the species richness in *BG Creek dam* is the highest. This might be that *BG Creek dam* is closer to a river and farther away from the human community.

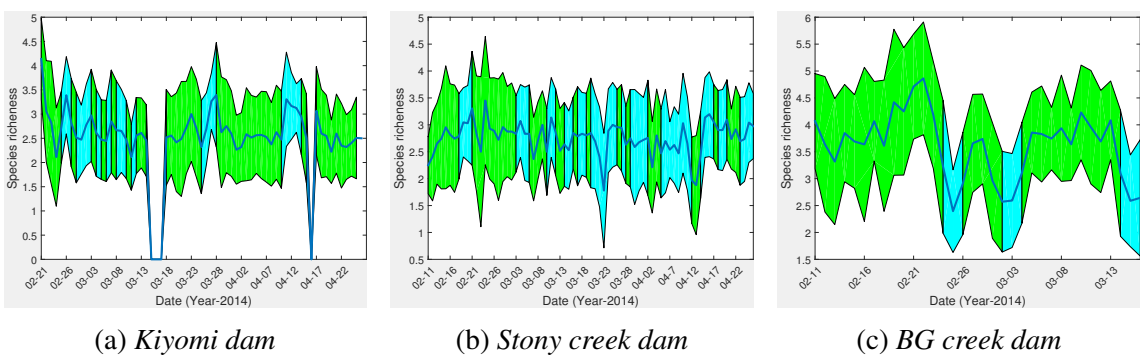


Figure 6.4: Frog species richness distribution of three selected sites. Here green bar represents the species variation, blue bar means there is no frog calls, zero value denotes the data loss of those particular days.

6.3.4 Comparison with MIML

In this chapter, ML learning is used to classify frog calls without syllable segmentation. Compared with the MIML learning (Table 5.1 in chapter 5), the ML classification has a better

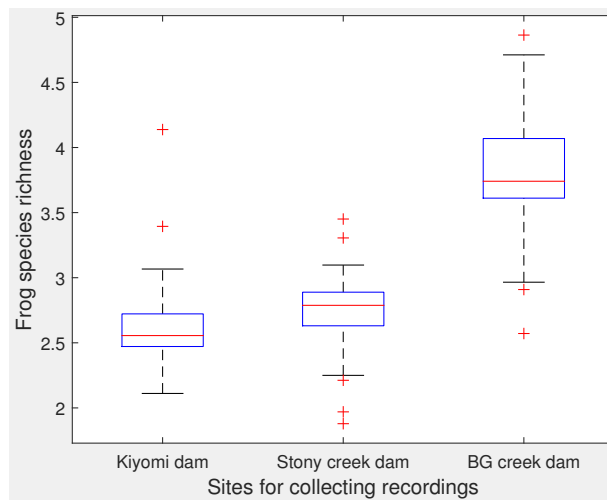


Figure 6.5: Averaged frog species richness of different sites.

classification performance. Although extracting global features for the ML classification will lose some detailed information, most frog vocalisations can still be successfully described when using cepstral features. Compared with other features, global cepstral features are often calculated from each windowed signal. Then, the statistical results, such as mean and standard deviation, of all the windowed signals are calculated, this process will compress the information in the time domain but keep the information of the frequency domain. Since most frogs tend to make calls continuously, the compression of the time domain information will not affect the discriminability of the cepstral features. In contrast, MIML classification needs to conduct the syllable segmentation before feature extraction. However, the use of AED often cannot accurately segment frog calls with low energies, which greatly affects the performance.

6.3.5 Statistical analysis

Multiple regression analysis is used to explore frog calling activity (frog abundance and frog species richness) along weather variables (mean temperature and rainfall)⁵. Frog calling activity is found to be highly correlated with mean temperature ($F=5.18$, $P<0.05$ for abundance, and $F=10.7$, $P<0.01$ for species richness). To calculate the correlation between rainfall and frog calling activity, we first set the rainfall value as the dummy variable. Then, the correlation between frog calling activity and rainfall value is also studied with multiple regression analysis ($F=4.63$, $P<0.05$ for abundance, and $F=4.64$, $P<0.05$ for species richness). The statistical analysis results indicate that frogs tend to make calls in the warm and humid environment,

⁵<http://www.bom.gov.au/?ref=hdr>

which is in accordance to previous studies Akmentins et al. [2015], Canavero et al. [2008].

6.4 Summary and limitations

Acoustic sensors are more widely used to monitor frog calling activity than the traditional field survey method. However, the use of acoustic sensors generates large volumes of audio data, which makes it necessary to develop automated methods. This paper proposes a novel method for detecting frog calling activity based on acoustic event detection and multi-label learning. Specifically, acoustic event detection is the first step to calculate frog abundance. Meanwhile, each 10-second recording is analysed to decide whether it contains frog calls or not. For those recordings with frog calls, multi-label learning is further used for calculating frog species richness with multi-stage WP-based features and LPCs. Finally, statistical analysis is utilised to reflect the relationship between frog calling activity (frog abundance and frog species richness) and weather variables (mean temperature and rainfall). Experiment results show that our proposed method can accurately detect frog calling activity and reflect its relationship with weather variables. Future work will focus on a wider frog call database, including a larger number of frog species, and frog calls collected over a longer period.

Chapter 7

Conclusion and future work

This thesis has addressed frog call classification using both high and low SNR recordings. For high SNR recordings, both feature extraction methods and classification frameworks for frog call classification are investigated. For feature extraction, enhanced feature representations and a novel feature representation based on wavelet packet decomposition are proposed. To study multiple simultaneously vocalising frog species in low SNR recordings, a spectrum of machine learning algorithms were explored including single-instance single-label classification, multiple-instance multiple-label classification, and multiple-label classification.

Many challenges of this thesis lie in the designing and identifying the effective feature extraction algorithms and adopting novel classification frameworks that can successfully classify low SNR recordings with multiple simultaneously vocalising frog species. In this chapter, key contributions of this research to the challenges will be summarised. Furthermore, useful avenues of inquiry for improving the methods described in this thesis will be explored.

7.1 Summary of contributions

The contributions of this research are mainly two folds.

1. Feature representation: Identifying characteristics of Australian frog vocalisations and developing corresponding novel feature representations.
2. System integration: Designing a new framework that combines multiple signal processing and machine learning techniques into a unified and effective system to classify frogs using

acoustics.

Below is the summary of the contributions of this thesis:

1) Enhanced acoustic feature representation for frog call classification in high SNR recordings.

A systematic scheme was developed towards the goal of automatic classification of frog calls. The performances of various classification methods such as LDA, K-NN, SVM, RF, MLP were evaluated together with different feature representations. The experience gained and experimental results demonstrate that: 1) Compared with previous feature representation, an enhanced feature representation including temporal, perceptual, and cepstral features can achieve the best classification performance. 2) The best classification performance is achieved by SVM and RF, in comparison with LDA, K-NN, and MLP. 3) The cepstral features are very sensitive to the background noise, but can achieve good classification accuracy in the high SNR recordings.

2) A novel feature representation via adaptive wavelet packet decomposition for frog call classification in both high and low SNR recordings.

To improve the anti-noise ability of cepstral features, wavelet packet decomposition is utilised to design a novel cepstral feature representation. Compared with other cepstral features such as MFCCs, Mel-scale wavelet packet decomposition coefficients, our proposed feature representation shows both good classification performance and excellent anti-noise ability.

3) Design a MIML classification framework for frog call classification in low SNR recordings.

Since most frog field recordings consist of multiple simultaneously vocalising frog species, both MIML and ML classification frameworks are first introduced to study frog calls. For MIML learning, a novel acoustic event detection algorithm is designed to segment acoustic events by using event filtering. Then, different MIML classifiers are evaluated together with various acoustic features based on the content and shape of the segmented events. The results show that MIML-RBF achieves the best classification results.

4) Design a ML classification framework for long-term monitoring of frogs in low SNR recordings.

For an ML classification framework, acoustic event detection is first used to filter all the recordings to find those that have frog calls. Meanwhile, frog abundance is detected based on the shape and content of segmented acoustic events. Then, those recordings with frog calls are

classified via ML learning. The feature representation used is a modified *adaptive WPD sub-band cepstral coefficients feature*. Compared with MIML learning, ML learning can achieve a better classification performance, because the MIML learning results are greatly affected by the syllable segmentation results. Lastly, the correlation between the frog calling activity (frog abundance and frog species richness) and weather variables (mean temperature and rainfall) are studied.

7.2 Limitations and future work

Although our proposed frog call classification system shows promising classification performance, there is still much work that can be done to help scientists and researchers in data collection and analysis in the bioacoustics communities.

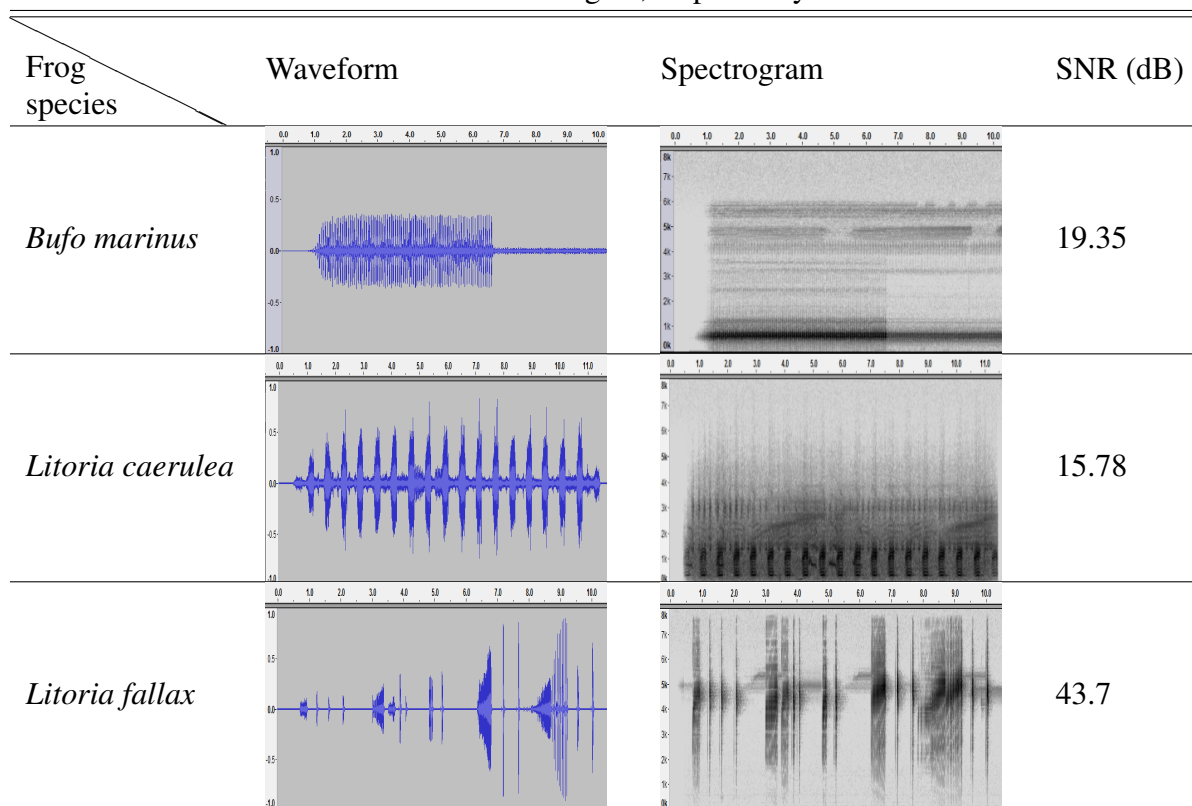
- One of the most important issues when dealing with frog recordings is the need for the standardised species-specific data with behavioural labels. Therefore, the algorithms we developed for frog call classification can be evaluated on a larger dataset. Consequently, researchers can use the outcomes of such automatic call classification methods for field studies effectively and precisely. However, it is very time-consuming to perform manual labelling. It is necessary to develop automatic or semi-automatic methods to perform the labelling.
- Another aspect that requires tremendous improvement is the need for an advanced frog syllable segmentation method for the field recordings so as to extract more accurate event-based features and conduct more thorough analysis on frog vocalisations. The problem of syllable segmentation is very complicated, because there are many simultaneous overlapping calling activities from birds, frogs, insects, and many other sources.
- Since collected low SNR recordings often contain much background noise, it is important to develop effective noise reduction algorithms to improve the classification performance.
- In addition, the *adaptive WPD sub-band cepstral coefficients feature* has been successfully used for frog call classification, which is used to capture the frequency domain information. The time-varying information has been attempted heuristically but there is still a lack of systematic exploration.

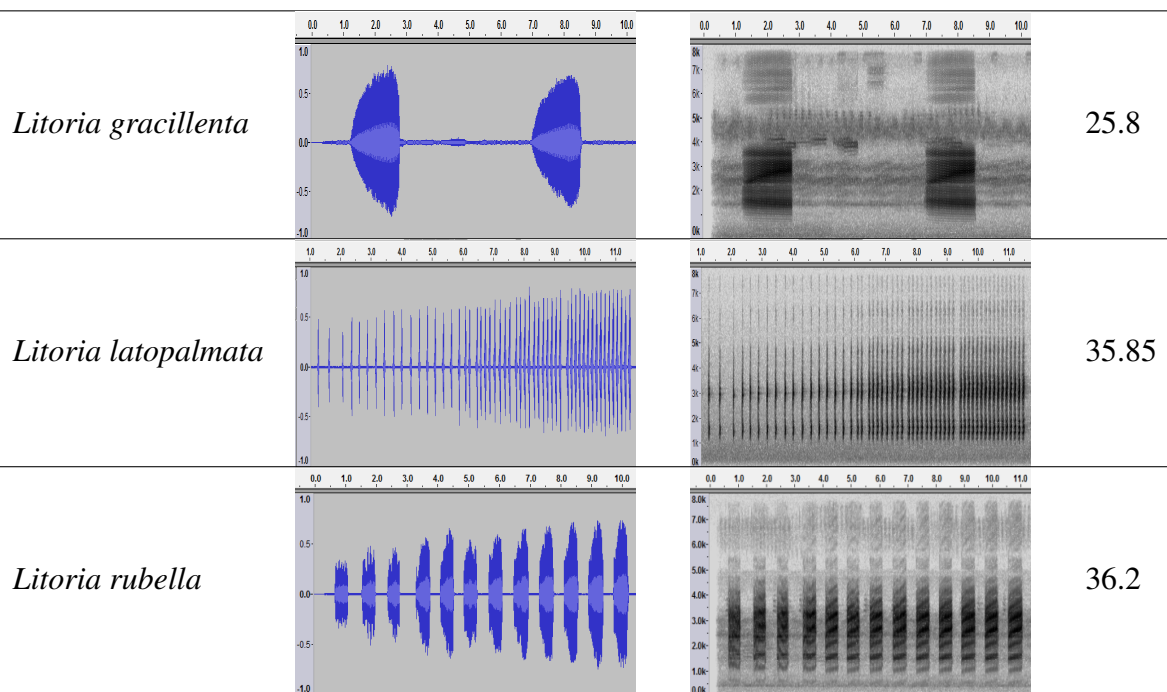
- Chapters 3 and 4 focus on the classification of segmented frog syllables using SISL algorithms. In Chapters 5 and 6, the classification is realised by tagging the small audio clip (10-second recording) with MIML/ML algorithms. There is no direct comparison between MIML/ML and SISL, because MIML/ML and SISL algorithms make different types of predictions, and are evaluated according to different performance measures.
- Our developed frog call classification system aims to help ecologists to study frogs over larger spatial and temporal scales. However, there is still no a generic platform for running the frog calls recordings. It is necessary to develop a toolbox with an easy user interface for frog call classification, and then ecologists can conduct the analysis on their own. We focus on efficacy in this research, however efficiency is also very important in big data analysis. For this purpose, the MATLAB code corresponding to feature extractors and classifiers needs to be optimised to perform real-time frog call classification in the field.

Appendix A

Waveform, spectrogram and SNR of frog species from David Stewart's CD

Table A.1: Waveform, spectrogram, and SNR of selected six frog species from David Stewart's CD. The SNR is calculated as $SNR = 10 * \log_{10}(\frac{\sum_{i=n}^{m+L} S_i^2}{\sum_{j=n}^{n+L} N_j^2})$ where L is the length of the signal and noise used for calculating SNR, and set at 6000 samples here, n and m are manual selected start location in the waveform for noise and signal, respectively.



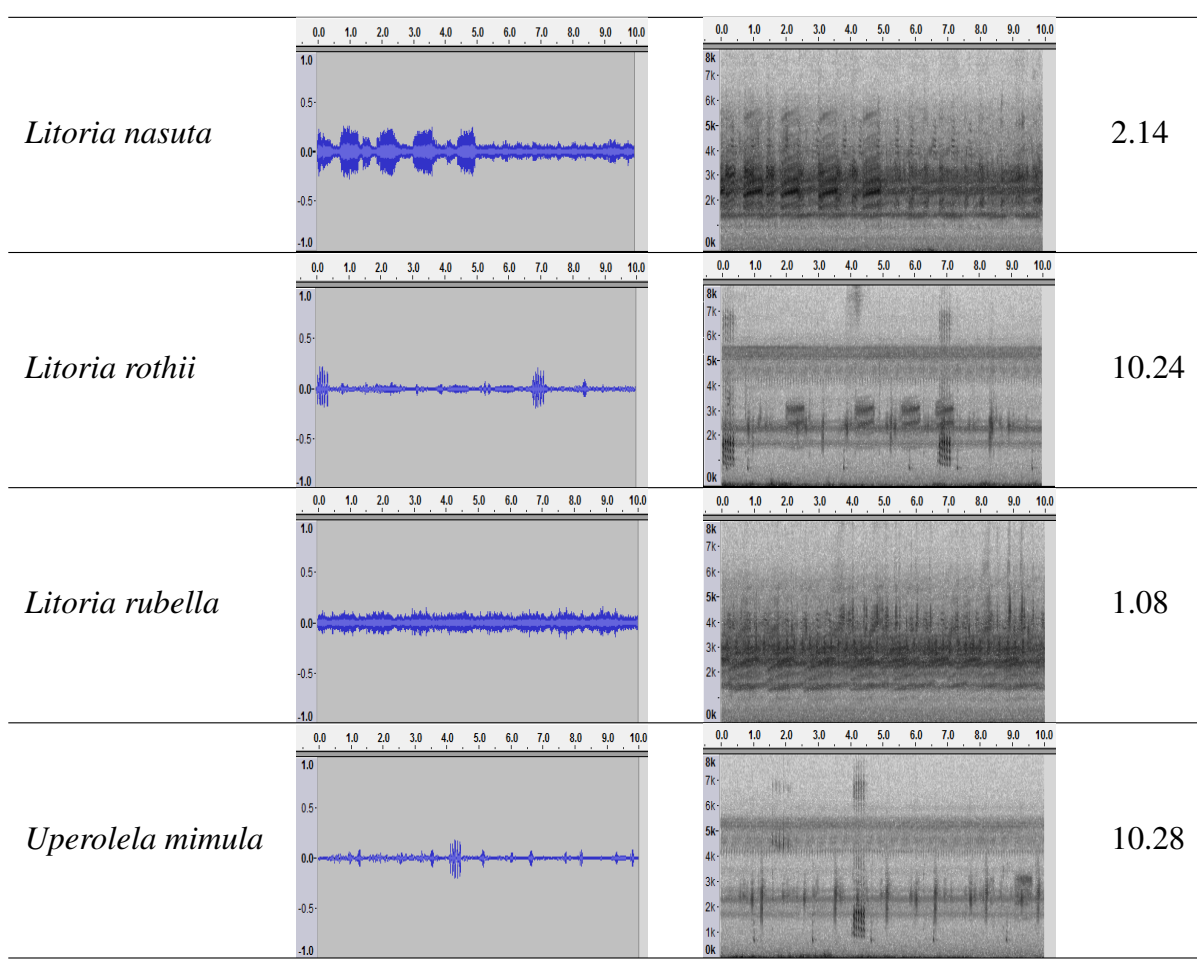


Appendix B

Waveform, spectrogram and SNR of six frog species from JCU recordings

Table B.1: Waveform, spectrogram, and SNR of eight frog species (recordings from JCU)

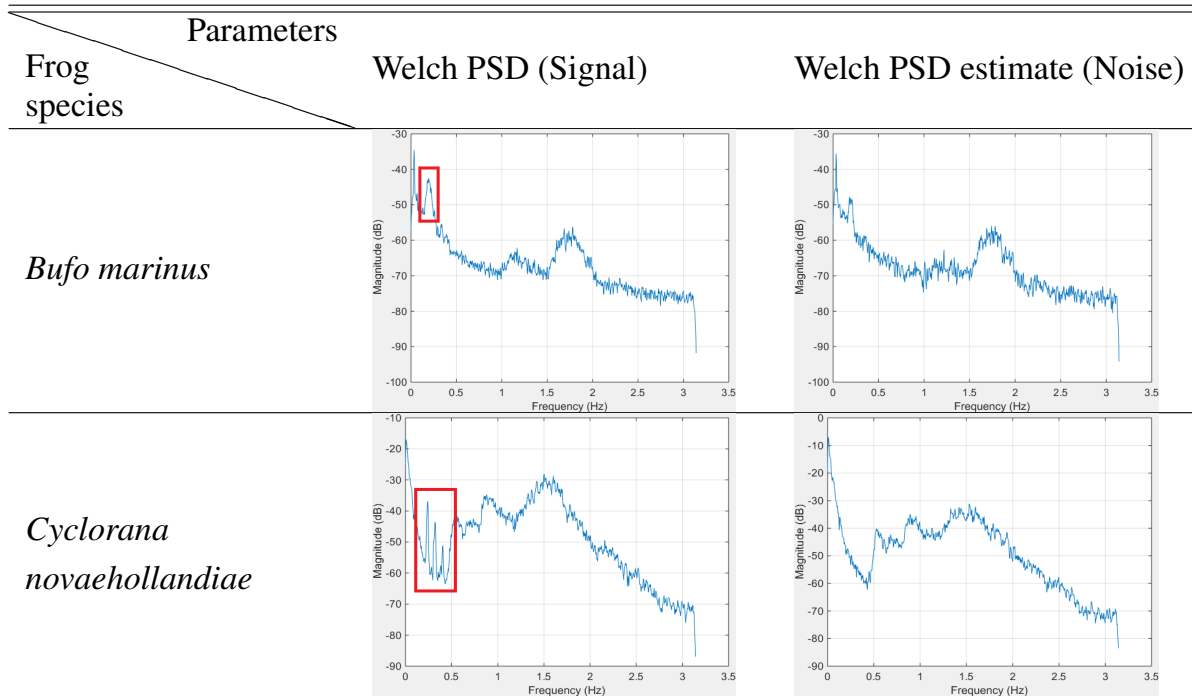
	Waveform	Spectrogram	SNR (dB)
<i>Bufo marinus</i>			1.86
<i>Cyclorana novaehollandiae</i>			-0.13
<i>Limnodynastes terraereginae</i>			-2.88
<i>Litoria fallax</i>			1.52



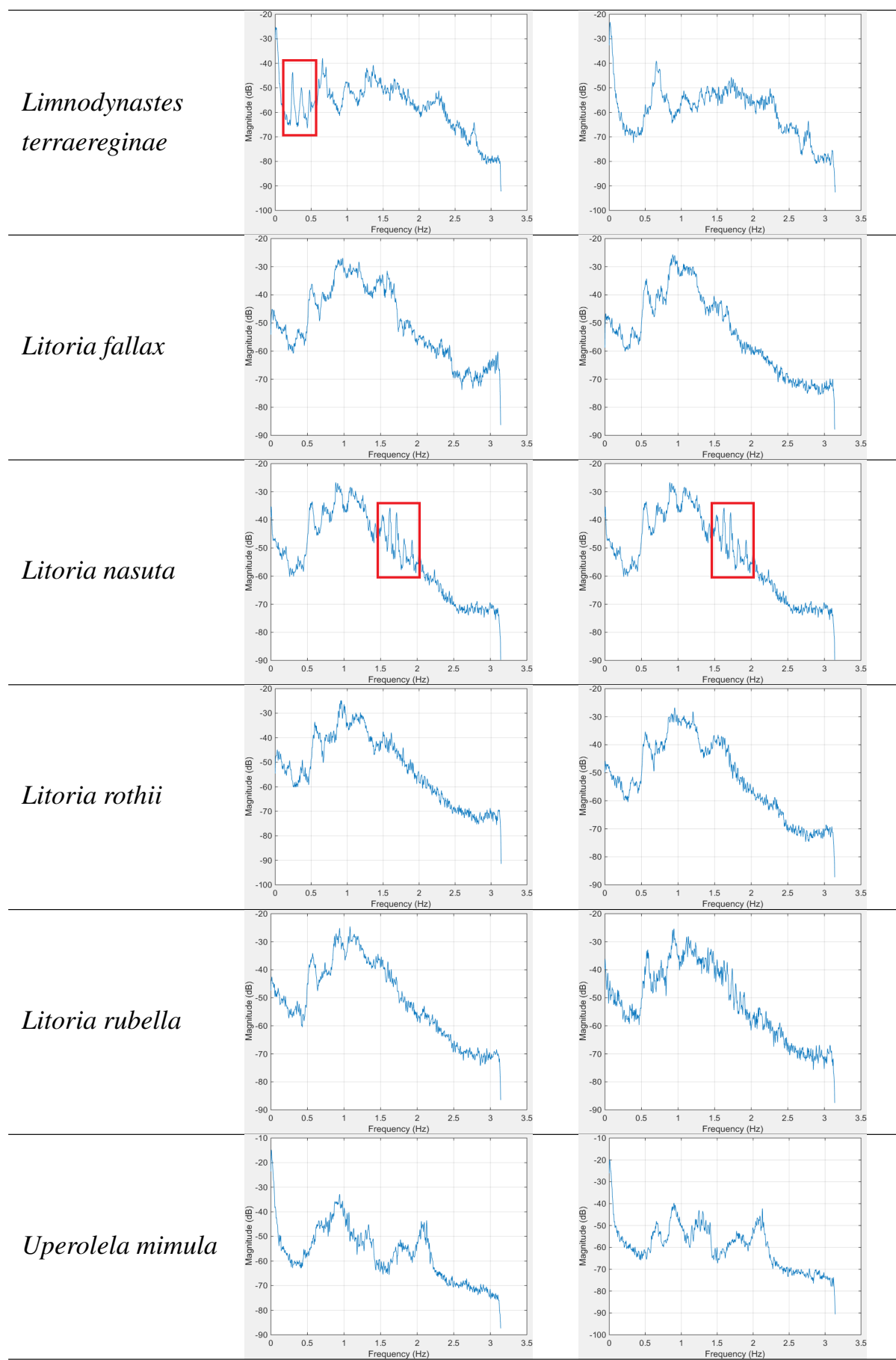
Appendix C

Power spectral density (PSD) estimate of signal and noise (JCU recordings)

Table C.1: Power spectral density (PSD) estimate of signal and noise (JCU recordings); for some frog species, the PSD difference between the signal and background noise is marked with the red rectangle, which indicates the frequency location of specific frog species; for others, the PSD of signal and noise is very similar, which means that some sources have similar frequency information with frog species



**APPENDIX C. POWER SPECTRAL DENSITY (PSD) ESTIMATE OF SIGNAL AND NOISE
108 (JCU RECORDINGS)**



Appendix D

Confidence interval of signal and noise

Table D.1: Confidence interval of signal and noise (David Stewart's CD). The calculation of confidence interval is defined as $CI = \mu \pm Z * \frac{\sigma}{\sqrt{L}}$, where μ and σ are the mean and standard deviation, respectively, Z is the upper $\frac{(1-C)}{2}$ critical value for the standard normal distribution, C is the confidence level, and set at 0.95.

Frog species \ Parameters	Confidence intervals of signal	Confidence intervals of noise
<i>Bufo marinus</i>	$-9.27*10^{-6} \pm 2.10*10^{-3}$	$-2.67*10^{-5} \pm 2.26*10^{-4}$
<i>Litoria caerulea</i>	$-6.73*10^{-5} \pm 2.40*10^{-3}$	$-6.89*10^{-5} \pm 3.90*10^{-4}$
<i>Litoria fallax</i>	$-5.85*10^{-6} \pm 1.50*10^{-3}$	$-2.73*10^{-5} \pm 9.62*10^{-6}$
<i>Litoria gracilenta</i>	$-7.12*10^{-5} \pm 2.00*10^{-3}$	$-7.70*10^{-5} \pm 1.00*10^{-4}$
<i>Litoria latopalmata</i>	$-6.58*10^{-5} \pm 2.70*10^{-3}$	$-1.02*10^{-4} \pm 4.36*10^{-5}$
<i>Litoria rubella</i>	$-3.13*10^{-5} \pm 3.00*10^{-3}$	$-9.87*10^{-5} \pm 4.70*10^{-5}$

Table D.2: Confidence interval of signal and noise for JCU recordings

Frog species \ Parameters	Confidence intervals of signal	Confidence intervals of noise
<i>Bufo marinus</i>	$-1.36*10^{-5} \pm 6.00*10^{-5}$	$-3.22*10^{-5} \pm 4.80*10^{-5}$
<i>Cyclorana novaehollandiae</i>	$1.30*10^{-3} \pm 8.70*10^{-4}$	$1.30*10^{-3} \pm 8.90*10^{-4}$
<i>Limnodynastes terraereginae</i>	$6.43*10^{-5} \pm 1.30*10^{-4}$	$1.86*10^{-4} \pm 1.89*10^{-4}$
<i>Litoria fallax</i>	$2.31*10^{-5} \pm 5.00*10^{-4}$	$5.75*10^{-6} \pm 4.22*10^{-4}$
<i>Litoria nasuta</i>	$-1.55*10^{-4} \pm 4.90*10^{-4}$	$6.25*10^{-6} \pm 3.85*10^{-4}$
<i>Litoria rothii</i>	$-3.32*10^{-4} \pm 9.2*10^{-4}$	$1.61*10^{-4} \pm 2.84*10^{-4}$
<i>Litoria rubella</i>	$-8.15*10^{-5} \pm 5.52*10^{-4}$	$-2.69*10^{-5} \pm 4.87*10^{-4}$
<i>Uperolela mimula</i>	$-1.20*10^{-3} \pm 1.10*10^{-3}$	$-9.36*10^{-4} \pm 3.35*10^{-4}$

References

- Acevedo, M. A., Corrada-Bravo, C. J., Corrada-Bravo, H., Villanueva-Rivera, L. J., and Aide, T. M. (2009). Automated classification of bird and amphibian calls using machine learning: A comparison of methods. *Ecological Informatics*, 4(4):206–214.
- Akmentins, M., Pereyra, L., Sanabria, E., and Vaira, M. (2015). Patterns of daily and seasonal calling activity of a direct-developing frog of the subtropical andean forests of argentina. *Bioacoustics*, 24(2):89–99.
- Allen, J. (1997). Short term spectral analysis, synthesis, and modification by discrete fourier transform. In *IEEE Trans. on Acoust., Speech, and Sig. Proc.*, volume 4, pages 21–24.
- Arch, V. S., Grafe, T. U., and Narins, P. M. (2008). Ultrasonic signalling by a bornean frog. *Biology Letters*, 4(1):19–22.
- Bao, L. and Cui, Y. (2005). Prediction of the phenotypic effects of non-synonymous single nucleotide polymorphisms using structural and evolutionary information. *Bioinformatics*, 21(10):2185–2190.
- Bedoya, C., Isaza, C., Daza, J. M., and López, J. D. (2014). Automatic recognition of anuran species based on syllable identification. *Ecological Informatics*, 24:200–209.
- Biswas, A., Sahu, P., and Chandra, M. (2014). Admissible wavelet packet features based on human inner ear frequency response for hindi consonant recognition. *Computers & Electrical Engineering*, 40(4):1111 – 1122.
- Brandes, T. S. (2008). Feature vector selection and use with hidden markov models to identify frequency-modulated bioacoustic signals amidst noise. *Audio, Speech, and Language Processing, IEEE Transactions on*, 16(6):1173–1180.

- Brandes, T. S., Naskrecki, P., and Figueroa, H. K. (2006). Using image processing to detect and classify narrow-band cricket and frog calls. *The Journal of the Acoustical Society of America*, 120(5):2950–2957.
- Briggs, F., Lakshminarayanan, B., Neal, L., Fern, X. Z., Raich, R., Hadley, S. J., Hadley, A. S., and Betts, M. G. (2012). Acoustic classification of multiple simultaneous bird species: A multi-instance multi-label approach. *The Journal of the Acoustical Society of America*, 131(6):4640–4650.
- Camacho, A., García-Rodríguez, A., and Bolaños, F. (2011). Automatic detection of vocalizations of the frog diasporus hylaformis in audio recordings. In *Proceedings of Meetings on Acoustics*, volume 14, page 010003. Acoustical Society of America.
- Canavero, A., Arim, M., Naya, D. E., Camargo, A., Da Rosa, I., and Maneyro, R. (2008). Calling activity patterns in an anuran assemblage: the role of seasonal trends and weather determinants. *North-Western Journal of Zoology*, 4(1):29–41.
- Chen, W., Zhao, G., and Li, X. (2013). A novel approach based on ensemble learning to nips4b challenge. In *proc. of int. symp. Neural Information Scaled for Bioacoustics, sabiod.org/nips4b, joint to NIPS, Nevada*.
- Chen, W.-P., Chen, S.-S., Lin, C.-C., Chen, Y.-Z., and Lin, W.-C. (2012). Automatic recognition of frog calls using a multi-stage average spectrum. *Computers & Mathematics with Applications*, 64(5):1270–1281.
- Chen, Z. and Maher, R. C. (2006). Semi-automatic classification of bird vocalizations using spectral peak tracks. *The Journal of the Acoustical Society of America*, 120(5):2974–2984.
- Colombia, C. and del Cauca, V. (2009). Frogs species classification using lpc and classification algorithms on wireless sensor network platform.
- Colonna, J., Ribas, A., dos Santos, E., and Nakamura, E. (2012a). Feature subset selection for automatically classifying anuran calls using sensor networks. In *Neural Networks (IJCNN), The 2012 International Joint Conference on*, pages 1–8.
- Colonna, J. G., Cristo, M., Junior, M. S., and Nakamura, E. F. (2015). An incremental technique for real-time bioacoustic signal segmentation. *Expert Systems with Applications*, 42(21):7367 – 7374.

- Colonna, J. G., Ribas, A. D., dos Santos, E. M., and Nakamura, E. F. (2012b). Feature subset selection for automatically classifying anuran calls using sensor networks. In *Neural Networks (IJCNN), The 2012 International Joint Conference on*, pages 1–8. IEEE.
- Cortes, C. and Vapnik, V. (1995). Support-vector networks. *Machine learning*, 20(3):273–297.
- Croker, B. and Kottege, N. (2012). Using feature vectors to detect frog calls in wireless sensor networks. *The Journal of the Acoustical Society of America*, 131(5):EL400–EL405.
- Dang, T., Bulusu, N., and Hu, W. (2008). Lightweight acoustic classification for cane-toad monitoring. In *Signals, Systems and Computers, 2008 42nd Asilomar Conference on*, pages 1601–1605. IEEE.
- Dayou, J., Han, N. C., Mun, H. C., Ahmad, A. H., Muniandy, S. V., and Dalimin, M. N. (2011). Classification and identification of frog sound based on entropy approach. In *International Conference on Life Science and Technology*, volume 3, pages 184–187.
- Deng, L. and O’Shaughnessy, D. (2003). *Speech processing: a dynamic and optimization-oriented approach*. CRC Press.
- Dorcas, M. E., Price, S. J., Walls, S. C., and Barichivich, W. J. (2009). Auditory monitoring of anuran populations. *Amphibian ecology and conservation: a hand book of techniques*. Oxford University Press, Oxford, pages 281–298.
- Dudgeon, D., Arthington, A. H., Gessner, M. O., Kawabata, Z.-I., Knowler, D. J., Lévéque, C., Naiman, R. J., Prieur-Richard, A.-H., Soto, D., Stiassny, M. L., et al. (2006). Freshwater biodiversity: importance, threats, status and conservation challenges. *Biological reviews*, 81(02):163–182.
- Dufour, O., Glotin, H., Artires, T., Bas, Y., and Giraudet, P. (2013). Multi-instance multi-label acoustic classification of plurality of animals: birds, insects & amphibian. *Workshop on Neural Information Processing Scaled for Bioacoustics*, pages 164–174.
- Farooq, O. and Datta, S. (2001). Mel filter-like admissible wavelet packet structure for speech recognition. *IEEE Signal Processing Letters*, 8(7):196–198.
- Fodor, G. (2013). The ninth annual mlsp competition: first place. In *Machine Learning for Signal Processing (MLSP), 2013 IEEE International Workshop on*, pages 1–2. IEEE.

- Fox, E. J. (2008). A new perspective on acoustic individual recognition in animals with limited call sharing or changing repertoires. *Animal Behaviour*, 75(3):1187 – 1194.
- Gingras, B. and Fitch, W. T. (2013). A three-parameter model for classifying anurans into four genera based on advertisement calls. *The Journal of the Acoustical Society of America*, 133(1):547–559.
- Glotin, H., Sueur, J., Artières, T., Adam, O., and Razik, J. (2013). Sparse coding for scaled bioacoustics: From humpback whale songs evolution to forest soundscape analyses. *The Journal of the Acoustical Society of America*, 133(5):3311–3311.
- Gordon, L., Chervonenkis, A. Y., Gammerman, A. J., Shahmuradov, I. A., and Solovyev, V. V. (2003). Sequence alignment kernel for recognition of promoter regions. *Bioinformatics*, 19(15):1964–1971.
- Grigg, G., Taylor, A., Mc Callum, H., and Watson, G. (1996). Monitoring frog communities: an application of machine learning. In *Proceedings of Eighth Innovative Applications of Artificial Intelligence Conference, Portland Oregon*, pages 1564–1569.
- Han, N. C., Muniandy, S. V., and Dayou, J. (2011). Acoustic classification of australian anurans based on hybrid spectral-entropy approach. *Applied Acoustics*, 72(9):639–645.
- Han, W., Chan, C.-F., Choy, C.-S., and Pun, K.-P. (2006). An efficient mfcc extraction method in speech recognition. In *Circuits and Systems, 2006. ISCAS 2006. Proceedings. 2006 IEEE International Symposium on*, pages 4–pp. IEEE.
- Harma, A. (2003). Automatic identification of bird species based on sinusoidal modeling of syllables. In *Acoustics, Speech, and Signal Processing, 2003. Proceedings.(ICASSP'03). 2003 IEEE International Conference on*, volume 5, pages V–545. IEEE.
- Heller, J. R. and Pinezich, J. D. (2008). Automatic recognition of harmonic bird sounds using a frequency track extraction algorithm. *The Journal of the Acoustical Society of America*, 124(3):1830–1837.
- Hsu, C.-W., Chang, C.-C., Lin, C.-J., et al. (2003). A practical guide to support vector classification.

- Huang, C.-J., Chen, Y.-J., Chen, H.-M., Jian, J.-J., Tseng, S.-C., Yang, Y.-J., and Hsu, P.-A. (2014). Intelligent feature extraction and classification of anuran vocalizations. *Applied Soft Computing*, 19(0):1 – 7.
- Huang, C.-J., Yang, Y.-J., Yang, D.-X., and Chen, Y.-J. (2009). Frog classification using machine learning techniques. *Expert Systems with Applications*, 36(2):3737–3743.
- Huang, C.-J., Yang, Y.-J., Yang, D.-X., Chen, Y.-J., and Wei, H.-Y. (2008). Realization of an intelligent frog call identification agent. In *Agent and Multi-Agent Systems: Technologies and Applications*, pages 93–102. Springer.
- Jaafar, H. and Ramli, D. (2013a). Automatic syllables segmentation for frog identification system. In *Signal Processing and its Applications (CSPA), 2013 IEEE 9th International Colloquium on*, pages 224–228.
- Jaafar, H. and Ramli, D. A. (2013b). Automatic syllables segmentation for frog identification system. In *Signal Processing and its Applications (CSPA), 2013 IEEE 9th International Colloquium on*, pages 224–228. IEEE.
- Jaafar, H., Ramli, D. A., and Shahrudin, S. (2013a). A comparative study of classification algorithms and feature extractions for frog identification system.
- Jaafar, H., Ramli, D. A., and Shahrudin, S. (2013b). Mfcc based frog identification system in noisy environment. In *Signal and Image Processing Applications (ICSIPA), 2013 IEEE International Conference on*, pages 123–127. IEEE.
- Jancovic, P. and Kokuer, M. (2015). Acoustic recognition of multiple bird species based on penalized maximum likelihood. *Signal Processing Letters, IEEE*, 22(10):1585–1589.
- Jang, Y., Hahm, E. H., Lee, H.-J., Park, S., Won, Y.-J., and Choe, J. C. (2011). Geographic variation in advertisement calls in a tree frog species: gene flow and selection hypotheses. *PloS one*, 6(8):e23297.
- Juan Mayor, L. M. M. (2009). Frogs species classification using lpc and classification algorithms on wireless sensor network platform. In *XVII General Assembly, Ibero-American Conference on Trends in Engineering Education and Collaboration, ISTEC, 2009*.

- Kular, D., Hollowood, K., Ommajaro, O., Smart, K., Bush, M., and Ribeiro, E. (2015). Classifying frog calls using gaussian mixture models. In *Advances in Visual Computing*, pages 347–354. Springer.
- Lasseck, M. (2013.). Bird song classification in field recordings: winning solution for nips4b 2013 competition. In *Proc. of int. symp. Neural Information Scaled for Bioacoustics, sabiod.org/nips4b, joint to NIPS, Nevada.*
- Lee, C.-H., Chou, C.-H., Han, C.-C., and Huang, R.-Z. (2006). Automatic recognition of animal vocalizations using averaged mfcc and linear discriminant analysis. *Pattern Recognition Letters*, 27(2):93–101.
- Litvin, Y. and Cohen, I. (2011). Single-channel source separation of audio signals using bark scale wavelet packet decomposition. *Journal of Signal Processing Systems*, 65(3):339–350.
- Madjarov, G., Kocev, D., Gjorgjevikj, D., and D?eroski, S. (2012). An extensive experimental comparison of methods for multi-label learning. *Pattern Recognition*, 45(9):3084 – 3104.
- Mallawaarachchi, A., Ong, S., Chitre, M., and Taylor, E. (2008). Spectrogram denoising and automated extraction of the fundamental frequency variation of dolphin whistles. *The Journal of the Acoustical Society of America*, 124(2):1159–1170.
- Massaron, L. (2013). Ensemble logistic regression and gradient boosting classifiers for multilabel bird song classification in noise (nips4b challenge). *Proc of Neural Information Processing Scaled for Bioacoustics, joint to NIPS.*
- Mellinger, D. K., Martin, S. W., Morrissey, R. P., Thomas, L., and Yosco, J. J. (2011). A method for detecting whistles, moans, and other frequency contour sounds. *The Journal of the Acoustical Society of America*, 129(6):4055–4061.
- Melter, R. A. (1987). Some characterizations of city block distance. *Pattern Recognition Letters*, 6(4):235 – 240.
- Mencia, E. L., Nam, J., and Lee, D.-H. (2013). Learning multi-labeled bioacoustic samples with an unsupervised feature learning approach. *Proc of Neural Information Processing Scaled for Bioacoustics, joint to NIPS*, 2013:184–189.

- Narins, P. M., Feng, A. S., and Shen, J.-X. (2007). Frogs communicate with ultrasound in noisy environments. In *Hearing—From sensory processing to perception*, pages 185–190. Springer.
- Noda, J. J., Travieso, C. M., and Sánchez-Rodríguez, D. (2016). Methodology for automatic bioacoustic classification of anurans based on feature fusion. *Expert Systems with Applications*, 50:100 – 106.
- Otsu, N. (1975). A threshold selection method from gray-level histograms. *Automatica*, 11(285-296):23–27.
- Potamitis, I. (2015). Unsupervised dictionary extraction of bird vocalisations and new tools on assessing and visualising bird activity. *Ecological Informatics*, 26:6–17.
- Razik, J., Hoeberichts, M., Doh, Y., et al. (2015). Sparse coding for efficient bioacoustic data mining: Preliminary application to analysis of whale songs. In *2015 IEEE International Conference on Data Mining Workshop (ICDMW)*, pages 780–787. IEEE.
- Ren, Y., Johnson, M. T., and Tao, J. (2008). Perceptually motivated wavelet packet transform for bioacoustic signal enhancement. *The Journal of the Acoustical Society of America*, 124(1):316–327.
- Rocchesso, D. (2003). *Introduction to sound processing*. Mondo estremo.
- Roch, M. A., Brandes, T. S., Patel, B., Barkley, Y., Baumann-Pickering, S., and Soldevilla, M. S. (2011). Automated extraction of odontocete whistle contours. *The Journal of the Acoustical Society of America*, 130(4):2212–2223.
- Ruiz-Munoz, J., Orozco-Alzate, M., and Castellanos-Dominguez, G. (2015). Multiple instance learning-based birdsong classification using unsupervised recording segmentation. *Proceedings of the Twenty-Fourth International Joint Conference On Artificial Intelligence (IJCAI 2015)*.
- Selin, A., Turunen, J., and Tanttu, J. T. (2007). Wavelets in recognition of bird sounds. *EURASIP Journal on Applied Signal Processing*, 2007(1):141–141.
- Somervuo, P. et al. (2004). Classification of the harmonic structure in bird vocalization. In *Acoustics, Speech, and Signal Processing, 2004. Proceedings.(ICASSP'04). IEEE International Conference on*, volume 5, pages V–701. IEEE.

- Somervuo, P., Härmä, A., and Fagerlund, S. (2006). Parametric representations of bird sounds for automatic species recognition. *Audio, Speech, and Language Processing, IEEE Transactions on*, 14(6):2252–2263.
- Stewart, D. (1999). Australian frog calls: subtropical east. Audio CD.
- Stowell, D. and Plumley, M. D. (2013). Feature design for multilabel bird song classification in noise (nips4b challenge). *Proceedings of NIPS4b: neural information processing scaled for bioacoustics, from neurons to big data*.
- Tan, W., Jaafar, H., Ramli, D., Rosdi, B., and Shahrudin, S. (2014). Intelligent frog species identification on android operating system. *International journal of circuits, systems and signal processing*.
- Tanton, J. S. (2005). *Encyclopedia of mathematics*. Facts On File.
- Tjahja, T. V., Fern, X. Z., Raich, R., and Pham, A. T. (2015). Supervised hierarchical segmentation for bird song recording. In *Acoustics, Speech and Signal Processing (ICASSP), 2015 IEEE International Conference on*, pages 763–767. IEEE.
- Towsey, M., Planitz, B., Nantes, A., Wimmer, J., and Roe, P. (2012). A toolbox for animal call recognition. *Bioacoustics*, 21(2):107–125.
- Towsey, M. W. and Planitz, B. (2011). Technical report : acoustic analysis of the natural environment. 2011.
- Vaca-Castano, G. and Rodriguez, D. (2010). Using syllabic mel cepstrum features and k-nearest neighbors to identify anurans and birds species. In *Signal Processing Systems (SIPS), 2010 IEEE Workshop on*, pages 466–471. IEEE.
- Wei, B., Yang, M., Rana, R. K., Chou, C. T., and Hu, W. (2012). Distributed sparse approximation for frog sound classification. In *Proceedings of the 11th international conference on Information Processing in Sensor Networks*, pages 105–106. ACM.
- Wimmer, J., Towsey, M., Planitz, B., Williamson, I., and Roe, P. (2013). Analysing environmental acoustic data through collaboration and automation. *Future Generation Computer Systems*, 29(2):560–568.

- Xie, J. (2016). Song meter (sm2) widelife acoustic. <http://www.wildlifeacoustics.com/products/song-meter-sm2-birds>.
- Xie, J., Towsey, M., Eichinski, P., Zhang, J., and Roe, P. (2015a). Acoustic feature extraction using perceptual wavelet packet decomposition for frog call classification. *11th IEEE International Conference on eScience*.
- Xie, J., Towsey, M., Truskinger, A., Eichinski, P., Zhang, J., and Roe, P. (2015b). Acoustic classification of australian anurans using syllable features. In *2015 IEEE Tenth International Conference on Intelligent Sensors, Sensor Networks and Information Processing (IEEE ISSNIP 2015)*, Singapore, Singapore.
- Xie, J., Towsey, M., Zhang, J., Dong, X., and Roe, P. (2015c). Application of image processing techniques for frog call classification. *International Conference on Image Processing*.
- Xie, J., Towsey, M., Zhang, J., and Roe, P. (2015d). Image processing and classification procedure for the analysis of australian frog vocalisations. In *Proceedings of the 2Nd International Workshop on Environmental Multimedia Retrieval*, EMR '15, pages 15–20, Shanghai, China. ACM.
- Xie, J., Towsey, M., Zhang, J., and Roe, P. (2016). Adaptive frequency scaled wavelet packet decomposition for frog call classification. *Ecological Informatics*, pages –.
- Yen, G. G. and Fu, Q. (2002). Automatic frog call monitoring system: a machine learning approach. In *AeroSense 2002*, pages 188–199. International Society for Optics and Photonics.
- Yuan, C. L. T. and Ramli, D. A. (2012). Frog sound identification system for frog species recognition. In *Context-Aware Systems and Applications*, pages 41–50. Springer.
- Zhang, M.-L. and Zhou, Z.-H. (2014). A review on multi-label learning algorithms. *Knowledge and Data Engineering, IEEE Transactions on*, 26(8):1819–1837.
- Zhang, X. and Li, Y. (2015). Adaptive energy detection for bird sound detection in complex environments. *Neurocomputing*, 155(0):108 – 116.
- Zhou, Z.-H., Zhang, M.-L., Huang, S.-J., and Li, Y.-F. (2008). Miml: a framework for learning with ambiguous objects. *CORR abs/0808.3231*.

